JOURNAL OF APPLIED PHYSICS

JOURNAL
OF
APPLIED PHYSICS

Vol. 16, No. 2 FEBRUARY, 1945

In This Issue

Page

Physics in 1944 THOMAS H. OSGOOD 61

Small Prism Infra-Red Spectrometry
R. BOWLING BARNES, ROBERT S. MCDONALD, VAN ZANDT WILLIAMS, AND RICHARD F. KINNAIRD 77

Contributed Original Research

General Theory of Stresses and Displacements in Layered Systems. I D. M. BURMISTER 89

Use of the Electron Diffraction Camera to Detect Insulating Films EILEEN I. ALESSANDRINI 94

Crystal Interference Phenomena in Electron Microscope Images R. D. HEIDENREICH AND L. STURKEY 97

Sustained Subharmonic Response in Non-Linear Series Circuits CHARLES F. SPITZER 105

X-Ray Diffraction Study of the Fatigue in Metals at High Stresses ARTHUR G. BARKOW 111

Erratum: Fatigue of Fabrics W. F. BUSSE, E. T. LESSIG, D. L. LOUGHBOROUGH, AND L. LARRICK 120

In Every Issue

Here and There 87

New Books 87

New Booklets 88

Index to Advertisers xxviii

BOARD OF EDITORS

ELMER HUTCHISSON,
Editor

Associate Editors
R. B. BARNES
OTTO BEECK
W. F. BUSSE
S. H. CALDWELL
CLARK GOODMAN
SELIG HECHT
W. J. LYONS
MORRIS MUSKAT
THOMAS H. OSGOOD
PAUL E. SABINE
FREDERICK SEITZ
J. R. TOWNSEND

Publication of the American Institute of Physics

ADMINISTRATIVE STAFF

HENRY A. BARTON,
Director

MADELINE M. MITCHELL,
Publications Manager

JOHN T. TATE,
Adviser on Publications

GOVERNING BOARD

PAUL E. KLOPSTEG,
Chairman

GEORGE B. PEGRAM,
Secretary

T. D. COPE
R. B. DOW
L. A. DUBRIDGE
FLOYD A. FIRESTONE
HARVEY FLETCHER
R. C. GIBBS
K. S. GIBSON
HERMANN MARK
A. G. WORTHING
JOHN T. TATE
L. W. TAYLOR
N. W. TAYLOR
WALLACE WATERFALL

The JOURNAL OF APPLIED PHYSICS, published monthly at Prince and Lemon Sts., Lancaster, Pa., is devoted to physics in its role as the science basic to other natural sciences and to the arts and industries. Previous to 1937 this publication was known as PHYSICS. The JOURNAL OF APPLIED PHYSICS publishes editorials, news of physicists, and reviews, as well as technical papers of applied physics.

Manuscripts should be submitted to Elmer Hutchisson, Editor, Case School of Applied Science, Cleveland 6, Ohio.

Subscriptions and orders for back numbers should be addressed to Prince and Lemon Streets, Lancaster, Pa. or to the American Institute of Physics, 57 East 55 Street, New York 22, N. Y.

Subscription Price

	U. S. AND CANADA	ELSEWHERE
To members of scientific societies	$5.00	$5.70
To all others	7.00	7.70

Back Number Prices
Complete set: Vol. 1, July, 1931–Vol. 15, 1944—**$94.50**
Yearly back number rate: **$7.70**
Single copies: **$0.70** each.

Changes of address and proofs should be addressed to the Publications Manager.

Advertising rates supplied on request. Orders, advertising copy, and cuts should be sent to the American Institute of Physics.

Entered as second class matter January 22, 1937, at the Post Office at Lancaster, Pennsylvania, under the Act of March 3, 1879
Accepted for mailing at the special rate of postage provided for in the Act of February 28, 1925, authorized May 2, 1932.

Copyright 1945, by the American Institute of Physics.

Journal
of
Applied Physics

Volume 16, Number 2 February, 1945

Physics in 1944

BY THOMAS H. OSGOOD
Michigan State College, East Lansing, Michigan

THE WAR AND RESEARCH

IN the years immediately preceding the war, attention was called frequently to the contrasting spirit of the research which was characteristic of industrial laboratories, and that which could be regarded as typical of university laboratories and other institutions whose primary function was the training and polishing of research workers. The signpost which pointed the way was, in the first case, the job to be done; in the second, the field or subject matter of study. Even when due allowances are made for the necessary restrictions in choice of research topics by which a beginner-in-research is hedged on account of the limitations of his special knowledge, it must be admitted that many universities followed an unduly narrow policy in this respect.

While no scientist could conscientiously argue for a complete reversal of traditional policy, it must be recognized that when the present war finally comes to an end, the men who return to their university laboratories will have had a liberal education in research as a cooperative undertaking in which the completion of a specified job was the immediate goal. During the past three years of war we have seen projects pushed to successful completion because psychologists became engineers, biologists became physicists, and physicists showed commendable versatility in turning their hands and heads to research in a dozen unfamiliar fields. Like a skilful artisan who can quickly learn a new trade, a competent research worker is soon at home in a new profession. The tonic effect of this intermingling of specialties will soon make itself felt in nearly all fields of research, and will undoubtedly be manifest in the literature when publication of material now shrouded in secrecy is permitted at the conclusion of hostilities.

X-RAYS

Nearly ten years ago Kossel and Voges used a single crystal as a target in an x-ray tube and found that the diverging rays characteristic of the crystal atoms were reflected by Bragg planes in such a way as to give, on a photographic film placed nearby, a pattern of very sharp curved lines superposed upon a fairly uniformly exposed background. Their techniques appear to have been elaborated by only a few other investigators. Recently, however, the matter has been taken up by Lonsdale[1] in connection with a study of the perfection of crystals.

Lonsdale finds that photographs of this type can be made without using the crystal itself as the target in the x-ray tube. Instead, the crystal being investigated is mounted on the anticathode, close beside the sharp focal spot where it is strongly irradiated by divergent rays from the target. That the crystal must be quite small is to be considered as one of the merits rather than a defect of this method of crystal photography. The pattern which is obtained depends on the kind of crystal which is used, on its orientation, and on the relation between the film (usually a plane) and the crystallographic axes. A typical pattern from Kossel's paper is reproduced in Fig. 1. This picture is a negative of the original

FIG. 1. Absorption lines obtained by the divergent-beam technique of crystal analysis by x-rays. [Reproduced from W. Kossel and H. Voges, Ann. d. Physik **23**, 694 (1935).]

film; the dark criss-cross lines therefore tell where less than the average amount of x-radiation reached the film, and thus give a clue to the crystal structure once the mechanism involved is understood. The beam of x-rays, it must be remembered, is widely divergent, and strongly loaded with characteristic rays typical of the target. If these rays pass through a perfectly homogeneous, amorphous material, they will, with a short exposure, cause nearly uniform blackening over any small region of the film. Since the rays pass through a crystal, however, there are many directions in which the monochromatic characteristic radiation is suppressed by Bragg reflection from planes which happen to lie at the proper angle. The curved network of lines (dark in the negative) is thus a graphical record of these directions of diminished intensity. They appear when the crystal is thick enough to provide absorbing material to give satisfactory contrast on the film, and when it is yet thin enough to transmit a considerable fraction of the primary characteristic radiation. The optimum thickness of a crystal will therefore vary from one experiment to another.

As an example of the application of this method of crystal analysis, Lonsdale's work on diamonds is of current interest. From a physical point of view, diamonds are of two kinds, which have been classified as type I and type II. Their characteristics, as determined by a variety of laboratory tests, are given in Table I.[2]

The only point which concerns us here is the quality of the divergent beam x-ray photographs which the two types produce. Upon finding that good type I diamonds gave poor photographs with fuzzy lines, and type II very good ones with sharp lines, Lonsdale suggested that this difference was attributable to a difference in crystal perfection, the perfect crystals giving poor divergent-beam photographs. In the language of the x-ray specialist, type I diamonds are characterized by strong primary extinction.

To put this in more descriptive language, let us suppose that divergent monochromatic x-rays of wave-length λ traverse a crystal which is geometrically perfect, a crystal in which every crystal plane is exactly parallel to others of the same kind, each separated from its neighbor by a grating space d. In a certain direction θ given by $\lambda = 2d \sin \theta$, a very small pencil of the divergent rays will not penetrate the crystal, but will be reflected. Now this process of reflection does not occur wholly at the first plane upon which the pencil of radiation falls. A layer of perfect crystal perhaps a few

TABLE I. Diamonds, natural and artificial.

Type I (relatively perfect)	Type II (mosaic)
1) Common.	Rare, in general.
2) Infra-red: absorbs at 8μ.	Transparent at 8μ.
3) Ultraviolet: absorbs beyond 3000A.	Transparent to 2250A.
4) Often perfect octahedra, with perfect surface.	Often lamellated.
5) Give streaks and triangles on Laue photographs.	No streaks or triangles on Laue photographs.
6) Bragg reflections of moderate intensity.	Bragg reflections very intense.
7) Divergent beam photographs with very blurred lines.	Divergent beam photographs with very sharp lines.
8) Slight photoconductivity.	Marked photoconductivity.

thousand planes thick is needed to suppress the pencil completely, or rather to turn it through 2θ to a new direction. This reflected radiation will, however, still fall on the same family of planes but from the other side at the appropriate angle for reflection, and will thus be reflected back into its original direction. The reflection, backwards and forwards among the members of one family of planes, will continue many many times until the radiation has traversed the crystal. Hence, a very considerable proportion of the original pencil of radiation which started at an angle θ will emerge from the other side of the crystal, traveling essentially in the same direction. It will be spread over a somewhat wider solid angle than it possessed at the beginning, but its general direction will still be θ. This radiation thus falls on the photographic film in a narrow region covering the place at which a suppression of the radiation might be expected, and instead of a line of diminished intensity, the film shows more or less uniform intensity distribution. In other words, the photograph is a poor one.

On the other hand, consider a crystal of mosaic structure. Here, a narrow pencil of radiation will be reflected at the angle θ by a tiny perfect crystallite, but this radiation, now traveling in a new direction, will not meet any planes in other crystallites at quite the correct angle to turn it back to its original direction. The orientations of the tiny crystallites of which the bulk is composed differ by enough to let the radiation, once deflected, traverse the crystal and emerge from it in a direction far away from the original one. Hence a deficiency of intensity in the direction θ is created, which is recorded satisfactorily on the photographic film.

To demonstrate that the absence of a clear divergent-beam photograph could be taken as an indication of crystal perfection, Lonsdale[3] first picked some organic crystals which gave poor pictures, then immersed them in liquid air for a few seconds. This harsh treatment would have the effect of straining the crystals violently, giving rise to somewhat less regular structures than before. Upon making photographs of the crystals after this treatment, it was found that the clarity and sharpness of the absorption lines were much improved. Lonsdale also calls attention to the necessity of allowing for primary extinction even in soft organic crystals when accurate analytical work is being done by x-ray methods. She finds, too, that large scale distortion of crystals can be detected by the blurring of some of the absorption lines in an otherwise good divergent-beam photograph. Such a large scale distortion affects a volume much greater than that of an elementary crystallite which is fundamentally characteristic of mosaic structure.

COSMIC RAYS

Papers dealing with cosmic rays occupy a larger and larger share of the pages of *The Physical Review*, not so much by reason of any great expansion of cosmic-ray programs, but rather because of the dwindling number of original papers on other subjects. Perhaps the most striking feature of these cosmic-ray researches is the great number of different particle-creating processes which they reveal. It is the secondary particles which are responsible for most of the ionization produced by cosmic rays in an unshielded ionization chamber. In the wealth of data which these papers present, and in the conclusions which their authors draw, it is easy to find many apparently contradictory statements. At the same time it is correspondingly difficult to tell a simple story of the latest discoveries. Without apology for the separation of the complicated phenomena (which are closely related) into three broad fields we shall give a brief account, first, of a recently developed theory of the penetrating component; second, of nuclear disintegrations demonstrated by cloud-chamber pictures; and third, of observations concerning the nature of showers made chiefly with counters and ionization chambers.

Although we may permit a Pooh-Bah who claims the right to many titles to enliven the scenes of comic opera, such ambiguous levity should not be allowed to clog the pages of scientific literature. The mesotron, *alias* meson, has by now justified its right to one universal name: Mesotron is used in this article, not for any subtle philological reasons, but merely in the presumptuous belief that the word falls more trippingly from an Anglo-Saxon tongue than the slightly halting meson.

Whatever we call them, mesotrons are something of an enigma. Born in the fields of nuclei, they hurtle through the atmosphere, blazing straight trails across cloud chambers, only to lose their identities in nuclear catastrophes or by radioactive disintegration a few millionths of a second later. Their tracks are difficult to recognize. Under some conditions they leave about the same trace as fast electrons; under others, they may be indistinguishable from fast protons. They

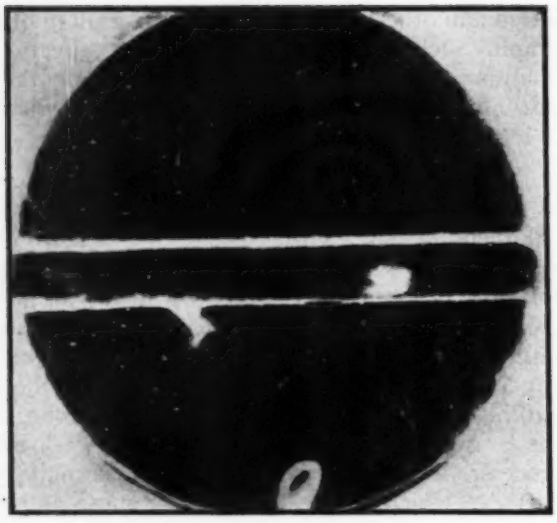

FIG. 2. Cloud-chamber photograph of a mesotron shower, showing three penetrating particles passing through a lead plate. The particles appear to have a common origin. Their slow divergence as they proceed downwards is a matter of current theoretical interest. [Reproduced from Phys. Rev. 64, 345 (1943).]

are generally believed to form the penetrating component of cosmic rays—a belief which has only occasionally been questioned.

Mesotrons have usually been observed singly, a fact which fits well with a theory of the production of these particles by the interaction of fast protons and neutrons, owing to Hamilton, Heitler, and Peng.[4] Only a bald outline of this theory can be given, based to a great extent on excerpts from a paper published in 1943.

The assumption is made that the primary radiation falling upon the earth's atmosphere consists of protons which produce mesotrons upon collision with nuclei after the fashion of the bremsstrahlung familiar to workers in x-rays. The energy of one of these protons is of great importance, there being a critical energy roughly equivalent to the mass energy of the particle, at which a startling change in the particle's behavior occurs. Denoting this critical energy by M, it is found that mesotrons created with energy $>M$ are all emitted in a forward direction, which is not true for mesotrons created with energy $<M$. The latter occur in significant numbers only near the top of the atmosphere.

The space-rate of loss of energy by protons of energy $\gg M$ is extraordinarily high. In 1 cm of lead a 3×10^9 ev proton ($3M$) loses two-thirds of its energy. This rapid drain on a proton's energy makes its range correspondingly small. A primary proton would need 7×10^{11} ev to be sure of penetrating the atmosphere and having energy M left at sea level. Since most primary protons do not have nearly such a large energy as this, the majority of mesotrons is born near the fringes of the earth's atmosphere. In creating a positively or a negatively charged mesotron, a proton must change to a neutron or a neutron to a proton in order that charge may be conserved. Since the primary radiation is assumed, with good experimental evidence, to consist of protons, the very process of creating positive mesotrons adds to the neutron population of the upper atmosphere.

After descending to energies of the order of M (10^9 ev), protons and neutrons lose their energy much more slowly than before. Thus there are many comparatively slow protons and neutrons in the high atmosphere. These are also mixed with protons produced by recoil processes, and with protons and neutrons arising from

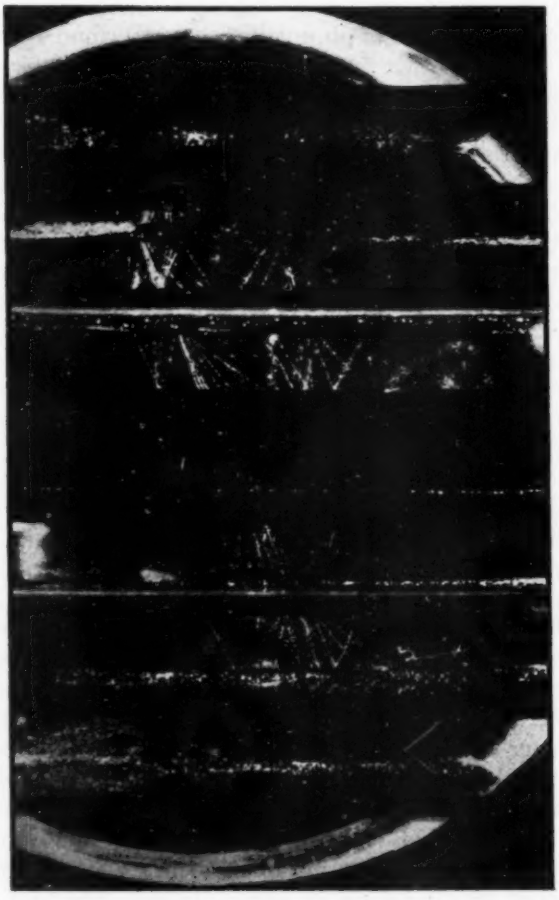

FIG. 3. Growth and decay of a cascade shower in lead. (Courtesy of W. E. Hazen.)

nuclear photoelectric effects. Most of the recoil particles have enough energy to produce only a few mesotrons.

Even near sea level there must be some fast protons having originally possessed energy in excess of 7×10^{11} ev, the energy necessary to penetrate the atmosphere. These particles are capable of creating several mesotrons in rapid succession, a phenomenon observed as a mesotron shower. Presumably the proton-neutron or neutron-proton switch in the identity of the primary particle occurs as the new mesotrons, alternately positive and negative, are created. There is also, however, a small probability that protons and neutrons not only create mesotrons one by one in succession, but liberate several simultaneously from the same disintegrating nucleus.

Mesotrons have been found to occur in large cascade showers, which are presumed to be initiated by very fast protons; the fast proton creates a mesotron which by decay produces an electron. All these particles have extremely high energies. The electron then starts the shower. Photons may also produce mesotrons according to the equation

$$\text{photon}+\text{proton}\rightarrow\text{neutron}+\text{positive mesotron},$$

though with a small probability compared with pair production of electrons by photons. At the maximum of a big shower, however, several thousand photons may be available, so that a few mesotrons should certainly be created. The mesotron-photon process, however, appears to be an indirect one, via an electron, so that the true cascade process, as it is understood of electrons, does not occur directly in the case of mesotrons.

During the last year, several photographs have been published which corroborate some of the details of this theory. Small groups of mesotrons have been observed appearing to diverge in a very narrow bundle from a common source. It is thus difficult to escape the conclusion that mesotrons may be produced in multiples perhaps more frequently than the theory suggests. Jánossy[5] discusses the theory and shows that within a certain range of energy of the primary particle, multiple collisions are likely to occur within a nucleus, which may therefore emit several mesotrons simultaneously. In a cloud-track photograph reproduced in Fig. 2, Jánossy recognizes a small, slightly divergent group of associated penetrating ionizing particles as mesotrons by the fact that in passing through a thick lead plate they produce no new particles. This is perhaps an over-statement, for Jánossy merely says that because of this behavior "they cannot be assumed to be electrons." Bose, Choudhuri, and Sinha[6] go much farther. Their picture of a narrow pencil of ionizing penetrating particles is captioned: "Wilson cloud chamber photograph showing production of mesons (*sic*) by a cascade process." This may be taken to imply that the Indian investigators consider that cascade processes involving mesotrons occur in the same way as cascade processes involving electrons occur. On the other hand, the difficulty[7] may merely be one of the interpretation of the phrase "cascade process." A true cascade shower of electrons is shown in Fig. 3.

Many experiments on the production of mesotrons cannot be analyzed immediately in the light of the theory which has been sketched above. In one of these, performed at Echo Lake and on top of Mount Evans by J. Tabin,[8] the production of mesotrons in different materials was investigated with the apparatus shown in Fig. 4. Single mesotrons were found to be created in paraffin, in aluminum, in iron, and in lead by non-ionizing primary radiation. Since the probability of occurrence in the various materials was found to be proportional to the cross section of the atomic nuclei it is certain that mesotrons in this case are created by nuclear processes. Furthermore, the mesotron-producing radiation was considerably absorbed by only 1 cm of lead, but could be detected below 60 cm of paraffin.

NUCLEAR DISINTEGRATIONS

A well-illustrated paper by Hazen[9] serves as a basis for this section. Thousands of photographs were taken of a Wilson cloud chamber, crossed at equal intervals of a few cm by eight lead plates, operated at 10,000 ft. in the High Sierras, far from the conveniences of a permanent laboratory (Fig. 5). The purpose of the lead plates in a chamber is merely to interpose in the path of the rays much more material than the gas of the chamber provides, thus increasing many fold the chance of observing interesting events. With these lead plates, the chamber was equivalent in stopping power to perhaps 2000 ft. of the atmosphere. Of course, the tracks of particles and their branchings cannot be observed in the plates but only in the intervening gas. However, allowances can be made in a statistical analysis of the results for the relative obstruction of lead and air, and fairly reliable conclusions may be drawn.

When a primary cosmic ray interacts with an

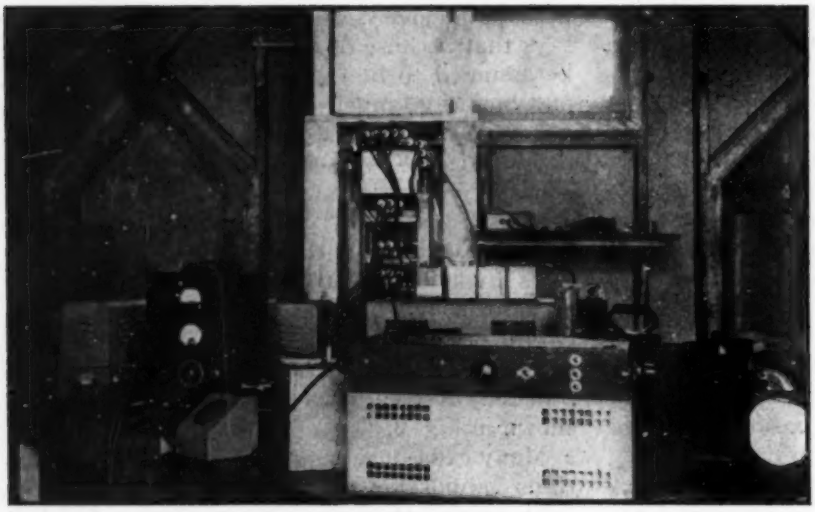

FIG. 4. Apparatus used by J. Tabin at Mt. Evans Laboratory, Colorado, to measure the production of mesotrons in paraffin. At the top is seen a thick layer of paraffin blocks, brightly illuminated by daylight which happens to be coming through the laboratory window (top right). Below the paraffin is a bank of Geiger-Mueller counters in a wooden frame. Almost in the center are four dry batteries on top of a voltage stabilizer unit. To the left of this are two coincidence units in light-colored boxes, half-hidden behind a black electrical control box. The case in the foreground contains the power supply. The location of the laboratory is shown in a picture in J. App. Phys. **14**, 62 (1943). (Courtesy of M. Schein.)

atomic nucleus in such a way as to disrupt it, a characteristic group of a few tracks, known as a star, is formed. Only when these stars by rare chance have their centers in the gas of the chamber can their component tracks be observed in their true relation. These disintegration stars, which have also been studied, although under certain handicaps, in the emulsion of photographic plates, are not to be confused with electron showers which contribute to localized bursts of intense ionization. The showers may contain thousands of particles, mostly electrons. The star tracks are broad and usually short, displaying the characteristics of heavy moving charged particles. In a few special cases,[10] individual stars have been the subject of considerable speculation. Hazen treats his 58 cases statistically.

On the assumption that the component tracks of a star are made by familiar particles, a tentative identification may be made by considering their linear ionization density, their change of ionization density as they approach the end of their range, or the scattering which they suffer as they move through matter. To these three criteria Hazen adds a fourth, a consideration of the tiny electron branches, or δ-rays, which are formed along the tracks. Of the 166 star tracks of range less than 0.7 cm of lead which Hazen observed,

FIG. 5. W. E. Hazen's cosmic-ray expedition entering Yosemite National Park en route to Tioga Pass. The load includes apparatus, knocked-down laboratory, power plant, living accommodations, and the cook. (Photograph and caption by W. E. Hazen.)

70 possessed the sparse ionization density characteristic of electrons or mesotrons, while the remaining 96 were much more massive, and could not have been electrons. Three of them were almost certainly α-particles. Of 80 star tracks with ranges greater than 0.7 cm in lead, twelve looked like electrons, three were α-particles, and the rest were probably protons or mesotrons. Four hundred other tracks starting simply from the lead plates without a visible cause were probably owing to nuclear fragments ejected from the lead by incoming neutrons. The tracks which constitute a star are thus mostly mesotrons and protons.

There remains the question of the nature of the rays which create the nuclear disintegrations. Some are ionizing particles, most are not. Hazen concludes that they are very seldom, if ever, electrons or photons, since they are not accompanied by cascade showers. Three possibilities compatible with the immediate evidence remain; neutrons, protons, and mesotrons. If mesotrons played an important part in the creation of stars, there should be a correlation between the increase in the frequencies of stars and of mesotrons with increase in altitude. Such a correlation is not observed. Therefore it seems probable that the ionizing primaries which produce nuclear disintegrations are protons, while the non-ionizing agents are neutrons. Most of the stars containing low energy components are produced by neutrons. Protons which produce disintegrations give stars with higher total kinetic energy. The two types of star are shown in Figs. 6 and 7.

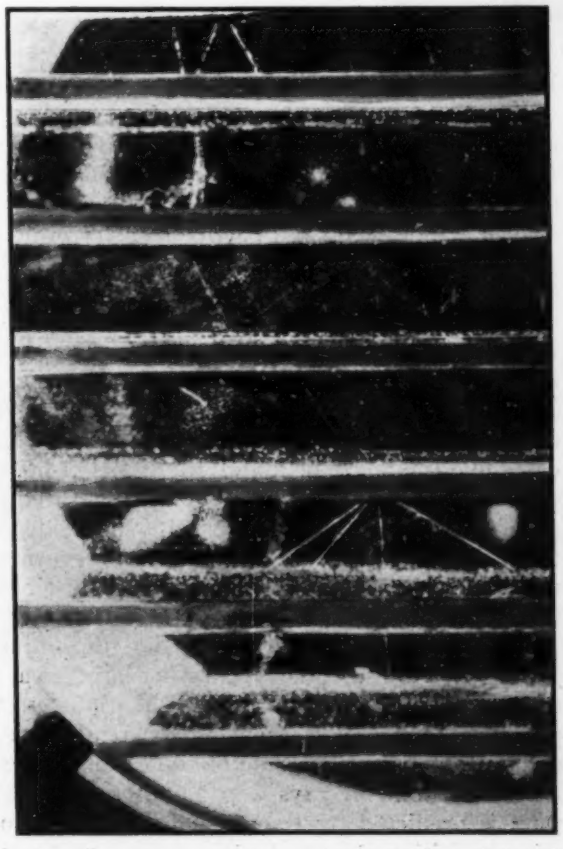

FIG. 6. A proton produces a nuclear disintegration in lead. The horizontal strips are 0.7-cm lead plates. (Courtesy of W. E. Hazen.)

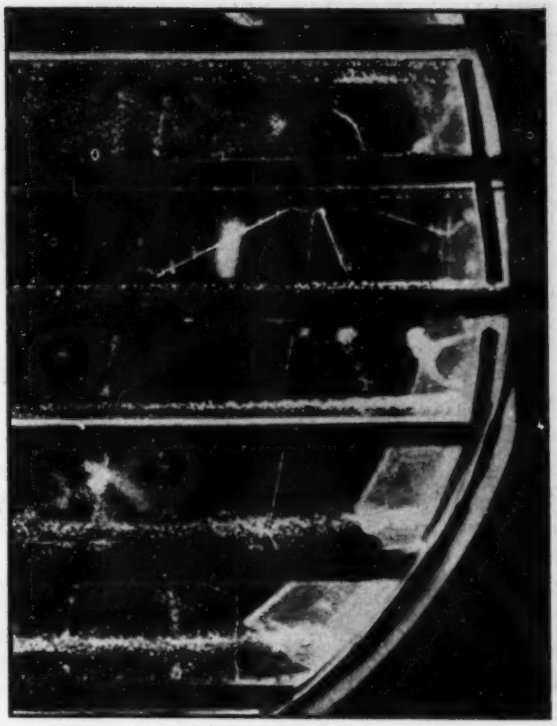

FIG. 7. A neutron produces a nuclear disintegration in lead. The horizontal bands are 0.7-cm lead plates. One of the star tracks is much more penetrating, and less heavily ionizing, than the other three. (Courtesy of W. E. Hazen.)

A theory propounded by W. Heitler[11] seems to be not inconsistent with these observed phenomena. He believes that nuclear disruption may occur in two ways. Either the nucleus retains the incident particle for a long enough time to distribute the excess energy more or less uniformly among the constituents of the nucleus, whereupon a few of the nuclear particles may be expelled; or else the process is a quicker one, involving only particles near the boundary of the

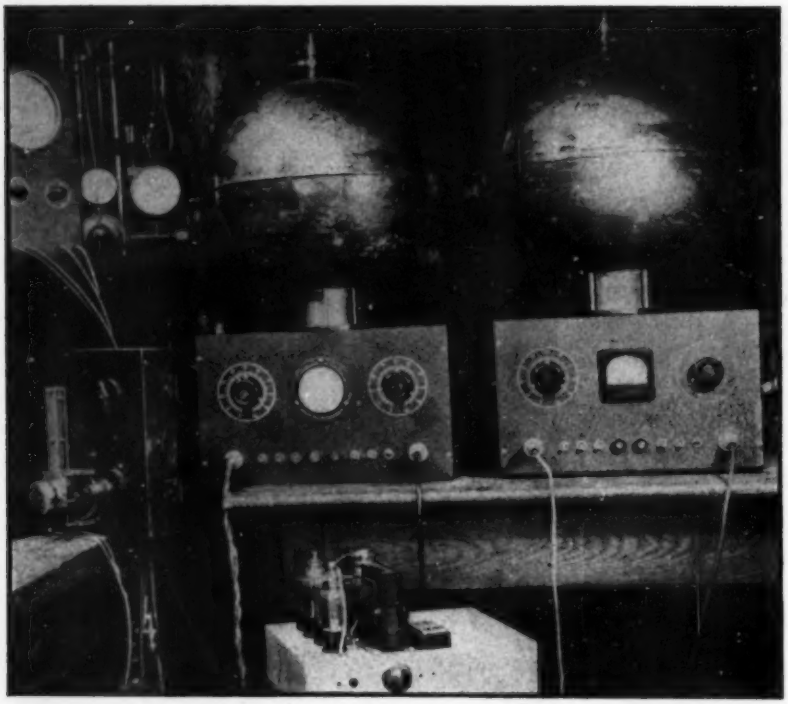

FIG. 8. Two large ionization chambers arranged to measure coincidences in bursts of ionization. (Courtesy of R. E. Lapp and M. Schein.)

nucleus, corresponding to a surface "heating." In the first case Heitler estimates that only 0.01 of the incoming energy may be carried away by the flying star particles, if the energy of the incident particle is 2×10^9 ev. Since Hazen finds that many of the stars he photographed possess a total energy considerably in excess of this fraction, he concludes that either the energy of the primary agents may be much higher than 2×10^9 ev, or the mechanism of the process may follow Heitler's second alternative. Of the relation of his observations to the cascade theory of the multiple production of mesotrons, Hazen says briefly that "none of the present photographs gives evidence for such a process."

ATMOSPHERIC SHOWERS

The most comprehensive and significant reports upon varied experiments with counters and ionization chambers during 1944 have come from the University of Chicago group. Their work deals mainly with the production, nature, and extent of atmospheric showers, and with the production of mesotrons. The method of investigating showers used by L. G. and E. W. Lewis[12] in one of their experiments consisted in observing coincidences between large bursts of ionization in two unshielded ionization chambers, such as are pictured in Fig. 8. It had been shown earlier by Lapp[13] that the large bursts in such chambers were coincident with wide Auger showers usually detected by Geiger-Mueller counters. By varying the separation of the ionization chambers it was discovered that the central core of an Auger shower sometimes had a particle density of 6000 per m^2. This high particle density extended only over the core of the shower, comprising an area of perhaps 100 m^2, whereas the whole shower, thinning out at the edges, may cover an area a hundred times as great. According to the generally accepted theory, each Auger shower is created by one primary ray, whose energy in cases like this must be about 10^{17} ev. It is interesting to note that the highest energy liberated in a single cosmic-ray event was, in 1937, considered to be about 10^{13} ev. In 1938 new observations raised this to 10^{16} ev; now it is one order of magnitude higher still.

While some of the showers, like those just described, were spread over a rather large area, a considerable number was found which possessed only a narrow spread, their cores extending one or two meters on each side of the center. These bundles of ionizing rays were far more compact than is predicted by the present-day theory of showers initiated by electrons, unless they were created not very far above the recording devices. There are, however, two objections to such an

interpretation; first, unshielded ionization chambers cannot be highly selective toward showers produced immediately above them, and second, the magnitude of the bursts seems to demand the presence of photons or electrons with energy higher than can be accounted for.

The experimental results are, however, in good agreement with observations made in the stratosphere by Auger, Rogozinski, and Schein.[14] In one of their balloon experiments, they sent aloft sets of counters spaced over a horizontal distance of 8 meters. The start of the flight and some of the details of the apparatus are shown in Figs. 9–11. By noting coincidences between various groups of counters, it was possible to tell how extensive were the showers of particles in the high atmosphere. The results showed that very few high density showers of large spread were present. High density showers were indeed observed, but they had a small spread, of the order of 1 m across the core, either because these showers were being recorded in an embryonic stage, or because the shower particles travelled in almost parallel directions.

THEORY OF COUNTERS

In experiments on cosmic rays or radioactivity, the word counter is used to describe a device which responds to the passage of single ionizing particles. In the original counter, known by the name of Geiger, a high electric field is maintained between a sharp-pointed needle and a metal envelope which surrounds it. This field, of itself, is hardly sufficient to cause a discharge between the point and the envelope, through the gas with which the counter is filled. But if an ionizing particle passes through the gas, enough ions are created to initiate an avalanche of ions which consititutes a pulse of current which (usually after amplification) actuates a mechanical recorder. In the last three decades, counters have been modified and developed, usually by empirical methods. The type most commonly used today, known as a Geiger-Mueller counter, consists of a thin wire stretched along the axis of a conducting cylinder. The thin axial wire takes the place of the point-electrode in Geiger's original design. Different experimenters have usually constructed counters following their own specifications as to size, contents, and activation technique. In many cases, extremely reliable counters have been developed; in others, the results have been disappointing, the counter characteristics varying in disconcerting fashion from one batch to the next, under apparently identical conditions of manufacture.

In the last few years, however, the processes occurring when a counter "fires" have been in-

FIG. 9. Start of a typical high altitude balloon flight from Stagg Field, University of Chicago, August 8, 1944. On this flight, the balloons carried apparatus to the stratosphere to measure the production of mesotrons in paraffin there. (Courtesy of R. E. Lapp and M. Schein.)

FIG. 10. Apparatus used by Auger, Rogozinski, and Schein taking off from Stagg Field, University of Chicago, June 13, 1944. The horizontal beam carries widely-spaced Geiger-Mueller counters to investigate the frequency of extensive cosmic-ray showers in the high atmosphere. The rectangular box in the middle of the beam is shown in more detail in Fig. 11. (Courtesy of R. E. Lapp and M. Schein.)

vestigated systematically, so that these Geiger-Mueller tubes can now be made to give predetermined performance characteristics of remarkable uniformity. Typical results of recent investigations which lead to better counter performance are contained in a series of papers by Korff and his colleagues at New York University.

The desirable characteristics of a counter vary with the job it has to do. Since most of the events recorded by counters occur at times which are distributed at random, it is necessary in the interests of accuracy that the counter be able to record separately two events which occur very close together in time. This requirement demands that the firing of the counter, the duration of the discharge, and the return of the counter to its waiting state be accomplished in as short a time as possible. Counters filled with simple permanent gases have the characteristic that once the discharge starts, it continues unless some scheme is employed to reduce the potential difference between wire and wall to a value below that which will sustain a discharge.

For this purpose a high resistance may be kept in series with the counter, or an auxiliary vacuum-tube circuit may be connected with it. Even so, the operation of such counters is comparatively slow. A faster quenching of the discharge can be accomplished inside the counter itself if the filler includes 5 or 10 percent of a polyatomic gas such as alcohol vapor. A group of experimental counters being prepared in this way is shown in Fig. 12.

Useful data concerning the effect of different proportions of alcohol in alcohol-argon counters (total pressure, 10 cm of mercury) have been published by Spatz.[15] His results deal with the variations in starting potentials, in flatness of plateaux, in permanence of initial performance characteristics, in useful life, and in total gas pressure which are caused by variations in the composition of the argon-alcohol filler. Simpson[16] has investigated methods of reducing the natural insensitive time of counters, caused by the positive ion space charge, by additional electronic circuits. We merely mention these before giving qualitatively the general theory which accounts for the quenching of the discharge by alcohol vapor inside fast counter tubes.

Since the quenching of a discharge involves the prevention of the formation of new carriers by whatever agency created, there are, as Korff and Present[17] point out, three important sources of electrons and ions to be considered. These are (a) photons in the initial avalanche, (b) collisions during the avalanche, and (c) secondary emission at the cathode. Owing to the recombination of argon ions in the counter, photons of energy between 11.5 and 15.7 ev are created. These, if they reach the wall or cathode of the counter, will be well able to liberate photoelectrons, since the photoelectric threshold of the cathode is only a few electron volts. The photoelectrons, driving toward a region of intense electrostatic field surrounding the axial wire, will create new ions by collision, and the discharge becomes continuous. Complex molecules like alcohol, however, have a peculiar ability to absorb comparatively large quanta of radiation and to convert them to other forms of energy which cannot contribute to a continuation of a discharge.

This excess energy of the excited alcohol molecules may cause their decomposition, as indeed

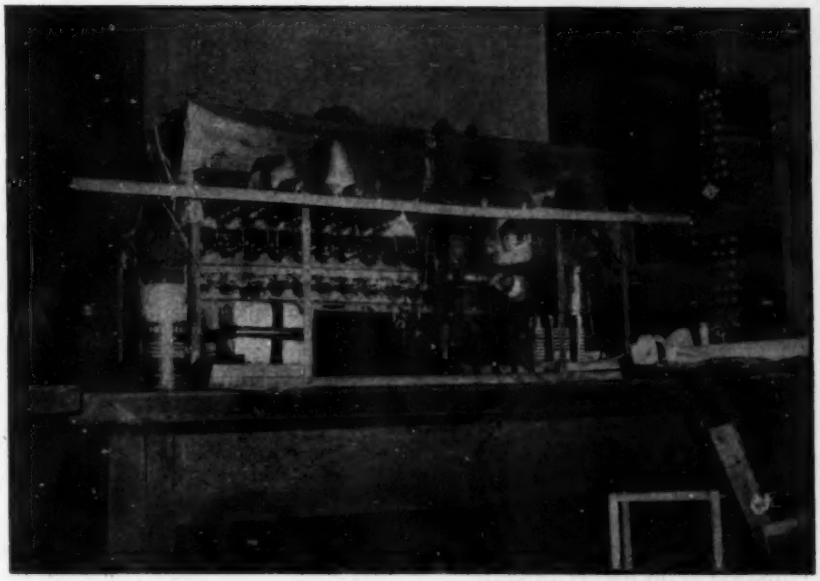

FIG. 11. Close-up of electrical circuits and automatic recording mechanism which are part of the apparatus supported by the balloons in Fig. 10. This was used by Auger, Rogozinski, and Schein in an investigation of the frequency of extensive showers of cosmic-ray particles in the upper atmosphere. (Courtesy of M. Schein.)

Spatz has inferred from the increase of pressure which accompanies prolonged use of counters; or the energy may be removed by molecular collisions, or it may be re-emitted as radiation. The time which is likely to elapse before this redistribution of energy is complete varies with the type of process. But that process will occur most frequently which is likely to take place in the shortest time. The last two processes are so slow (10^{-8} sec.) in comparison with the first (10^{-12} sec.) that they may be considered to play a negligible part in the redistribution process. A diatomic molecule, on the other hand, though it may absorb a photon as the polyatomic alcohol molecule does, has a good chance of re-emitting it in its entirety, so that the photon is not quenched.

A fast counter is normally operated in series with a comparatively low resistance, so that practically the full operating voltage is impressed continuously upon the counter. Were it not for the blanketing effect of a sheath of positive ions, there would always be a field around the central wire sufficient to cause ionization by collision. But as the positive space charge drifts towards the wall of the counter, it leaves behind it a space devoid of free electrons which could continue the discharge. However, if positive ions of the space charge, upon reaching the wall, liberate new electrons, the discharge will start again. An

FIG. 12. A bank of experimental Geiger-Mueller counters in process of manufacture. The counters are the vertical tubes at the bottom of the picture. Higher up are seen several spherical glass reservoirs of gas from which the counters are filled to a pressure determined by the mercury manometer on the left. (Courtesy of S. A. Korff.)

intermittent discharge would thus be set up in a pure argon-filled counter following the familiar continuous mechanism of an ordinary discharge tube. Alcohol or similar vapor apparently prevents the liberation of new electrons from the cathode in the following manner. As a polyatomic ion approaches the wall, its effect upon a metallic electron is first felt at a distance of perhaps 5×10^{-8} cm when the wave functions of the ionic and metallic electrons begin to overlap, and neutralization of the ion occurs at about this distance. Now the neutralized ion, under its own momentum, has still some distance to go, but its speed, though high, is not likely to carry it this small distance before it dissociates, which it will probably do in 10^{-12} sec. Thus, the neutralized excited polyatomic molecules usually never quite reach the wall before their energies are parcelled out among dissociation products, and secondary emission is no longer possible.

ARTIFICIAL DISINTEGRATION

What theoretical physicists who study atomic nuclei welcome most is accurate information concerning the behavior of light nuclei under a variety of conditions. When the structure and energy levels of a few simple nuclei have been worked out satisfactorily, there will be time enough to proceed with more complicated cases. The reaction $Li^7+H^1\rightarrow He^4+He^4+17$ Mev is therefore of great interest: The original nucleus is light; the projectile is the simplest available; and the products of the reaction are two identical particles. It is important to find out two things, how the number of alpha-particles per proton varies with the energy of the incident proton, and how the emitted alpha-particles are distributed in angle round the target in a plane which includes the proton beam. A good start was made on the problem about five years ago by Young, Ellett, and Plain, at the University of Iowa. Using protons of energy up to 400 kev, they found $I(\theta)$, the intensity of the alpha-particles as a function of angle of emission, to be well represented by an expression of the form $I(\theta)=1+A(E)\cos^2\theta$. Here θ is the angle between the direction of the incident proton and the direction of observation (in the center-of-mass coordinate system), and $A(E)$ is a function depending on the energy E of the proton. Although Young, Ellett, and Plain could not go to voltages high enough to prove the point conclusively, their observations suggested a maximum in the neighborhood of 400 kev for the function $A(E)$.

The matter was taken up next by Swartz, Rossi, Jennings, and Inglis[18] of the Johns Hopkins University, who published a report early in 1944. With their pressure-insulated Van de Graaff generator they were able to go as high as 900 kev. To make the obtaining of data less time-consuming than usual, they allowed the emerging alpha-particles to imbed themselves in photographic plates appropriately placed at various angles round a lithium target. Upon development, the tracks of the alpha-particles could be counted in the plates. Their results have confirmed those of the Iowa investigators as to the form of the function $I(\theta)$ but showed definitely that the maximum in $A(E)$ suspected earlier was spurious, and that a true maximum occurs at about 675 kev. Thus when observed values of $I(\theta)$ are plotted, for a particular value of E, against $\cos^2\theta$, they lie on a reasonably straight line. The slope of this line gives, at each separate voltage, the value of $A(E)$, which has a maximum at 675 kev. The symmetry which is implied by the proportionality of $I(\theta)$ to the square of $\cos\theta$ arises because the two alpha-particles resulting from the lithium reaction must of necessity be expelled in opposite directions.

The well-known fluorine reaction $F^{19}+H^1\rightarrow O^{16}+He^4+7.95$ Mev was also studied by Rossi and Swartz[19] by the same photographic plate technique. The observations were not, however, as straightforward as in the case of the lithium reaction, in which thin evaporated targets had been used. Relying on earlier results indicating that for the fluorine reaction the function $I(\theta)$ is reasonably constant for all values of E, and that $A(E)$ goes up very rapidly with increasing E, Rossi and Swartz felt that observations made with thick targets of CaF_2 would be reasonably simple to interpret, and would permit experiments to be done in a much shorter time than if a technique had to be worked out for making thin targets of some fluorine-bearing material.

Unfortunately it turned out that the earlier measurements of McLean, Ellett, and Jacobs led to a false conclusion regarding the constancy of $I(\theta)$ for all values of E. Rossi and Swartz found that for low values of E (330–435 kev), $I(\theta)$ is not describable by any simple function of θ. The angular distribution would, in any case, hardly be expected to show the symmetry which is characteristic of the lithium reaction. In addition, at low voltages, Rossi and Swartz were bothered by fogging of plates by undesired radiation from the source. Hence their data, at these low volt-

ages, are subject to considerable uncertainty. The general trend of the results, however, suggests a butterfly-shaped distribution, with a very low value at $\theta=180°$ and a maximum at about $\theta=50°$ or 60°. On the other hand, for all high voltages above 500 kev, the distribution is different. A plot of $I(\theta)$ against $\cos\theta$ shows definite maxima and minima which appear to be trustworthy on account of the much better experimental conditions. The angular distribution, indeed, possesses an unexpected suggestion of symmetry, with maxima at $\theta=0°$, 90°, and 180°, and with shallow minima between. It is obvious from a glance at the published graphs that the case of lithium is a much simpler one than that of fluorine.

The lithium reaction has been discussed by Eisner[20] in the light of these new results and in the light of existing theories. Using a variety of assumed nuclear potentials he calculates the corresponding proton penetration factors which are closely related to the yield of disintegration products from the reaction. The results of his calculations are rather inconclusive. They show, however, that the maximum of $A(E)$ which is observed occurs independently of the details of the nuclear model used, provided a repulsive force field is met at about 4×10^{-13} cm from the center of the nucleus. To make further progress, it is necessary to know the trend of the function $A(E)$ as it approaches the value zero after passing through its maximum; that is, whether it approaches zero asymptotically or with a finite slope. To settle this point, measurements are required at much higher energies than have yet been used. A waiting period of a few years is certainly to be anticipated.

MAGNETIC LENS SPECTROMETER

Information concerning nuclear energy levels is obtained from a study of the particles emitted by a disintegrating nucleus. When the particles are heavy, they can be studied well in a cloud chamber, since their tracks are short, strong, and straight; but when electrons are given out, this technique no longer suffices, for electrons produce tracks of comparatively light ionization, and so tortuous that the track length, and hence the energy of the particle, are hard to estimate. Recourse must be had to some type of electron spectrometer, operated under vacuum conditions. A magnetic field can be used to separate particles of different energies and their relative numbers may then be measured by photographic or electrical means. The desirable characteristics of such an instrument, as of an optical spectrometer, are high resolution and high intensity. It usually happens that it is difficult to secure both these characteristics under the same conditions.

Until electron optics became a recognized branch of physics, the standard electron spectrometer employed semicircular focusing of the particles emitted from a fine wire source, or from a narrow slit. This was the electrical counterpart of the prism spectrometer. If the prism is made with cylindrical symmetry, that is, essentially in the shape of a lens, the instrument becomes an optical focal isolation spectrometer, which depends for its functioning on the chromatic aberration of the lens which is used. Translating this into electrical terms, a focal isolation electron spectrometer is a single magnetic lens which has different focal lengths for electrons of different energy.

An instrument[21] of this kind, though not the first of its type to be constructed, has been in use for a few years at the Massachusetts Institute of Technology, where it has aided in studies of the energy levels of radioactive nuclei. The "thin" magnetic lens is actually a 300-lb. circular coil of square cross section with the following dimensions: inner radius 9.6 cm; outer radius, 25.6 cm; axial length, 16.0 cm. No. 12 copper wire is used. The focal length for electrons of 3.5 Mev is 25 cm; when the power expenditure is 2 kw. Through the center of the coil runs a brass tube, about 7.5 cm in radius, and 1 meter long. On its axis, at one end, the substance whose electron emission is to be studied is inserted; at the other, an electrical counter is placed. Some of these details are visible in Fig. 13. When the tube is placed symmetrically with respect to the lens, the source and counter corresponding to the object and image in the optical case are both equidistant from the lens. The magnification is unity and the distance from source to counter is four times the focal length. The central tube is, of course, evacuated.

If the adjustments are made so that electrons of definite momentum whose trajectories all lie near the axis are focused correctly, then it is found that the same conditions bring to the same focus faster electrons whose trajectories reach out nearly to the walls of the central tube. This is a consequence of spherical aberration. The difference in momentum for electrons near the axis and at the periphery of the lens is nearly 10 percent. The aperture of the lens must therefore be cut down, and for the sake of high intensity it should

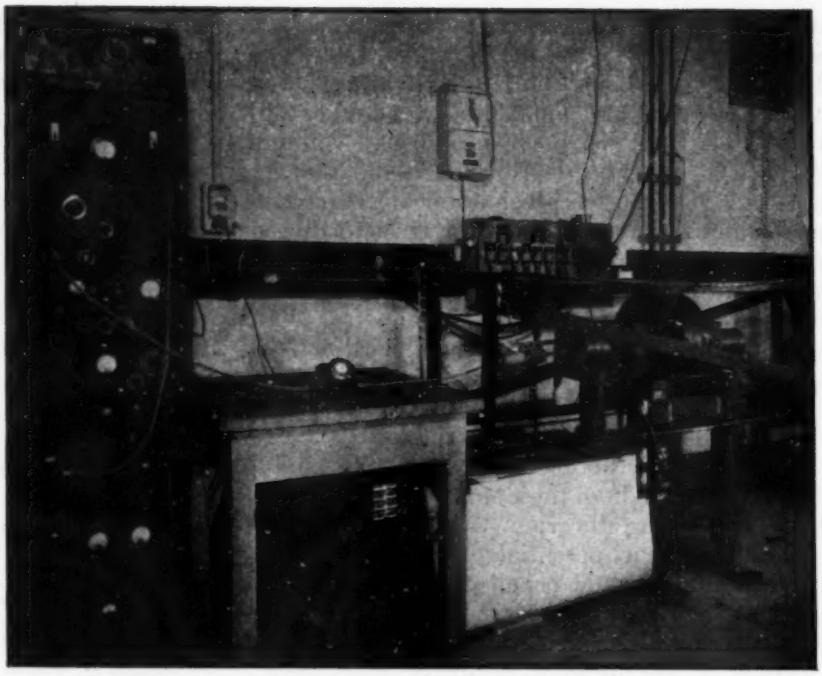

FIG. 13. The M. I. T. magnetic lens electron spectrometer. At the right, immediately below the three parallel vertical pipes on the wall, are seen the cylindrical evacuated deflection chamber and the magnetic lens. These units are centered in a set of rectangular Helmholtz coils which annul the earth's magnetic field. At the left is the control panel for all circuits, together with single and coincidence counter amplifiers and pulse scaling circuits. The motor generator is under the table. (Photograph by M. I. T., courtesy of R. D. Evans.)

be blocked out where the least area is sacrificed, that is, near the center of the lens.

To indicate the nature of the considerations which enter into the design of the instrument, we quote some of the arguments of Deutsch, Elliott, and Evans[21] concerning the dimensions of the coil. They give an equation for the product of the amount of copper M and the power H which reads $H \times M = K 4\pi^2 \bar{a}^2 (\rho/\sigma)(\bar{a}/t)(t/f) p_0^2$ where K is a constant depending on the shape and size of the coil, ρ and σ are the density and conductivity, respectively, of copper, $\bar{a}$ is the mean radius of the coil, f is its focal length for electrons of momentum p_0, and t/f is its numerical aperture. Now the power which can be dissipated is proportional to the surface area of the coil for any given design, making $H/\bar{a}^2$ constant. At the same time, the mass of copper is proportional to $\bar{a}^3$, so that, for the same design $M/\bar{a}^3$ is constant. The product HM can therefore be written as $HM = A\bar{a}^5$, with A constant for any one design. If $\bar{a}$ be made too small, either the amount of power or the amount of copper will be too small to give the desired performance. By combining the equations quoted, the minimum value of $\bar{a}$ is found to be $\bar{a}^3 = 4\pi^2 K A^{-1} (\rho/\sigma)(\bar{a}/t)(t/f) p_0^2$. Electron-optical considerations show, however, that only a certain value of $\bar{a}$ is needed for a source of a specified diameter, so that if $\bar{a}$ from the last equation turns out to be larger than this, there are two alternatives, either changing the design of the lens or making a lens coil larger than would otherwise be required. The value of A could be increased by more efficient cooling, thus reducing the necessary value of $\bar{a}$, but the improvement which can be achieved by this method is rather limited. To achieve a significant reduction in $\bar{a}$, therefore, the last resort is to reduce K, which can be done by strengthening the field by the use of iron. But this brings in its train many difficulties affecting the linearity of the calibration and the extent of spherical aberration.

One of the advantages of this spectrometer is its versatility in that it can be adjusted for high intensity or high resolution as desired. It is, therefore, possible to use it for the study of continuous β-ray spectra, or for a study of line intensities; it possesses distinct advantages when coincidence studies have to be made to determine the order in which successive nuclear events take place; and it can be adapted nicely for a study of gamma-rays by measuring the energies either of photoelectrons or of Compton recoil electrons. This new instrument will not displace the older type when strong sources are available, but it will be of the greatest value in exploratory work which is not within the range of the semicircular-focusing electron spectrometer.

NEWTON'S RINGS

Tolansky[22] has published some observations on Newton's rings which promise to change a traditional laboratory demonstration into an instrument of startling precision. In the usual arrangement, interference occurs between two beams of light, one reflected from the top, the other from the bottom, of a thin film of air. The lag of one beam behind the other is at most a few dozen wave-lengths. To obtain the highest resolution in any optical instrument it is necessary to produce interference between beams whose paths differ by as many wave-lengths as possible. This condition is achieved in Tolansky's method by the simple expedient of using, not plain surfaces (say of glass), but surfaces which have previously been coated with thin reflecting layers of silver. These coatings are thick enough to be strongly reflecting, yet thin enough to allow an incident or emergent beam to be partially transmitted. Reflection may therefore occur a great many times in the air film, with a consequent increase in the order of interference. To obtain the sharpest definition, it is necessary to restrict the incident light to a single angle of incidence by employing a small source at the principal focus of a lens. According to Tolansky, this multiple beam interference technique used at normal incidence possesses the following features of superiority over the two-beam standard technique. (1) The fringes are much more intense. (2) They are so sharp that very high precision in measurement can be obtained. A change of 0.01 of an order can be measured with an accuracy of about 5 percent. This corresponds to measuring a displacement of the optical components amounting to 25A with an error of $\pm$1A. (3) The fringes are so sharp that fine-scale defects and irregularities on the glass surfaces are reproduced as detail in the fringes.

Many applications of practical importance will undoubtedly occur to the reader. One which has already been made is the examination of natural crystal faces. In the photographs which are reproduced in *Nature*,[23] imperfections of the faces stand out clearly. Portions of a large surface which deviate even a small fraction of a minute of arc from the general level can be picked out. The boundaries between small areas of differing orientation are sharply visible in spite of the covering of reflecting material. It will be interesting to compare data obtained by this method and those derived from electron microscope pictures of the surfaces of metallic crystals. Tolansky states that the experimental arrangements are critical, though in what respects no information is directly available in the publications upon which this brief account is based.

LOOKING AHEAD

As the war draws towards a close, several general problems of importance to all physicists will present themselves for solution. Some of these have already been considered elsewhere; they are mentioned again in the hope that the interest of as wide an audience as possible may be focused on them.

Now that physicists have their own national headquarters at 57 East 55 Street, New York, the organization of the various societies and of the profession as a whole should be reviewed. As matters stand at present, an individual is a member of one or more societies which are, in turn, members of the American Institute of Physics. But there is no one organization which embraces all physicists as individuals. The advantages and disadvantages of this state of affairs were considered by a group of some fifty physicists representing all branches of the profession at a conference held under the sponsorship of the National Research Council in the Philosophical Society's chambers at Philadelphia in May, 1944. Among the frank discussions which characterized the meetings, several important suggestions were made which will serve as tentative lines of approach toward a more satisfactory organization than exists at present.

There is no doubt that the number of men and women classed as physicists has increased during the last three years. There is good reason to believe that the demand for their services will continue to increase when once again we live at peace. Not only are industrial organizations keenly aware of the specific value of research in physics, but colleges and universities expect a general increase in enrollment quite apart from the temporary gains which will accompany any partial demobilization of the armed forces. Whatever the level of instruction in physics, expert physicists will be required in greater numbers than before. Colleges and universities may find themselves more than ever in competition with industry and with research foundations for the most able men.

If the scientific professions are to attract the best brains, their rewards must from the very beginning be just. Most physicists have gone through an apprenticeship as graduate assistants in universities and must be aware of the diffi-

culties of living on an inadequate income. The problem is one for all branches of science. A steady investment of effort aimed at raising the average stipend of graduate assistants to the level of a young person's living wage would pay rich dividends. This is the level at which the profession now runs the greatest risk of losing good recruits.

At a higher stage in the development of the physical scientist there are clear signs that the need of providing encouragement and adequate rewards for promising research talent is being recognized. One of these welcome signs is the establishment by the American Telephone and Telegraph Company of the Frank B. Jewett fellowships in the physical sciences for post-doctoral study and research. An unusual feature of the fellowships guarantees the payment of a grant to the institution which plays host to the investigator.

There appeared in the October, 1944 issue of *The Review of Scientific Instruments* a thoughtful editorial which advocates setting up, after the war, fellowships for research in military and naval science. Anyone who has read the special number of the *Journal of Applied Physics* (March, 1944) devoted to research in the Navy will realize that the services offer wide opportunities for pure as well as for applied research. The creation of fellowships of this type would go a long way toward preventing any large part of the research in pure science which has been fostered by the war from being locked up unproductively for years in confidential files.

ACKNOWLEDGMENTS

The writer is pleased to have this opportunity of thanking the scientists who have helped him by lending photographs, especially Dr. Marcel Schein who also gave him permission to use some results which were in process of publication while the present article was being written. He has profited from friendly discussions with his colleagues at Michigan State College and is particularly indebted to Dr. J. W. McGrath, Dr. C. Kikuchi, and Mr. A. R. Laufer who read parts of the manuscript and made valuable suggestions for improving its clarity.

REFERENCES

(1) K. Lonsdale, Nature **151**, 52 (1943).
(2) K. Lonsdale, Nature **153**, 669 (1944).
(3) K. Lonsdale, Nature **153**, 433 (1944).
(4) J. Hamilton, W. Heitler, and H. W. Peng, Phys. Rev. **64**, 78 (1943).
(5) L. Jánossy, Phys. Rev. **64**, 345 (1943).
(6) D. M. Bose, B. Choudhuri, and M. Sinha, Phys. Rev. **65**, 341 (1944).
(7) G. D. Rochester, Nature **154**, 399 (1944).
(8) J. Tabin, Phys. Rev. **65**, 64A (1944).
(9) W. E. Hazen, Phys. Rev. **65**, 67 (1944).
(10) M. Sinha, Nature **152**, 568 (1943); M. Goldhaber, Nature **153**, 221 (1944).
(11) W. Heitler, Phys. Rev. **54**, 873 (1938).
(12) L. G. Lewis and E. W. Lewis, Phys. Rev. **65**, 346A (1944); K. L. Kingshill and L. G. Lewis, Bull. Am. Phys. Soc. **19**, No. 5, 9 (1944).
(13) R. E. Lapp, Phys. Rev. **64**, 129 (1943).
(14) P. Auger, A. Rogozinski, and M. Schein, Bull. Am. Phys. Soc. **19**, No. 5, 9 (1944).
(15) W. D. B. Spatz, Phys. Rev. **64**, 236 (1943).
(16) J. A. Simpson, Jr., Phys. Rev. **66**, 39 (1944).
(17) S. A. Korff and R. D. Present, Phys. Rev. **65**, 274 (1944).
(18) C. D. Swartz, H. H. Rossi, B. Jennings, and D. R. Inglis, Phys. Rev. **65**, 80 (1944).
(19) H. H. Rossi and C. D. Swartz, Phys. Rev. **65**, 83 (1944).
(20) E. Eisner, Phys. Rev. **65**, 85 (1944).
(21) M. Deutsch, L. G. Elliott, and R. D. Evans, Rev. Sci. Inst. **15**, 178 (1944).
(22) S. Tolansky, Nature **153**, 314 (1944).
(23) S. Tolansky, Nature **153**, 195 (1944).

Small Prism Infra-Red Spectrometry

R. BOWLING BARNES, ROBERT S. MCDONALD, VAN ZANDT WILLIAMS
Stamford Research Laboratories, American Cyanamid Company, Stamford, Connecticut

AND

RICHARD F. KINNAIRD
The Perkin-Elmer Corporation, Glenbrook, Connecticut

A NUMBER of articles describing the application of infra-red spectroscopy to problems of chemical research and analysis have recently appeared. In almost all of these the experimental results discussed were obtained through the use of spectrometers built according to the individual designs of various spectroscopists. This situation may present certain difficulties for those people who desire to undertake work in this field. Thus, while the research worker who is unfamiliar with the past history of infra-red spectroscopy may survey these recent papers and fully realize that this technique offers many advantages in connection with his work, he may at the same time become confused by the bewildering array of spectrometers, which vary so widely as to size, optical paths, dispersing agents, and methods of signal detection and amplification. He is offered little fundamental information regarding the reasons for the differences in instrument construction. He is offered few criteria as to the optical dispersion and resolution or as to the degree of sensitivity and reproducibility of spectral characteristics which must be met by an instrument in order for it to be satisfactory for the particular chemical applications desired. Since only the successful applications are published, it is also difficult for the reader to know the limitations of the various spectrometers. Although these criteria and limitations may be derived by a careful study of the published results, he still has little idea of the size spectrometer or the order of optical or instrumental precision required to achieve experimental results of the required quality.

In partial answer to this problem we should like to describe, and present experimental data from, a small all-purpose infra-red spectrometer* which has been developed recently. The theoretical and experimental resolution obtainable with this instrument throughout the near infra-red is discussed. The relative merits of various prism materials are illustrated as well as the over-all performance of the instrument under several conditions of use.

THE SPECTROMETER

A view of the completely housed spectrometer is shown in Fig. 1, and a similar view with the covers removed is shown in Fig. 2. Its compact, sturdy design (31″×12″×9″) and light weight (100 lb.) permit small housing space and mobility if operation at various sites is desired. The base is normalized cast iron and the covers are cast aluminum.

The optical path of the spectrometer is shown in Figs. 3 and 4. Infra-red radiation from the source *G* is reflected by the plane mirror *Mi* to the spherical mirror *Mii* which focuses the beam on the entrance slit *Si*. The radiation from the slit is collimated by the 18° off-axis parabola *Miii* onto the prism *P* and the Littrow mirror *Miiii*. The returning beam from *Miiii* is focused by *Miii* and the offset mirror *Mv* onto the exit slit *Sii*. The combination of the plane mirror *Mvi*

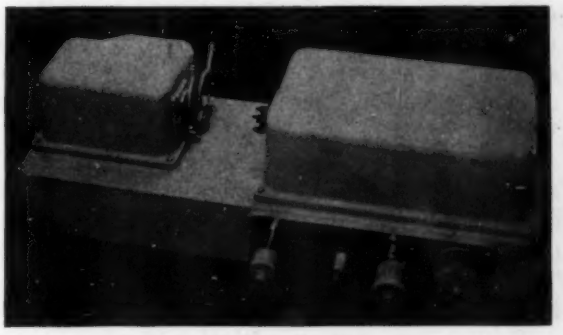

FIG. 1. Small prism infra-red spectrometer.

* The Perkin-Elmer Infra-Red Spectrometer Model 12A, manufactured and sold by The Perkin-Elmer Corporation, Glenbrook, Connecticut.

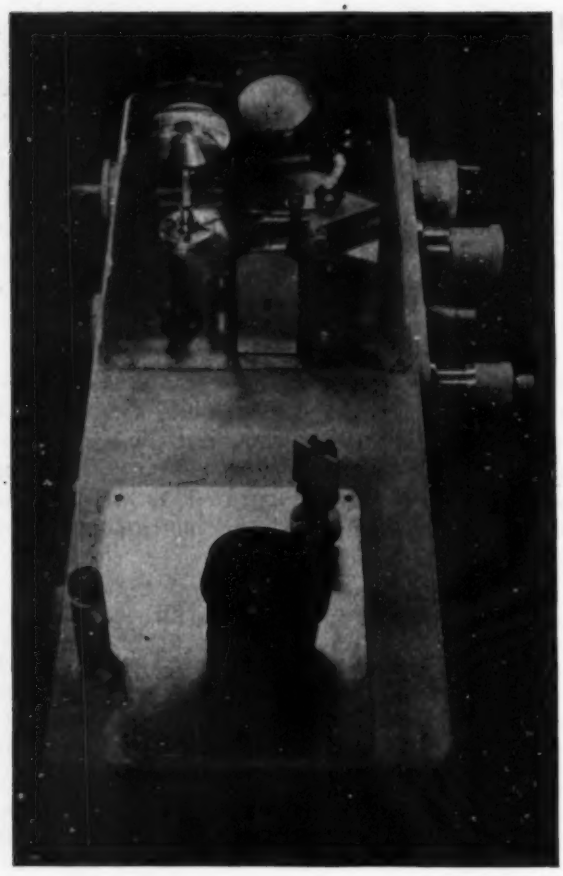

FIG. 2. Spectrometer with covers removed.

and the spherical mirror *Mvii* focuses an image of the exit slit on the thermocouple *Tc*. The current from *Tc* is measured by a galvanometer system. The focal length of the collimator is 27 cm and its effective aperture is f:4.5. The overall optical path length is 195 cm.

The source *G* is a Globar (average life, 6 weeks) 2″ long by $\frac{3}{16}$″ in diameter mounted in a water-cooled jacket which permits easy replacement of units. Silver-to-silver contacts ensure electrical stability. The source consumes about 250 watts at 50 to 60 volts a.c. and can be run off a standard voltage regulator and Variac.

The slits *Si* and *Sii* are 12 mm high, bilateral, and simultaneously operating. The slit width is controlled by the slit micrometer *Ms* which reads directly in microns (1/1000 mm) from 0 to 2 mm. The entrance slit is curved to compensate for image curvature introduced by the prism.

The most important optical part of the spectrometer is the accurately figured off-axis parabola *Miii*. Because the spectrometer dimensions are small, critical focusing adjustment is necessary. For example, rotation of the parabola about its axis by 2° from critical focus or translation by a fraction of a millimeter are sufficient to cause pronounced loss of resolution. For this reason, all the mirror mounts are sturdy but flexible in control. They permit rotation and translation with respect to the mirror axis, and tilt about horizontal and vertical axes.

The prism *P* is mounted on an individual spectrometer table which may be removed and locked back in place accurately. Thus rapid interchange of prisms allows work in any region of the spectrum for which sources and detectors are available.

Automatic temperature compensation *D* which may be adjusted for an arbitrary prism material and wave-length is provided.

Frequency (wave-length) setting is controlled by the specially designed micrometer barrel *Mw* which will rotate the Littrow mirror *Miv* through 9° over a normal range of 2000 divisions.

For analytical work at predetermined frequencies, a turret stop mechanism *T* is provided. The adjacent plunger *Tr* disengages the Littrow mirror lever arm and the turret may be rotated readily to any one of six adjustable stop positions.

In order to eliminate continual pumping, the thermocouple vacuum is maintained for a period of months by a charcoal trap. However, the thermocouple mounting *Tc* is provided with a standard tapered joint for use if any operator desires to attach a pumping system directly. The detector itself consists of two opposed thermal elements of which one measures the radiation passing through the spectrometer and the other corrects for ambient temperature changes. (The bismuth, bismuth-tin thermocouples, made by Dr. Donald F. Hornig, have a receiver area 4 mm×0.6 mm, a sensitivity of about 0.4 μv/erg/sec., and a period of about 1 sec. The two junctions are compensated to better than 5 percent.)

The optical parts, except for the source, are enclosed in the two covers which may be rendered airtight for removal of atmospheric absorption. The space between the housings permits easy access to the radiation beam for the introduction of solid or liquid samples, or vapor cells *C* up to 10 cm in length. Where longer absorption paths are necessary for gas studies, the smaller housing is tapped for inlet and outlet tubes and can be made airtight to provide an additional

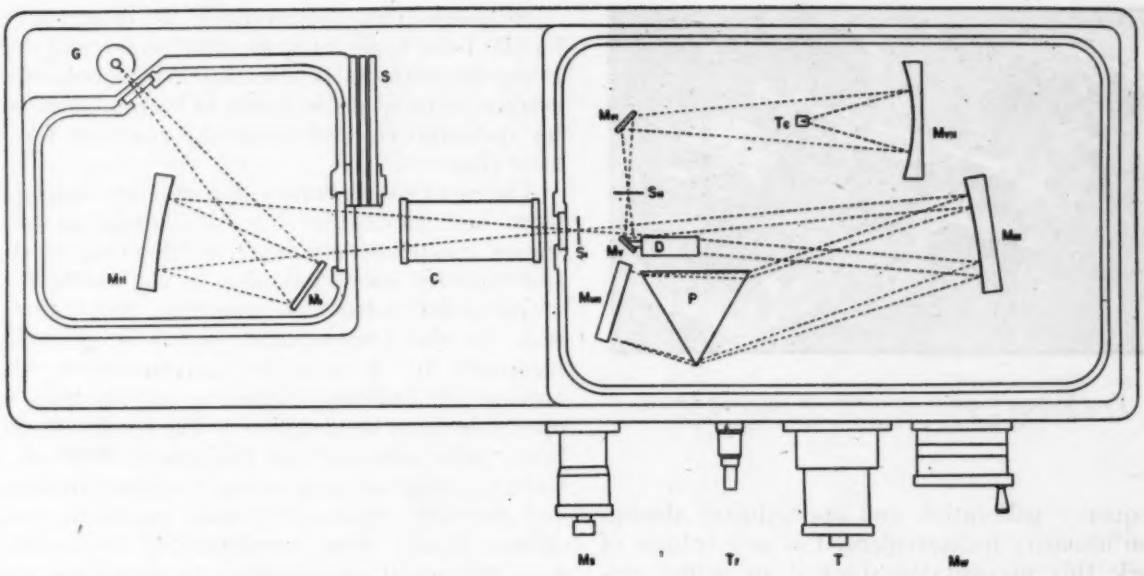

FIG. 3. Schematic optical path of small prism spectrometer. *C* is sample cell; *G*, global source; *Mi*, *Miiii*, *Mv*, *Mvi*, flat mirrors; *Mii*, *Mvii*, spherical mirrors, *Miii*, off-axis paraboloid; *Ms*, slit micrometer; *Mw*, wave-length micrometer; *P*, prism; *S*, shutters, *Si*, entrance slit; *Sii*, exit slit; *T*, turret drum; *Tr*, turret release; *Tc*, thermocouple; and *D*, temperature compensator.

40-cm absorption path. The three shutters *S* allow for various shutter and filter materials to be used alone or in combination. All the controls are very legible and grouped on a single panel board where they are convenient to the operator. The construction is such that the spectrometer proper and its controls are a unit occupying about half the base. For special work—emission, study of a catalytic process *in situ*, etc.—the other half may be cleared off to permit the addition of special equipment.

The shaft of the micrometer barrel *Mw* is brought out the rear of the spectrometer so that a motor may be coupled to give a continuous drive for automatic recording and calibration. This can be done simply as shown in Fig. 5. A small 1/75 hp motor, coupled to the shaft through a gear shift drive, permits variable scanning speeds. Fiducial calibration marks are attained by means of a studded disk on the micrometer shaft. Upon rotation, the studs open and close a microswitch, which charges and discharges a condenser. The discharge through a solenoid moves the recording pen sharply, superimposing a mark on the curve. These marks can be numbered to correspond with micrometer readings and calibrated against frequency.

DISCUSSION AND PERFORMANCE

In general, the present-day applications of infra-red spectroscopy may be divided into two categories, qualitative and quantitative. The particular problem determines the qualifications which a spectrometer and its accessory equipment should possess and the experimental techniques which should be used.

Qualitative work includes such applications as the identification of characteristic atomic groups and unknown materials, structure studies (isomerism, tautomerism, association), and rough analyses or purity determinations from visual comparison of absorption spectra. Such studies usually require a complete survey of the infra-red spectrum at high resolution with fairly accurate

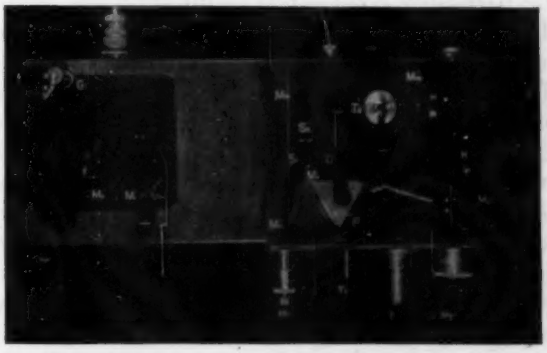

FIG. 4. Top view of spectrometer.

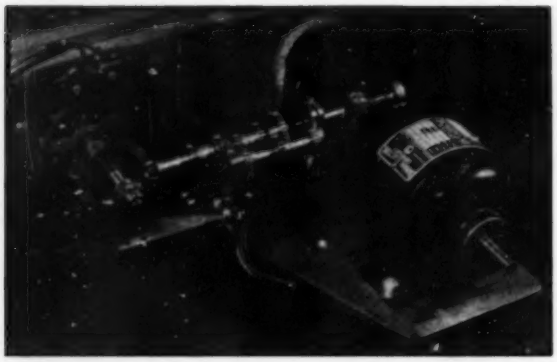

FIG. 5. Rear view of spectrometer showing motor coupled for automatic recording.

frequency calibration and approximate absorption intensity measurement. For any volume of work this necessitates spectral recording employing both high amplification and automatic record calibration. The speed in obtaining this complete spectrum is attained at some loss of repetitive accuracy.

Quantitative measurements require very accurate repetition both of frequency setting and of intensity measurements. At present this accuracy is attained at some loss of either analytical speed or spectral resolution. If analysis at high resolution is desired, several measurements are necessary for accuracy. If speed is desired, wide slits (hence poorer resolution) are necessary to give enough energy for precise single measurement and to minimize the effects of errors in frequency setting. These analyses are usually performed at a few predetermined frequencies and measurements are often made by visual observation of the deflection of a single galvanometer. Automatic recording is not an absolute necessity if sufficient data regarding the particular compounds in question are available in the literature to permit a choice of analytical frequencies. If the data are not available, a necessary preliminary step to analysis is the recording of the complete spectra of the various materials thought or known to be present in the unknown mixture so that a choice of the best combination of analytical frequencies can be made. Moreover, unless the analysis is exceptionally routine, it is often useful to obtain rapid spectral surveys to ensure that no new material is appearing in the process or to determine the approximate concentrations of the components.

Although this spectrometer is designed to handle both types of work, this paper will deal primarily with its potentialities for qualitative studies, a detailed discussion of its qualifications for quantitative analysis being reserved for a later time.

The repetitive accuracy of frequency measurement and absorption intensity under spectral survey conditions are functions not only of the spectrometer itself, but also of the method of amplification, automatic recording, and calibration. As the thermocouple signal is generally measured by a sensitive galvanometer, the amount of building vibration at the site of operation must be considered. The results shown below were obtained on the fourth floor of a building adjacent to a heavy trucking highway and probably represent average operating conditions. Under these conditions, it is possible with this small spectrometer to determine the frequency of the center of a sharp absorption band to ± 2 cm^{-1} with careful measurement and to repeat to ± 5 cm^{-1} with routine recording. The absorption deflection repeats to ± 5 percent under normal operating conditions of marking shutter zeros at the beginning and end of each sectional run and assuming a linear galvanometer zero between.* These criteria are not difficult to attain and depend largely on the care exercised by the operator in repeating spectrometer and amplification settings.

However, the criterion of the resolution, or spectral slit width, necessary to conduct research infra-red spectroscopy requires more discussion as it is the determining factor in deciding the size and cost of the spectrometer. Again there is no absolute way of deciding this condition and the writers can only give an opinion based on some years of experience in the field. Inasmuch as the natural width of a vibrational band of the average size molecule encountered is rarely less than 5 cm^{-1}, two such bands occurring about 7 cm^{-1} apart would not be very clearly defined, if a spectral slit width of 5 cm^{-1} were to be used. Therefore, it is probably safe to say that almost all industrial research could be conducted if a

* This figure of ± 5 percent may seem excessive for careful work. Such an error may occur in routine recording if galvanometer drift should occur in that portion of a sectional run where the energy is low. If that portion is of importance, the error can be greatly reduced by shortening the range between zero markings. Where extreme accuracy is desired, the spectrometer may be set at a fixed wavelength and transmissions measured to better than ± 0.5 percent.

spectral slit of 3 cm^{-1} could be achieved throughout the spectrum from 4000 cm^{-1} (2.5μ) to 500 cm^{-1} (20μ). At the present stage of prism spectroscopy, this is difficult to attain. Fortunately, the cases where such extreme resolution is necessary are rare. In our experience, better than 95 percent of the work can be handled with a spectral slit width of 5–7 cm^{-1}. The subsequent curves show that such spectral slit widths can be attained with a small prism spectrometer.

The need for good resolution in special cases is shown in Fig. 6 where the absorption of mixtures of ortho- and para-chloraniline in carbon tetrachloride are shown at 1490 cm^{-1}. Disubstituted benzene molecules generally have a characteristic absorption in this region and the para isomer has a higher frequency value than the ortho. For the curves marked *A*, the spectral slit width was 11.8 cm^{-1} while for *B* it was 7.2 cm^{-1}. The *A* curves appear very similar in that each shows a single broad absorption and only on careful inspection are differences in the shapes of the bands observed which might permit an indication or a rough measure of the proportions present. The *B* curves, on the other hand, show the presence of two absorption bands and permit fair quantitative estimates. It is known that disubstituted benzene has only one absorption frequency at this point. From an *A* curve it would be difficult to say that two components were present, but it is immediately obvious from a *B* curve that one is not dealing with a single isomer.

The spectral slit width of a spectrometer is defined as one-half the total frequency (or wavelength) interval passing out the exit slit. It represents a frequency difference which can exist between two monochromatic bands such that the instrument just fails to resolve them. For the case of a spectrometer employing a Littrow mount and assuming a non-absorbing prism at minimum deviation and perfect optics, the spectral slit width $\Delta\nu$ is given by the expression:

$$\Delta\nu(\mathrm{cm}^{-1}) = \underset{\text{A}}{\frac{\nu^2(1-n^2\sin^2\alpha/2)^{\frac{1}{2}}}{4\sin\alpha/2\dfrac{dn}{d\lambda}}}\ \frac{S_1+S_2}{f} + \underset{\text{B}}{\frac{\nu}{2b\dfrac{dn}{d\lambda}}}, \quad (1)$$

where ν is the frequency in cm^{-1}; n, the index of refraction of the prism at frequency ν; α, the prism angle; $dn/d\lambda$ the dispersion in cm^{-1}; S_1 and S_2, the mechanical slit widths in cm; f, the focal length in cm; and b, the effective prism base in cm. Term A represents the frequency spread as a result of the prism dispersion and finite slit widths and term B is the limiting resolving power of the prism, assuming the somewhat arbitrary Rayleigh definition of resolution. Where one is not working at minimum deviation, an accurate calculation requires tracing the rays through the prism system. In attempting to estimate the spectral slit width experimentally at any given frequency, the best one can do is to study a material which has absorption bands of various separations in the region of interest and measure the closest pair for which resolution is just achieved. Unfortunately, such materials are not always available and hence the experimental slit widths given represent observed resolution but not necessarily limiting resolution.

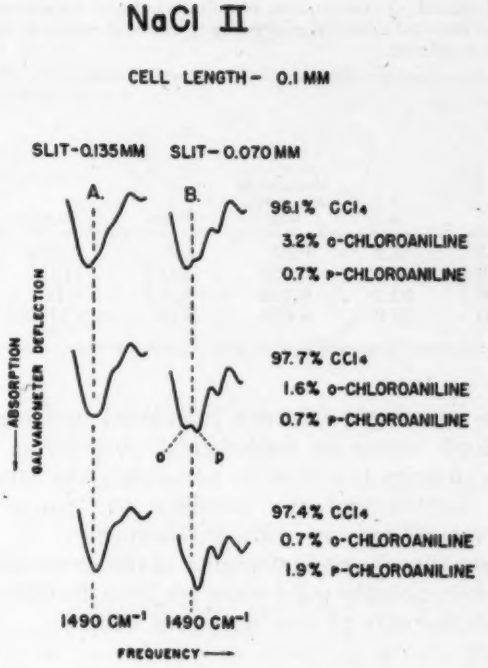

FIG. 6. Infra-red absorption of mixtures of ortho- and para-chloraniline near 1490 cm^{-1} illustrating loss of band structure with increase of spectral slit width. Spectral slit widths: *A* curves 11.8 cm^{-1}; *B* curves 7.2 cm^{-1}.

Table I gives some calculated spectral slit widths and observed resolved bands at a signal to noise ratio of approximately 100 to 1. The "exact" spectral slit was calculated by ray tracing for the finite slit contribution, and by a more stringent expression than Rayleigh's for minimum prism resolution, while the minimum deviation values were calculated from formula (1).

TABLE I. A comparison of calculated and experimental spectral slit widths in (cm^{-1}). There is evidence that the true experimental spectral slit widths, in some cases, is smaller than the calculated value, although no explanation for this fact is offered.

ν cm^{-1}	λ μ	Mechanical slit width mm	Prism	Sample	Minimum deviation spectral slit width (cm^{-1}) formula (1) Finite slits A	Prism resolution B	"Exact" spectral slit width (cm^{-1}) Finite slits A	Prism resolution B	Minimum deviation $\Delta\nu(cm^{-1})$ $A+B$	"Exact" $\Delta\nu(cm^{-1})$ $A+B$	Experimental spectral slit width (minimum observed resolution) $\Delta\nu(cm^{-1})$
3132	3.2	0.04	LiF	C_2H_4	3.5	1.4	3.3	1.2	4.9	4.5	7.2
1618	6.3	0.055	NaCl	H_2O	4.4	2.6	4.1	2.2	7.0	6.3	6.2
950	10.5	0.120	NaCl	NH_3	1.9	0.9	1.9	0.7	2.8	2.6	2.7
500	20.0	0.670	KBr	CH_3OH	3.5	0.6	3.5	0.5	4.1	4.0	5.0

The agreement between calculated and experimental values is fairly good considering the inaccuracies involved in measuring the smaller slit widths and the inability to change slit curvature for an arbitrary frequency. It also shows that the optical quality of the spectrometer is exceptionally good since its imperfections are observed only at very small slit widths.

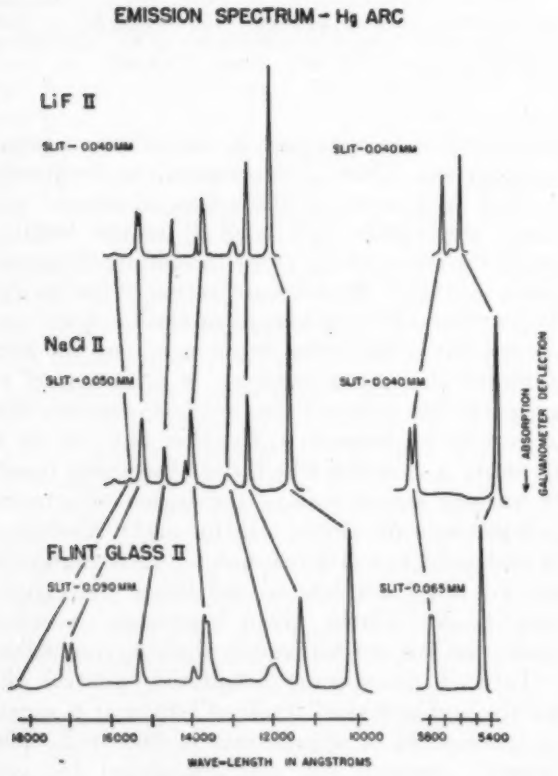

FIG. 7. Emission spectra of an H-3 mercury arc using various prism materials and double galvanometer recording.
Reference: E. D. McAlister, Phys. Rev. **34**, 1142–47 (1929).

The good resolution obtained with such a small spectrometer naturally leads to some speculation as to the size instrument which would be

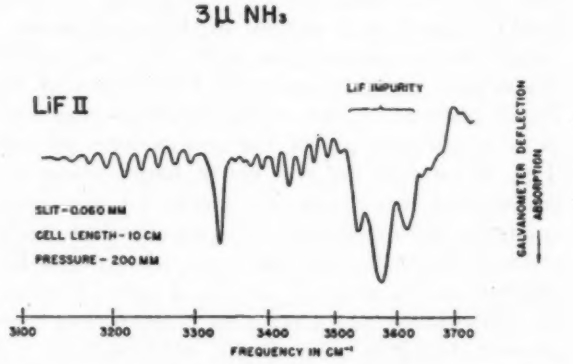

FIG. 8. Ammonia absorption at 3330 cm^{-1} using LiF prism and double galvanometer recording.
Reference: G. A. Stinchcomb and E. F. Barker, Phys. Rev. **33**, 305–8 (1929).

desirable if one wished to build a spectrometer to furnish equivalent spectral slit width with increased energy for accurate automatic recording measurement. Such a discussion would be too lengthy for inclusion in this paper as it would involve not only the dimensions of the spectrometer proper but also the extent of image reduction that could be achieved at the heat detector. Obviously, a short focal length imposes several difficulties to instrument design. The increased degree to which the optics are off-axis requires precise figuring of the parabola, errors in focusing are exaggerated, the slit jaw curvature is sharp, etc. Still, an increase in focal length to minimize these difficulties becomes uneconomical if carried too far. It now seems that the popular dimension of 100-cm focal length and a 10×15-cm prism may be larger than necessary since it

should be possible to get the instrument characteristics desired with 50- to 60-cm focus and an 8×12-cm prism.

In order to illustrate the nature of the results obtained from the present small spectrometer, Figs. 7 to 13 show the spectra of some common substances taken with various prism materials* and two different methods of signal measurement. Each curve is a trace of the direct record of the galvanometer deflection obtained with the pen recorder previously described.† In each case the prism material is designated. The Roman numeral I signifies that the thermocouple output was measured by a single galvanometer (Leeds and Northrup HS type, 0.05 μv/mm); while II signifies that the conventional double galvanometer photo-relay amplification‡ was used. The increase in sensitivity of method II over

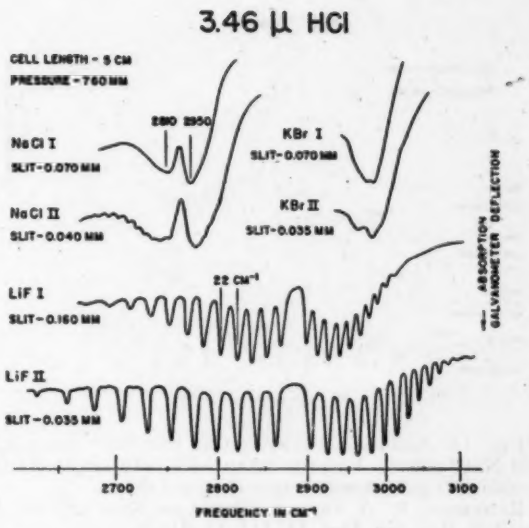

FIG. 10. Hydrogen chloride absorption at 2990 cm^{-1} using various prism materials. The Roman numeral I indicates single galvanometer recording, while II indicates double galvanometer recording.
Reference: E. S. Imes, Astrophys. J. **50**, 251–76 (1919).

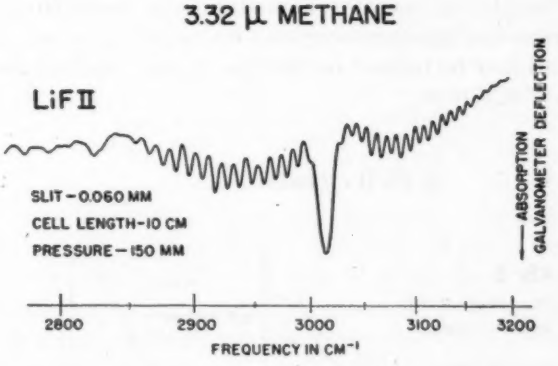

FIG. 9. Methane absorption at 3020 cm^{-1} using LiF prism and double galvanometer recording.
Reference: A. H. Nielsen and H. H. Nielsen, Phys. Rev. **48**, 864–7 (1935).

method I is of the order of 40 to 50 times. It is estimated that for 10-cm deflection of the galvanometer beam at a meter distance, the thermocouple develops 5 to 10 μv in method I; 0.2 to 0.5 μv in method II. Inasmuch as these compounds are useful for frequency calibration, the caption of each figure bears a reference to the literature where accurate frequencies of the rotation peaks may be obtained.

There is no need for a detailed discussion of each curve. They serve to illustrate the relative dispersion of the various materials throughout the spectrum and to show the loss of resolving power with the use of wider slits necessary to obtain sufficient energy for the single galva-

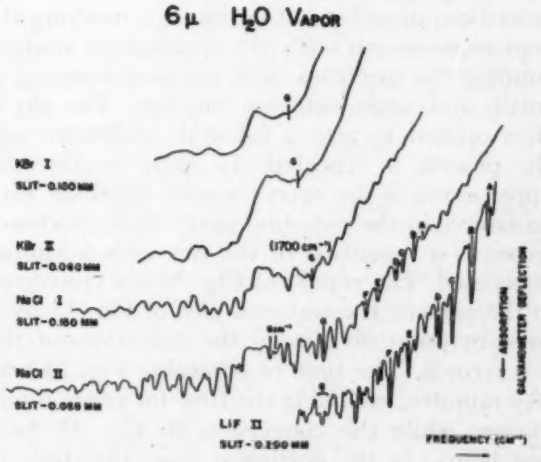

FIG. 11. Water vapor absorption at 1596 cm^{-1} using various prisms. I indicates single galvanometer recording, II indicates double galvanometer recording.
Reference: R. A. Oetgen, Chao-Lan Kao, and H. M. Randall, Rev. Sci. Inst. **13**, 515–23 (1942).

* The lithium fluoride, sodium chloride, and potassium bromide prism blanks were supplied by the Harshaw Chemical Company of Cleveland, Ohio.

† Barnes, Liddel, and Williams, Ind. Eng. Chem. **15**, 659–709 (1943).

‡ R. Bowling Barnes and F. Matossi, Zeits. f. Physik **76**, 24–37 (1932).

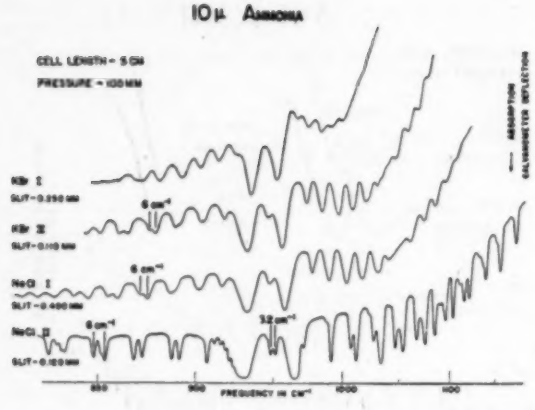

FIG. 12. Ammonia absorption at 950 cm^{-1} using KBr and NaCl prisms. Records taken with both single (I) and double (II) galvanometer recording are shown.
Reference: R. A. Oetgen, Chao-Lan Kao, and H. M. Randall, Rev. Sci. Inst. 13, 515–23 (1942).

nometer measurements. It can be seen that adequate resolution for research work is available (using method II) with the use of lithium fluoride from 3800 cm^{-1} to 2000 cm^{-1}; sodium chloride from 2000 cm^{-1} to 750 cm^{-1}; and potassium bromide from 750 cm^{-1} to 400 cm^{-1}. For many purposes, such as determining the choice of analytical frequencies for single galvanometer measurements, the lower resolution (single galvanometer) curves are sufficient.

To clarify the typical results obtained from the spectrometer, the absorption spectrum of para-methyl styrene is shown from 3600 cm^{-1} to 400 cm^{-1}. Figure 14 is a reproduction of the actual record obtained by setting the slit, marking the zero transmission with the appropriate shutter, running the spectrum until the source energy is small, and again marking the zero. The slit is then opened to give a full-scale deflection and the process is repeated. In each section, the upper curve is the energy record obtained with no sample in the radiation path, while the lower record is a repetition of the run with a sample interposed. The results of Fig. 14 are converted to the percent transmission plot of Fig. 15 by a point-by-point division of the deflections of the two records. The time of obtaining Fig. 14 was fifty minutes, excluding the time for prism interchange, while the conversion to Fig. 15 took four hours. In the particular case, therefore, it is quicker and easier to determine results directly from the record. However, in some cases, the fact that the energy background is not constant gives rise to artifacts which can be eliminated only by plotting. Moreover, it is difficult to compare records taken from instruments which are not identical so that interchange of information must generally be made on a basis of percent or log percent transmission graphs.

The fact that instruments of this caliber are now commercially available should make possible a considerable increase in the infra-red spectroscopic work done in this country. Smaller companies have evinced interest in the field but have not undertaken work because all-purpose instruments which might be applied to any problem were not available at a reasonable cost. Moreover, research instruments in the past have required considerable housing space, personnel, and facilities. The results of this paper were obtained with the instrument and recorder set up as shown in Fig. 16. The spectrometer and portable pen recorder can be placed on a laboratory desk or table and the galvanometer system mounted on the wall above. Whereas one formerly thought of devoting a medium-size room to an infra-red spectrometer and its appurtenances, it can now be housed on the floor space required for a 3′×5′ desk.

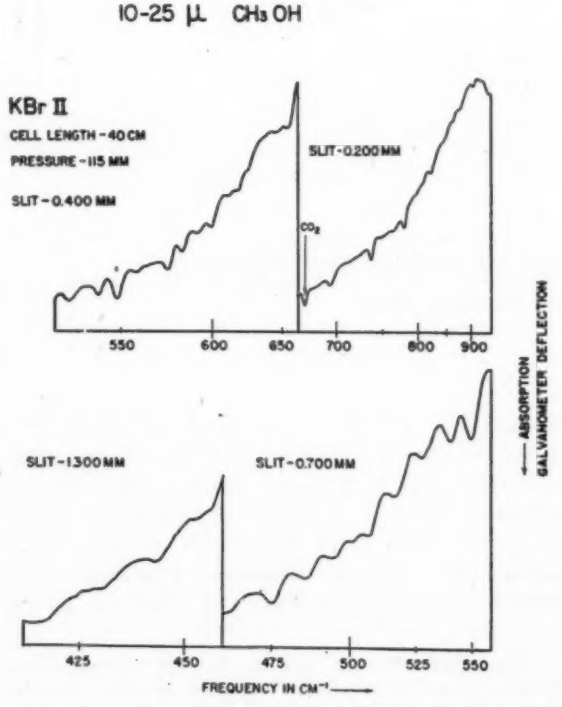

FIG. 13. Absorption of methyl alcohol vapor from 900 to 400 cm^{-1}.
Reference: A. Borden and E. F. Barker, J. Chem. Phys. 6, 553–63 (1938).

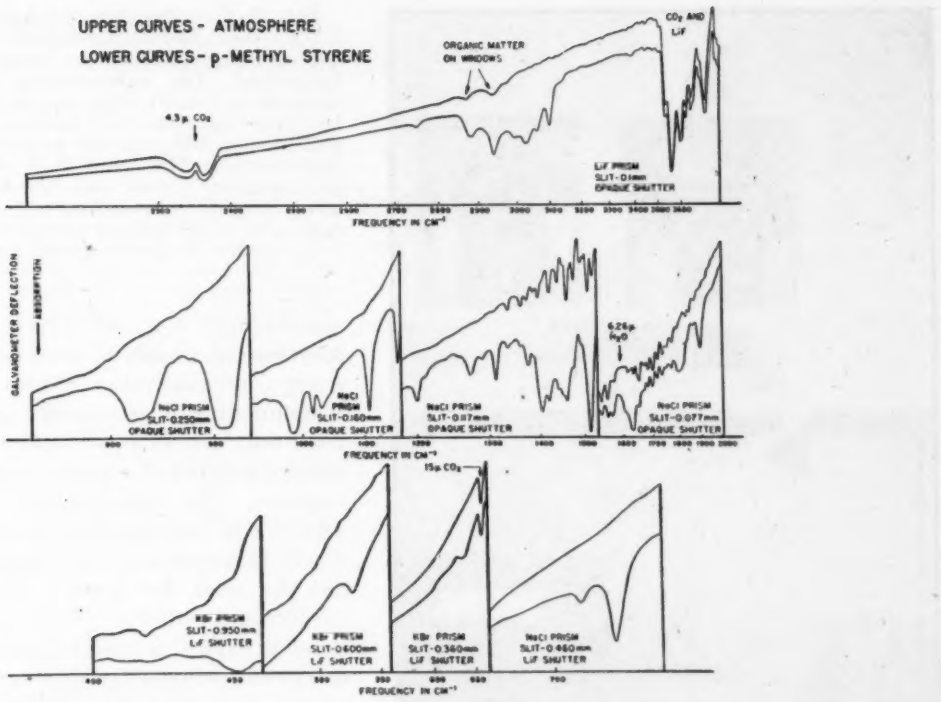

FIG. 14. The lower curve in each case is the infra-red absorption of para-methyl styrene. The upper curve is the background energy record obtained with no sample in the beam.

This spectrometer should also bring a change in technique to the larger laboratories which are doing considerable infra-red work. So long as a single expensive spectrometer was the rule, it was necessary to have two or three operators using the instrument, and each individual's sample preparation, spectral recording, and interpretation of results had to be dovetailed on a close schedule to obtain maximum efficiency from the spectrometer. With the advent of these small instruments, an infra-red laboratory can be set up on the same basis as a microscopy laboratory. Each physicist can have his own spectrometer and can handle a complete problem of research or analysis without the necessity for waiting for the large instrument to be free.

It is to be emphasized that it is not the authors' intention to present this spectrometer as the ultimate for either research or analytical work. In fact, the distinction that has been drawn between qualitative and quantitative uses of a spectrometer is a somewhat artificial one based on the present situation of infra-red instruments. As the applications in this field grow, there will undoubtedly appear on the market a variety of instruments (as is now the case in visible spectroscopy) whose range of resolution, accuracy, and cost is such that a specific instrument can be purchased for a specific job. At one end of this range there must be a rapid, percent recording

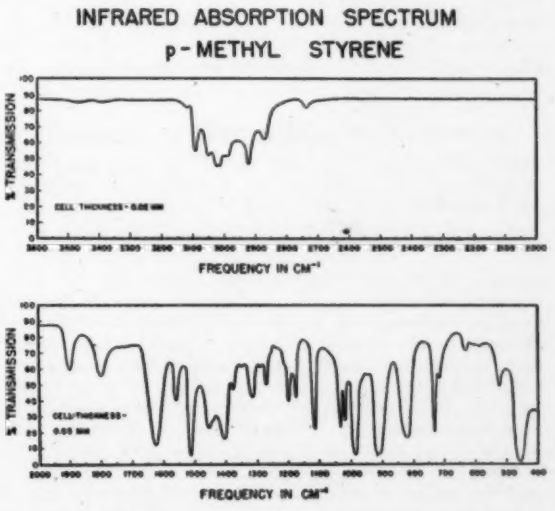

FIG. 15. Infra-red absorption spectrum of para-methyl styrene. Percent transmission values were obtained from a point-by-point division of the ordinates of the sample and energy curves of Fig. 14.

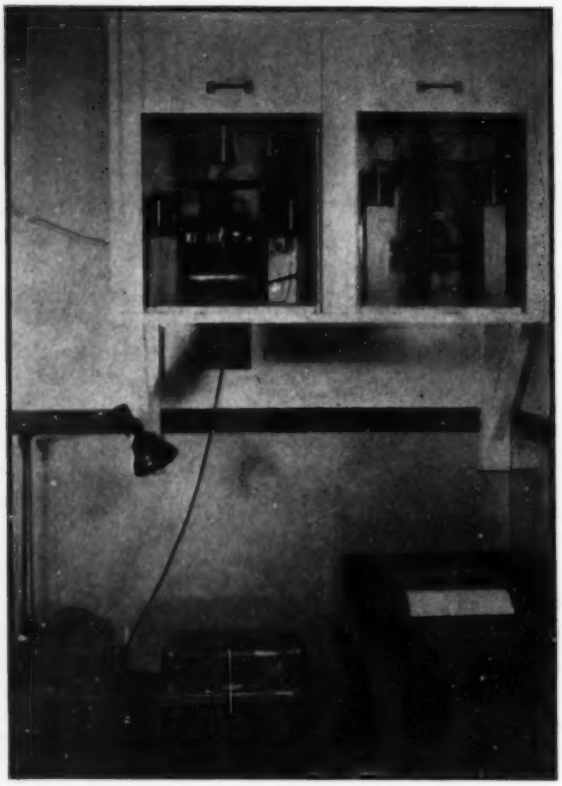

FIG. 16. Complete infra-red spectroscopic equipment on a 3′×5′ desk. The instrument is in the left foreground and the recording galvanometer beam follower in the right foreground. The galvanometer amplifying system is mounted in a draft-tight case on the wall above. On the left Julius suspension are mounted a bulb, photronic cell with double grid, and the primary galvanometer (Leeds and Northrup HS 2284X 0.17 μv/mm). The recording galvanometer (Leeds and Northrup R-2500 E, 0.003 μamp./mm) is mounted on a Julius suspension on the right. The factor limiting the sensitivity of such a system is the amount of vibration in the primary galvanometer.

spectrometer that will have high resolution at no sacrifice of absolute accuracy in frequency or energy measurement. However, this ultimate instrument will necessarily be costly and can be used only where the extent of research work or the importance of complex analyses warrants this expense. The spectrometer described in this article will take its place in this range as a relatively inexpensive, all-purpose instrument which can be used for general analytical work, for exploratory studies where a company or university wishes to investigate the application of infra-red spectroscopy to its particular problems, or for industrial research work that does not require the more expensive instrument of the future.

Here and There

News Notes

Dr. Peter L. Bellaschi, research engineer of the Westinghouse Electric and Manufacturing Company at Sharon, Pennsylvania, concluded a tour of South America in the interests of inter-American scientific and industrial coordination with a series of lectures in Brazil. He visited Argentina, Peru, Brazil, Uruguay, Chile, Colombia, and Venezuela in his study of Latin America's industrial needs. Dr. Bellaschi's artificial production of lightning strokes has contributed to the development of surgeproof power, distribution and instrument transformers, and aided the development of impulse testing techniques and sphere gap calibrations.

Dr. Harvey A. Zinszer, Professor of Physics and Astronomy at the Kansas State College at Fort Hays, has leave of absence to assist in the pre-radar course for Army and Navy officers at the Cruft Laboratory, Harvard University.

Dr. Robert Clark Jones, recent recipient of the Adolph Lomb Medal from the Optical Society of America for "noteworthy accomplishment in the field of optics," has rejoined the research staff of Polaroid Corporation in Cambridge. The Lomb Medal was awarded to Jones for developing an ingenious mathematical system used in calculations related to applications of polarized light. Since working out the system for Polaroid several years ago, Jones has been with the Bell Telephone Laboratories.

The Simpson Optical Manufacturing Company was recently awarded the fourth star for their Army-Navy "E" pennant by the Navy Board for Production Awards. This is the fifth citation they have been granted for their contributions to the war effort in the way of sustained production and high quality optics.

New Appointments

Dr. Paul R. Gleason, Professor of Physics at Colgate University, was elected Chairman of the New York State Section of the American Physical Society at the final session of its annual meeting at Union College, Schenectady. Dr. Gleason succeeds Dr. W. B. Rayton of the Bausch and Lomb Optical Company, Rochester.

Mr. R. V. Wilson has been appointed Director of Customer Service of Continental Can Company's Research Department, succeeding Mr. L. F. Pratt who has resigned to take a position with Hunt Brothers of Hayward, California, according to A. L. Malone, General Manager of the Research Department. Mr. Wilson was formerly Manager of General Line Customer Service.

The appointment of Dr. George A. Works of the University of Chicago to succeed Dr. Leonard Carmichael as Director of the National Roster of Scientific and Specialized Personnel has been announced by Paul V. McNutt, Chairman of the War Manpower Commission. In accepting his resignation, Mr. McNutt said he was doing so to permit Dr. Carmichael to devote a larger portion of his time to his duties as President of Tufts College, Medford, Massachusetts. Dr. Carmichael will continue as Chairman of the Committee on Scientific Research Personnel and as Consultant to the Roster, Mr. McNutt said.

Dr. William D. Coolidge retired on December 31 as Vice President and Director of Research of the General Electric Company. Dr. C. G. Suits, Assistant to the Director, has been elected a vice president of the company and has been placed in charge of the research laboratory.

Electron Microscope Society of America

At a meeting of the Electron Microscope Society of America held in Chicago, Illinois, on November 16–18, 1944, the following officers were elected to the Executive Council for 1945:

President: JAMES, HILLIER, *RCA Laboratories, Princeton, New Jersey*
Vice President: ERNEST FULLAM, *Interchemical Corporation, 432 West 45 Street, New York, New York*
Secretary-Treasurer: M. C. BANCA, *Apartment B-2, 306 Cooper Street, Camden, New Jersey.*

Directors (three years each)—newly elected Directors

Term expires Fall meeting 1947:

F. O. SCHMITT, *Department of Biology and Biological Engineering, Massachusetts Institute of Technology, Cambridge, Massachusetts*
R. B. BARNES, *American Cyanamid Company, Stamford, Connecticut.*

Term expires Fall meeting 1946:

R. D. HEIDENREICH, *The Dow Chemical Company, Midland, Michigan*
T. F. ANDERSON, *University of Pennsylvania, Johnson Foundation, Philadelphia, Pennsylvania.*

Term expires Fall meeting 1945:

L. MARTON, *Division of Electron Optics, Stanford University, California*
DAVID HARKER, *General Electric Company, Schenectady, New York.*

New Books

Steel in Action

BY CHARLES M. PARKER. Pp. 221+vi, Figs. 18, 13½×20 cm. The Jaques Cattell Press, Lancaster, Pennsylvania, 1943. Price $2.50.

The purpose of this little book is to tell what steel is, how it is made, and what part it has played in the industrial life of the nation. A short historical introduction is followed by a description of the blast furnace, the open hearth furnace, the Bessemer converter, the electric furnace, and the rolling mill as used in the manufacture of steel. Carbon and alloy steel are described, and a very illuminating chapter is included on the distribution and control of raw materials. International trade, wartime expansion, and "Steel in the postwar world" are among the topics treated in the last few chapters. To one who has not followed actively the progress of the steel industry in the past few years, this book will be gratefully and enthusiastically received.

The Technique of Motion Picture Production

A Symposium of Papers Presented at the 51st Semi-Annual Convention of the Society of Motion Picture Engineers, Hollywood, California. Pp. 150+viii, Figs. 41, 15½×23½ cm. Interscience Publishers, Inc., New York, 1944. Price $3.50.

At the Spring, 1942 Technical Conference of the Society of Motion Picture Engineers in Hollywood, California, a symposium was presented covering the current technical practices in the motion picture industry as applied to actual motion picture production. While information with regard to many of the subjects treated is scattered through the literature, no such complete descriptions of the various techniques involved had hitherto been assembled in a single volume. The papers of the symposium are presented here in the general order of the steps taken in the production and presentation of motion pictures in the studios, laboratories, and theaters. Each section has been prepared by a man well fitted by his knowledge and experience in a particular field to give authentic information on the various problems arising in the manufacture of this entertainment and educational medium.

Physical Chemistry

By Frank H. MacDougall. Pp. 722+viii, Figs. 130, 15×22 cm. The Macmillan Company, New York, 1943. Price $4.25.

It is quite apparent in reading this revised text on physical chemistry that the author has taken great care to present the material in a logical order and to treat the subject in as rigorous a manner as possible in an introductory text. Following brief chapters on atomic theory and the first law of thermodynamics, there are rather detailed treatments of the gaseous, liquid, and solid states. The next few chapters deal with the structure of atoms. Here the author confines his remarks on quantum mechanics to only two or three sentences and excuses further mention because of mathematical difficulties involved. In the reviewer's opinion, it should be possible to introduce the general philosophy of quantum mechanics and carry this throughout the remainder of the book even for students meeting the subject for the first time. The next few chapters give an excellent account of the second-law equilibrium and chemical kinetics. Electrical conductance in solutions and electrolysis are followed by brief chapters on photochemistry and the colloidal state. Except for the almost complete omission of the present-day ideas on the structure of the atom, this text will be found quite useful.

New Booklets

The Clarostat "Interim Line" catalog has just been issued to help span the gap between present wartime restrictions and postwar abundance. It lists such items as composition-element and wire-wound controls, switches, constant-impedance attenuators, universal metal-tube plug-in resistors, power rheostats, power resistors, voltage regulators, and glass-insulated flexible resistors which are in regular production and, priorities permitting, may be made available to the jobbing trade. A copy of this "Interim Line" catalog may be obtained by writing Clarostat Manufacturing Company, Inc., 285–7 North 6 Street, Brooklyn, New York.

Manufacturers of electrical equipment—wire, cable, instruments, motors, appliances, and insulating materials—who need to measure accurately and easily the insulation resistance of their products should be interested in an 8-page catalog, E-54-460(1), "To measure insulation resistance—L&N test set assemblies." This publication describes assemblies which are completely guarded from the effects of leakage currents. To receive this catalog, write to Leeds & Northrup Company, 4934 Stenton Avenue, Philadelphia, Pennsylvania.

Industrial Bulletin, a publication of Arthur D. Little, Inc., has for its purpose "to place before industrial, financial, and research executives early and authoritative information bearing upon the present status of industrial development or indicative of its probable trend." Further information regarding this booklet may be obtained from Arthur D. Little, Inc., Cambridge, Massachusetts.

Aminco Laboratory News is a publication devoted to the application of scientific instruments to modern laboratory technique, engineering, materials testing, and production control. Requests for the booklet should be addressed to American Instrument Company, 8030–8050 Georgia Avenue, Silver Springs, Maryland.

Specifications and prices of Engineers Specialties Division Products for use on all optical comparators, measuring projectors, microprojectors, and shadowgraphs are given in a 15-page booklet which announces two new products: the two types of Detail Engineers' Glass and the new Grid Comparator Charts. Requests for copies or additional information should be addressed to Engineers Specialties Division, The Universal Engraving and Colorplate Company, Inc., 980 Ellicott Street, Buffalo 8, New York.

A new 8-page folder entitled "Some problems influencing the drawing of fine wire" by H. P. Edinga, Wire Division Manager, has been announced by North American Philips Company, Inc., 100 East 42 Street, New York. It is a reprint of a technical paper presented by Mr. Edinga on October 17, 1944 before the annual meeting of the Wire Association at Pittsburgh. The folder describes the importance of fine wire in the world of today. It discusses drawing problems particularly with respect to the cold-drawn types.

Leeds & Northrup Company recently published a "general catalog" issue of "Modern Precision" which not only describes briefly all their laboratory instruments but also all of their equipment for regulating industrial processes and for heat-treating metals, as well as those for use in power plants. A copy of this 28-page booklet may be obtained by writing to Leeds & Northrup Company, 4934 Stenton Avenue, Philadelphia 44, Pennsylvania. Specify Folder ENT(7).

"Industrial Research and Development," a 2-page publication, will be sent gratis, providing requests are made on letterheads, to Richard Rimbach, Consulting Engineer, 1117 Wolfendale Street, Pittsburgh 12, Pennsylvania.

The Allied News, published by the Allied Radio Corporation, will be sent regularly without charge to engineers, purchasing agents, department heads, etc., who are interested in the maintenance and development of radio and electronic equipment. Requests on company letterhead should be addressed to: Editor, Allied News, 833 W. Jackson Boulevard, Chicago 7, Illinois.

A new permanent magnet manual of interest to everybody concerned with the application of the permanent magnet to various industries has been prepared by The Arnold Engineering Company, 147 East Ontario Street, Chicago 11, Illinois. Contents include such subjects as magnet materials, resistance comparisons, physical and magnetic properties, demagnetization and energy curves, fabrication, design, and testing. Charts and tables are included to illustrate and explain various aspects of the discussion. The new manual is available on request to The Arnold Engineering Company.

Contributed Original Research

The General Theory of Stresses and Displacements in Layered Systems. I*

D. M. Burmister
Columbia University, New York, New York

(Received August 24, 1944)

The problems of airport and foundation engineering have become increasingly important in the war construction program. These problems frequently involve the consideration of stresses and settlements in layered soil deposits. The well-known Boussinesq equations apply strictly only to homogeneous soil deposits. The general theory of stresses and displacements in a two-layer system is developed in order to provide the engineer with a useful tool which is more directly applicable to the analysis of actual conditions encountered in soil deposits. The basic equations of stresses and settlements are derived. The numerical evaluation of the surface settlement equation for the simplest case of Poisson's ratio equal to one-half has been completed as the first of a series, and is presented in the form of influence curves for the analysis of practical problems.

INTRODUCTION

THE war construction program has enormously increased the problems to be solved by the engineer in foundation engineering and particularly in airport design and construction. The engineer is dealing primarily with layered soil deposits in such problems. Frequently the consideration of stresses and settlements is of paramount importance. The surface layer may be either stronger or weaker than the underlying layer. In airport design, the surface or pavement layer must be made sufficiently strong to provide adequate support for heavy airplane wheel loads. In foundation work, a weaker surface layer is frequently encountered. On the other hand, a stronger surface layer has a considerable reinforcing and load-spreading effect, which is very important in foundation work. A two-layer system represents a step toward a closer approximation to actual conditions encountered in airport and foundation engineering.

The theory of stresses and displacements in a two-layer system is developed in accordance with the methods of the theory of elasticity in order to provide the engineer with a useful and important tool for the analysis of foundation and airport problems, which is more directly applicable to the actual conditions encountered in soil deposits. The theory reveals the fundamental relations existing between the physical factors, which control the magnitude and distribution of stresses and displacements in a two-layer system. A special case of this general problem has been treated elsewhere.[1]

1. ASSUMPTIONS AND CONDITIONS

It must be realized that all theories deal with ideal materials and ideal conditions, which are only imperfectly satisfied in natural soil deposits. The two-layer system, as a step toward a closer approximation to actual conditions, is illustrated in Fig. 1. It consists of a surface layer No. 1 having a finite thickness h which rests continuously upon layer No. 2 of infinite thickness, having different strength properties.

The general solution of the two-layer problem requires that the necessary assumptions of the theory of elasticity be made and, in addition, that certain essential boundary and continuity conditions be satisfied across the interface between the two layers.

(a) The soils of each of the two layers are assumed to be homogeneous, isotropic, elastic materials, for which Hooke's law is valid.

(b) The surface layer No. 1 is assumed to be infinite in extent in the horizontal direction, but of finite thickness h. The underlying layer No. 2

* Publication assisted by the Ernest Kempton Adams Fund for Physical Research of Columbia University.

[1] D. M. Burmister, "Theory of stresses and displacements in layered systems and application to the design of airport runways," Proc. 23rd Annual Meeting of the Highway Research Board (1943).

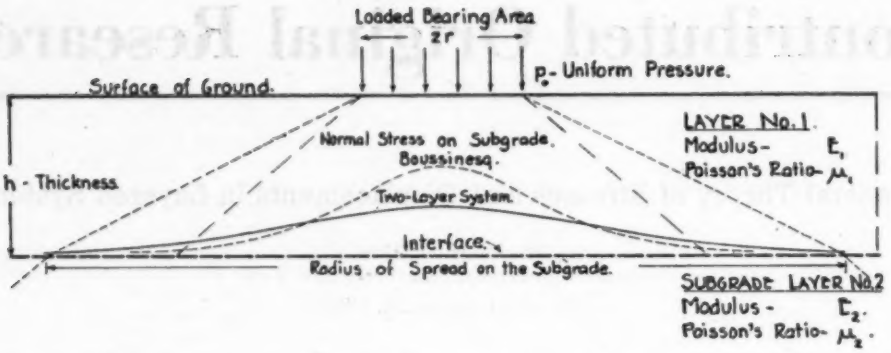

FIG. 1. The two-layer system.

is assumed to be infinite in extent in the horizontal and vertical (downward) directions.

(c) The boundary conditions require that the surface of layer No. 1 be free of shearing stresses and free of normal stresses outside the limits of the surface loading. Also the stresses and displacements must be equal to zero in layer No. 2 at infinite depth.

(d) *Continuity Conditions—Case 1.* It is assumed that the two layers of the system are continuously in contact with shearing resistance fully active between them, so that the two layers act together as an elastic medium of composite nature with a full continuity of stress and displacement across the interface between the layers.

Case 2. It is assumed that the two layers of the system are continuously in contact but with a frictionless interface and a continuity of normal stress and normal displacement only.

2. EQUATIONS OF THE THEORY OF ELASTICITY

In developing the theory of the two-layer system, the equations of the theory of elasticity for the three-dimensional problem in cylindrical coordinates were employed, which were derived by Love to satisfy the equations of equilibrium and compatibility.[2]

Equations of equilibrium (1).

$$\frac{\partial \sigma_r}{\partial r}+\frac{\partial \tau_{rz}}{\partial z}+\frac{\sigma_r-\sigma_\theta}{r}=0,$$

$$\frac{\partial \tau_{rz}}{\partial r}+\frac{\partial \sigma_z}{\partial z}+\frac{\tau_{rz}}{r}=0.$$

Equations of compatibility (2).

$$\nabla^4\phi=0,$$

$$\nabla^2=\left[\frac{\partial^2}{\partial r^2}+\frac{1}{r}\frac{\partial}{\partial r}+\frac{\partial^2}{\partial z^2}\right].$$

Elasticity equations of stress (3).

$$\sigma_z=\frac{\partial}{\partial z}\left[(2-\mu)\nabla^2\phi-\frac{\partial^2\phi}{\partial z^2}\right],$$

$$\sigma_r=\frac{\partial}{\partial z}\left[\mu\nabla^2\phi-\frac{\partial^2\phi}{\partial r^2}\right],$$

$$\sigma_\theta=\frac{\partial}{\partial z}\left[\mu\nabla^2\phi-\frac{1}{r}\frac{\partial\phi}{\partial r}\right],$$

$$\tau_{rz}=\frac{\partial}{\partial r}\left[(1-\mu)\nabla^2\phi-\frac{\partial^2\phi}{\partial z^2}\right].$$

Elasticity equations of displacement (4).

$$w=\frac{1+\mu}{E}\left[(1-2\mu)\nabla^2\phi+\frac{\partial^2\phi}{\partial r^2}+\frac{1}{r}\frac{\partial\phi}{\partial r}\right],$$

$$u=-\frac{1+\mu}{E}\left[\frac{\partial^2\phi}{\partial r^2}\right].$$

Where strain components $\partial w/\partial z$ and $\partial w/\partial r$ are made compatible.

A general solution of the stress equations (3) and the displacement equations (4) may be obtained by employing a stress function, ϕ which must satisfy the equation of compatibility (2).

[2] A. E. H. Love, *Treatise on the Mathematical Theory of Elasticity* (University Press, Cambridge, England, 1923), p. 274.

3. EQUATIONS FOR THE TWO-LAYER SYSTEM FULL CONTINUITY

The following form of stress function ϕ for the three-dimensional problem was found to satisfy the compatibility equation (2) which involves Bessel functions and a parameter m.

Stress Function $\phi = J_0(mr)[Ae^{mz} - Be^{-mz} + Cze^{mz} - Dze^{-mz}]$. (5)

The following stress and displacement equations were obtained by substituting this stress function in Eqs. (3) and (4).

(a) Equations for Surface Layer No. 1 (Subscripts, 1)

Normal stress

$$\sigma_{z1} = -mJ_0(mr)[A_1m^2e^{mz} + B_1m^2e^{-mz} - C_1m(1-2\mu_1-mz)e^{mz} + D_1m(1-2\mu_1+mz)e^{-mz}]. \quad (6a)$$

Shearing stress

$$\tau_{rz1} = +mJ_1(mr)[A_1m^2e^{mz} - B_1m^2e^{-mz} + C_1m(2\mu_1+mz)e^{mz} + D_1m(2\mu_1-mz)e^{-mz}]. \quad (6b)$$

Radial stress

$$\sigma_{r1} = +mJ_0(mr)[A_1m^2e^{mz} + B_1m^2e^{-mz} + C_1m(1+2\mu_1+mz)e^{mz} - D_1m(1+2\mu_1-mz)e^{-mz}] - m\frac{J_1(mr)}{mr}[A_1m^2e^{mz} + B_1m^2e^{-mz} + C_1m(1+mz)e^{mz} - D_1m(1-mz)e^{-mz}]. \quad (6c)$$

Settlement

$$w_1 = -\frac{1+\mu_1}{E_1}J_0(mr)[A_1m^2e^{mz} - B_1m^2e^{-mz} - C_1m(2-4\mu_1-mz)e^{mz} - D_1m(2-4\mu_1+mz)e^{-mz}]. \quad (6d)$$

Horizontal displacement

$$u_1 = +\frac{1+\mu_1}{E_1}J_1(mr)[A_1m^2e^{mz} + B_1m^2e^{-mz} + C_1m(1+mz)e^{mz} - D_1m(1-mz)e^{-mz}]. \quad (6e)$$

(b) Equations for Layer No. 2 (Subscripts, 2)

A similar set of equations was obtained with elastic properties E_2 and μ_2 and coefficients B_2 and D_2. The coefficients A_2 and C_2 are equal to zero to satisfy the boundary condition that the stresses and displacements be equal to zero at infinite depth.

4. BOUNDARY AND CONTINUITY CONDITIONS

Case 1. Full Continuity

The boundary and continuity conditions which must be satisfied for Case 1 are expressed mathematically in the following equations:

(a) Boundary Conditions at the Surface of the Ground, $z = -h$.

Distribution of surface loading, $\sigma_z = -mJ_0(mr)$.

$$-mJ_0(mr)[A_1m^2e^{-mh} + B_1m^2e^{mh} - C_1m(1-2\mu_1+mh)e^{-mh} + D_1m(1-2\mu_1-mh)e^{mh}] = -mJ_0(mr). \quad (8a)$$

Shearing stress at surface, $\tau_{rz} = 0$.

$$mJ_1(mr)[A_1m^2e^{-mh} - B_1m^2e^{mh} + C_1m(2\mu_1-mh)e^{-mh} + D_1m(2\mu_1+mh)e^{mh}] = 0. \quad (8b)$$

(b) Continuity Conditions at the Interface, $z = 0$.

Vertical settlements must be equal, $w_1 = w_2$.

$$-\frac{1+\mu_1}{E_1}[A_1m^2 - B_1m^2 - 2(1-2\mu_1)C_1m - 2(1-2\mu_1)D_1m] = -\frac{1+\mu_2}{E_2}[-B_2m^2 - 2(1-2\mu_2)D_2m]. \quad (9a)$$

Horizontal displacements must be equal, $u_1=u_2$.

$$+\frac{1+\mu_1}{E_1}[A_1m^2+B_1m^2+C_1m-D_1m]=+\frac{1+\mu_2}{E_2}[B_2m^2-D_2m]. \tag{9b}$$

Normal stresses, $\sigma_{z1}=\sigma_{z2}$.

$$-[A_1m^2+B_1m^2-(1-2\mu_1)C_1m+(1-2\mu_1)D_1m]=-[B_2m^2+(1-2\mu_2)D_2m]. \tag{9c}$$

Shearing stresses, $\tau_{rz1}=\tau_{rz2}$.

$$+[A_1m^2-B_1m^2+2\mu_1C_1m+2\mu_1D_1m]=+[-B_2m^2+2\mu_2D_2m]. \tag{9d}$$

(c) *Discontinuity at the Interface*

There is a discontinuity in the radial stress σ_r across the interface because, with horizontal displacements equal, $u_1=u_2$ the stresses σ_{r1} and σ_{r2} will be determined by the modulii E_1 and E_2, respectively, of the two layers.

5. TWO-LAYER SYSTEM. EQUATIONS OF STRESS AND DISPLACEMENT

The coefficients A_1, B_1, C_1, and D_1 were determined so as to satisfy these boundary and continuity conditions, as follows:

$$2A_1m^2=[K(1-4\mu_1)(1+2mh)e^{mh}-Le^{mh}+KL(4\mu_1-2mh)e^{-mh}]\frac{1}{\Delta}, \tag{10a}$$

$$2B_1m^2=[(4\mu_1+2mh)e^{mh}-Le^{-mh}+K(1-4\mu_1)(1-2mh)e^{-mh}]\frac{1}{\Delta}, \tag{10b}$$

$$C_1m=[K(1+2mh)e^{mh}-KLe^{-mh}]\frac{1}{\Delta}, \tag{10c}$$

$$D_1m=[e^{mh}-K(1-2mh)e^{-mh}]\frac{1}{\Delta}, \tag{10d}$$

where Δ is the common denominator,

$$\Delta=[e^{2mh}-(L+K+4Km^2h^2)+KLe^{-2mh}], \tag{10e}$$

and where the coefficients of the strength properties of the two layers are:

$$n=\frac{E_2}{E_1}\left[\frac{1+\mu_1}{1+\mu_2}\right],\quad K=\left[\frac{1-n}{1+n(3-4\mu_1)}\right],\quad L=\left[\frac{(3-4\mu_2)-n(3-4\mu_1)}{(3-4\mu_2)+n}\right]. \tag{10f}$$

Substituting these values of the coefficients A_1, B_1, C_1, and D_1 into Eqs. (6) for layer No. 1, the general stress and displacement equations were obtained for the two-layer system for a surface loading with a distribution, $\sigma_z=-mJ_0(mr)$.

(a) At the Surface of Layer No. 1

Settlement.

$$w=J_0(mr)\frac{2(1-\mu_1^2)}{E_1}\left[\frac{1+4Kmhe^{-2mh}-KLe^{-4mh}}{1-(L+K+4Km^2h^2)e^{-2mh}+KLe^{-4mh}}\right]. \tag{11}$$

Approximate radius of curvature of surface $\frac{1}{R}=\frac{\partial^2 w}{\partial r_2}$.

$$\frac{1}{R}=-\left[m^2J_0(mr)-\frac{m^2J_1(mr)}{mr}\right]\left[\frac{1-\mu_1^2}{E_1}\right]\left[\frac{1+4Kmhe^{-2mh}-KLe^{-4mh}}{1-(L+K+4Km^2h^2)e^{-2mh}+KLe^{-4mh}}\right]. \tag{12}$$

(b) At the Interface Between Layers No. 1 and No. 2

Normal stress.

$$\sigma_z = -mJ_0(mr)\left[\frac{[1+mh-L/2-0.5K(1+2mh)]e^{-mh}+[KL(1-mh)-L/2-0.5K(1-2mh)]e^{-3mh}}{1-(L+K+4Km^2h^2)e^{-2mh}+KLe^{-4mh}}\right]. \quad (13)$$

Shearing stress.

$$\tau_{rz} = -mJ_1(mr)\left[\frac{[mh+L/2-0.5K(1+2mh)]e^{-mh}+[KLmh-L/2+0.5K(1-2mh)]e^{-3mh}]}{1-(L+K+4Km^2h^2)e^{-2mh}+KLe^{-4mh}}\right]. \quad (14)$$

Radial stress.

$$\sigma_r = -mJ_0(mr)\left[\frac{[1-mh+L/2-1.5K(1+2mh)]e^{-mh} + [KL(1+mh)+L/2-1.5K(1-2mh)]e^{-3mh}}{1-(L+K+4Km^2h^2)e^{-2mh}+KLe^{-4mh}}\right]$$

$$+\frac{mJ_1(mr)}{mr}\left[\frac{[1-2\mu_1-mh+L/2-0.5K(3-4\mu_1)(1+2mh)]e^{-mh} + [KL(1-2\mu_1+mh)+L/2-0.5K(3-4\mu_1)(1-2mh)]e^{-3mh}}{1-(L+K+4Km^2h^2)e^{-2mh}+KLe^{-4mh}}\right]. \quad (15)$$

Settlement.

$$w = J_0(mr)\frac{1+\mu_1}{E_1}\left[\frac{[2-2\mu_1+mh+L/2+0.5K(3-4\mu_1)(1+2mh)]e^{-mh} - [KL(2-2\mu_1-mh)+L/2+0.5K(3-4\mu_1)(1-2mh)]e^{-3mh}}{1-(L+K+4Km^2h^2)e^{-2mh}+KLe^{-4mh}}\right]. \quad (16)$$

Approximate radius of curvature of the interface

$$\frac{1}{R} = -\left[m^2J_0(mr)-\frac{m^2J_1(mr)}{mr}\right]\left[\frac{1+\mu_1}{E_1}\right][\text{Bracket of Settlement Equation (16)}]. \quad (17)$$

The following checks were made on these equations as to their correctness of form:

(1) If the elastic properties E and μ are equal in the two layers, that is, a homogeneous deposit throughout, the strength coefficients L and K equal zero and Eqs. (11) to (17) reduce to the familiar forms from which the well-known Boussinesq equations may be readily derived.

(2) If the modulus E_2 becomes infinite, that is, a rough rock surface at the base of Layer No. 1 and Poisson's ratio, $\mu_1=\mu_2=\frac{1}{2}$, the strength coefficients L and K both become equal to minus one (-1) and Eq. (13) for the normal stress at the rock surface becomes identical with that given first by Biot,[3] and later by Pickett.[4] Also the stresses σ_z and σ_r are equal at the rock surface and the settlement w equal to zero.

The numerical evaluation has been completed as the first of a series for the settlement at the surface of layer No. 1 for Poisson's ratio equal to one-half in both layers by the application of well-known methods which were presented in detail elsewhere.[5] The basic equation of settlement at the center of a flexible circular bearing area for the two-layer system reduces to the simple form of the Boussinesq equation (Poisson's ratio, $\frac{1}{2}$) with a multiplying or correction coefficient

$$w = \frac{1.5pr}{E_2}F\left[\frac{r}{h}, \frac{E_2}{E_1}\right] = \frac{1.5pr}{E_2}F_w. \quad (18)$$

---

[3] M. A. Biot, Physics **6**, 367 (1935).

[4] G. Pickett, "Stress distribution in a loaded soil with some rigid boundaries," Proc. 18th Annual Meeting of the Highway Research Board (1938), Part II, p. 35.

[5] See reference 1.

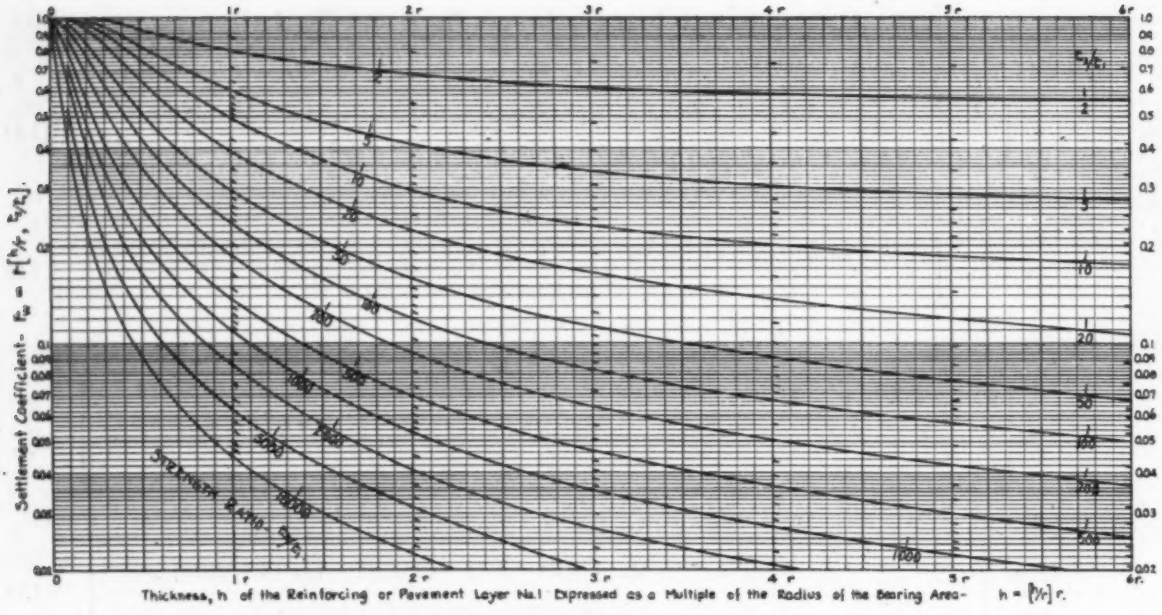
Settlement Coefficient- $F_w = F[h/r, E_2/E_1]$
Poisson's Ratio, μ_2
Thickness, h of the Reinforcing or Pavement Layer Not Expressed as a Multiple of the Radius of the Bearing Area- $h = [h/r]\,r$.

FIG. 2. Influence curves of the settlement coefficient, F_w for the two-layer system. Poisson's ratio, $\mu_1 = \mu_2 = 0.5$. Basic settlement equation at surface of ground $w = \frac{1.5pr}{E_2} F_w$. $F_w = F[h/r,\ E_2/E_1]$.

The coefficient F_w is a function of two basic ratios of the two-layer system, the ratio of the radius of the bearing area to the thickness of the surface layer r/h; and the ratio of the moduli of the two layers E_2/E_1. The theory reveals the controlling influence of these two basic ratios on the load-settlement characteristics of the system. For practical design purposes, the results of the theory of the two-layer system are expressed in the influence curves of Fig. 2 for a practical range of values of the ratios h/r and E_2/E_1.

The Use of the Electron Diffraction Camera to Detect Insulating Films

EILEEN I. ALESSANDRINI
Research Laboratory, General Electric Company, Schenectady, New York

(Received August 31, 1944)

Electron diffraction offers a solution to the problem of distinguishing between conducting and insulating surface films on conducting objects. An electron beam striking an insulating surface behaves in a different manner than with a conducting surface because of a charging up of the insulating surface. This enables the observer to recognize an insulating film on the surface of a sample.

DISTINGUISHING between insulating and conducting surface films is important in many investigations and the electron diffraction camera offers a simple means of obtaining this information. The presence of an insulating film on the surface of a metal or other conducting sample can be detected without the necessity of identifying the pattern obtained. In many cases, even if a pattern cannot be obtained from a particular sample, the behavior of the beam will show whether the surface is conducting or not. Sometimes this bit of information is all that is

necessary to tell the investigator whether the sample is applicable to the job for which it is being considered.

The sample to be analyzed is mounted in the specimen holder and placed in the camera. Its position in the electron beam is such that the electrons just graze the surface film (Fig. 1).

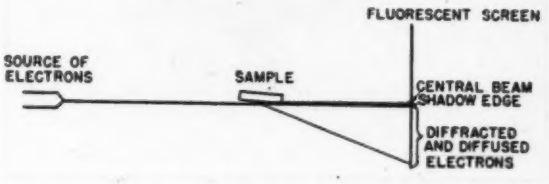

FIG. 1. Relation of sample position to the beam.

If the sample has a *conducting* surface, the main beam can be seen on the fluorescent screen,

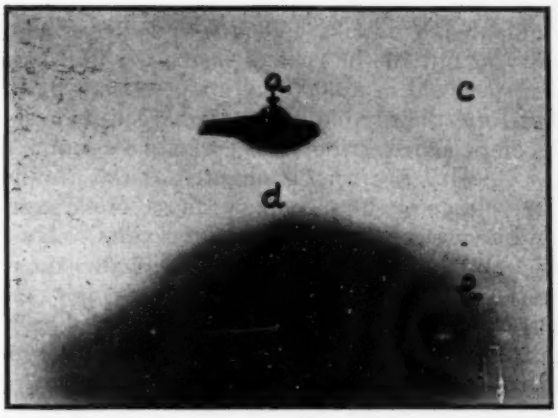

FIG. 2. Plate showing behavior of beam on conducting surface. No pattern present. Sample: Silver oxides on copper. *a*, Central beam. *b*, Diffracted beam. *c*, Shadowed area. *d*, Shadow edge.

and below it diffracted and diffused electrons—often showing pattern rings. A shadow edge appears because minute irregularities of the surface film block out a portion of the pattern of diffracted electrons. The central beam itself is broad enough so that a large part can pass the bumps in the surface and be seen above the shadow edge (Figs. 2 and 3). In other words, the bumps on the surface film have cut off some of the diffracted pattern because of the low intensity of the diffracted beams, whereas a large portion of the main beam has not been obstructed by any of the surface irregularities. The shadow edge appears as a straight line to the naked eye; however, if it were examined microscopically, many irregularities would be visible.

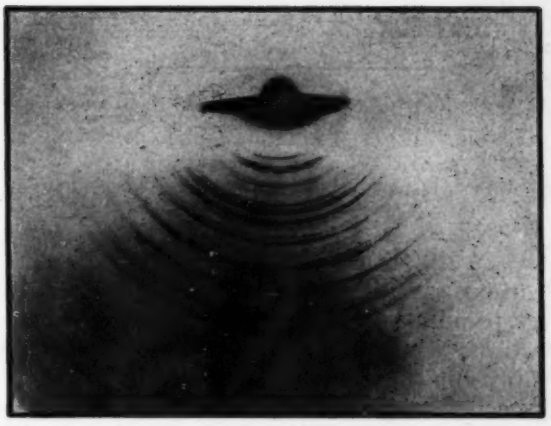

FIG. 3. Plate showing behavior of beam on conducting surface. Pattern present. Sample: Oxidized silicon steel.

A sample, whose surface is *insulating*, causes the beam to behave differently. When the sample is lowered into the beam, as described above, it charges up. This charging effect can be seen on the fluorescent screen as soon as the insulating surface enters the beam. When this effect is obtained, no shadow edge is visible and no central beam is defined. The beam, because of the charging up, is seen on the screen as a large spot 1 mm to 2 mm in size rather than 0.1 mm to 0.2 mm. Broad regions of scattered electrons extend out from the large central beam in several different directions (Fig. 4). However, the beam can be brought into focus by directing a secondary source of low velocity electrons at the insulating surface. A "spray gun" supplying secondary

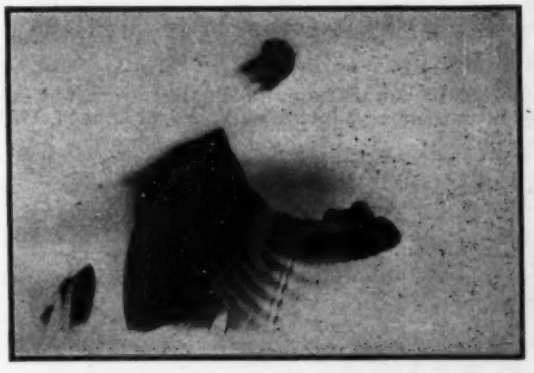

FIG. 4. Plate showing charging effect obtained from insulating surface. Sample: Sodium chloride on stainless steel block.

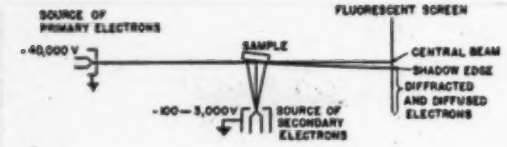

FIG. 5. Diagram showing "spray gun" as source of secondary electrons.

electrons is utilized (Fig. 5). The plates of Figs. 6 and 7 show how the diffracted and diffused electrons appear below the shadow edge after the "spray gun" is put in operation.

When the high velocity electrons of the central beam graze the insulating film, secondary electrons are given off. The number of secondary electrons has been found to depend on the number of primary electrons, their speed, and the surface of the sample on which they are directed.[1] The ratio of the electron yield of primaries to secondaries is a function of the voltage. As the voltage is increased the curve of this yield passes unity (one secondary for every primary), reaches a maximum, then gradually falls off, and drops below unity again. In the case of insulating films, the electron yield at 40,000 volts is less than unity; therefore, the sample becomes charged. In order to compensate for this loss, a secondary source of low velocity electrons is directed at the sample. The voltage of the secondary source of electrons can be varied from a few hundred volts to three thousand volts, the exact voltage being dependent on the nature of the sample. In this way, the ratio of primaries to secondaries is brought to unity—one electron hitting the sample and one being knocked out of it—thus eliminating charging up. This enables the investigator to bring the beam in focus, obtain a shadow edge, and observe the diffracted and diffused electrons.

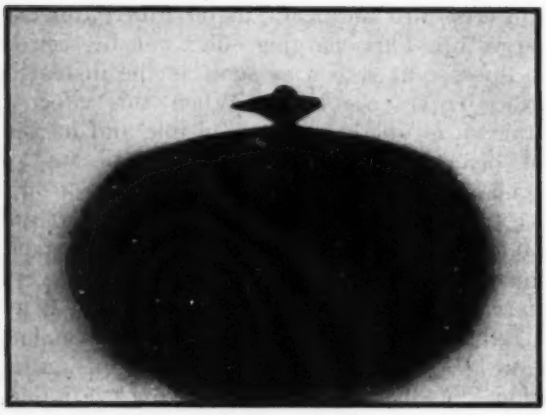

FIG. 6. Plate showing behavior of beam on insulating film with "spray gun." Sample: Magnesium oxide on stainless steel block. No pattern present.

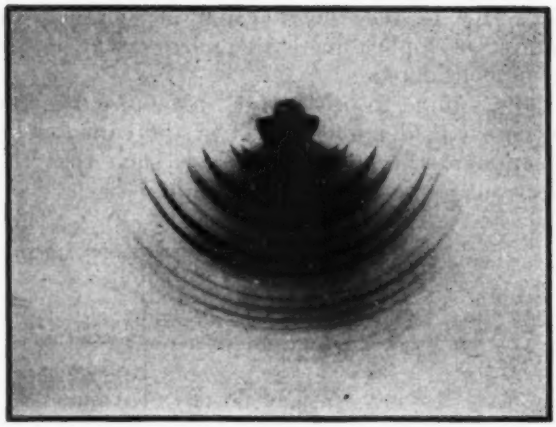

FIG. 7. Plate showing behavior of beam on insulating film with "spray gun." Sample: Sodium chloride on stainless steel block. Pattern present.

ACKNOWLEDGMENT

The author wishes to express her appreciation to Dr. David Harker, Mr. William Grams, and Mrs. Beulah Decker for helpful criticism and advice in the preparation of this paper.

[1] Jacob Millman and Samuel Seely, *Electronics* (McGraw-Hill Book Company, Inc., New York and London, 1941), pp. 173–175.

Crystal Interference Phenomena in Electron Microscope Images

R. D. HEIDENREICH AND L. STURKEY
The Dow Chemical Company, Midland, Michigan

(Received September 23, 1944)

The observation of electron reflections in electron microscope images is reviewed and further data are presented. The observations of the reflected beams with the objective limiting diaphragm removed and the determination of the planes responsible for the reflections by this means are described. The results of the dynamical theory of electron diffraction are briefly discussed and the values of the "characteristic" crystal thickness D_0 are computed. These values of D_0 are compared with the experimental values and are in reasonably good agreement for the MgO (200) reflections at 60, 96, and 103 kv, MgO (220) reflections and CdO (200) reflections at 60 kv. The dynamical theory accounts satisfactorily for the intensity variations except as modified by inelastic scattering and the results may be considered as experimental verification of the theory.

INTRODUCTION

NUMEROUS instances of "anomalous" intensity variations in electron microscope images of crystalline materials have been reported during the past few years. The term "anomalous" refers to the fact that the observations could not be explained on a simple mass-thickness variation to which the ordinary formulae could be applied.[1,2] Observations on the alteration in transmitted intensity in chromic oxide smoke[3] when the illuminating aperture was varied, Bragg reflections by local regions of Gibbsite crystals,[4] and the regular intensity maxima and minima in images of properly oriented magnesium oxide crystals[5,6] are among the instances in which crystal reflections were noted. Boersch[7–9] has published several examples of crystal interference effects with a qualitative explanation of the observations. Kossel[10] has offered an explanation of the striations observed by Kinder[6] based on the dynamical theory of diffraction developed by Bethe[11] and MacGillavry.[12] Earlier work by Kossel and Möllenstedt[13,14] on directing convergent electron beams through mica crystals of different thicknesses indicated that the intensity of the transmitted beam was dependent upon the orientation and thickness of the crystal.

It is the purpose of this paper to present electron micrographs further illustrating the occurrence and consequences of electron reflections in crystals and to show how the observations can be accounted for by diffraction theory.

EXPERIMENTAL OBSERVATIONS

It has been noted numerous times that changing the angle of illumination in the electron microscope resulted in alterations of intensity in the images of crystals such as those of MgO smoke shown in Fig. 1. If the aperture of the illuminating beam is maintained constant and the orientation of the crystal is changed relative to the optic axis of the instrument such as in taking stereomicrographs, the phenomena illustrated in Fig. 2a and Fig. 2b are often observed. Examination of Fig. 2 will show that although the general crystal shapes are easily recognizable in the individuals of the stereo pair, the internal markings and average intensity may be considerably different, indicating that the transmitted intensity is quite sensitive to orientation and that the markings do not originate with actual thickness variations within the crystal.

In the case of crystals which form with a

[1] M. v. Ardenne, *Elektronen—Uber mikroskopie* (Julius Springer, Berlin, 1940).
[2] L. Marton and L. I. Schiff, J. App. Phys. **12**, 759 (1941).
[3] B. v. Borries and E. Ruska, Naturwiss. **28**, 366 (1940).
[4] J. Hillier and R. F. Baker, Phys. Rev. **61**, 722 (1942).
[5] R. D. Heidenreich, Phys. Rev. **62**, 291 (1942).
[6] E. Kinder, Naturwiss. **31**, 149 (1943).
[7] H. Boersch, Zeits. f. Physik **118**, 706 (1942).
[8] H. Boersch, Zeits. f. Physik **121**, 746 (1943).
[9] H. Boersch, Kolloid Zeits. **106**, 169 (1944).
[10] W. Kossel, Naturwiss. **31**, 323 (1943).
[11] H. A. Bethe, Ann. d. Physik **87**, 55 (1928).
[12] C. H. MacGillavry, Physica **7**, 334 (1940).
[13] W. Kossel and G. Möllenstedt, Naturwiss. **26**, 660 (1938).
[14] W. Kossel and G. Möllenstedt, Ann. d. Physik **42**, 287 (1943).

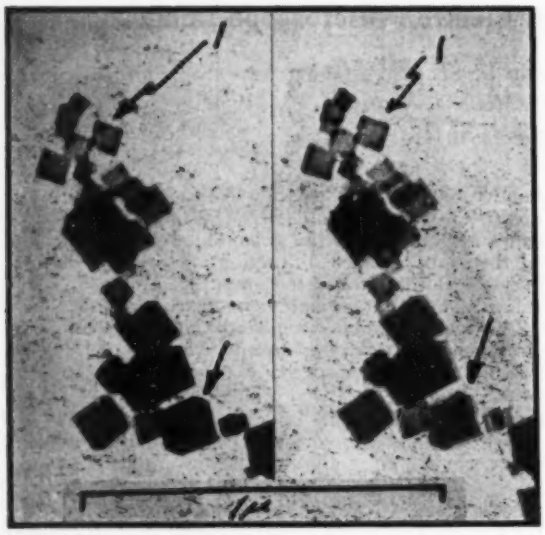

FIG. 1. Effect of change in illuminating aperture on intensity in image of MgO crystals. Prints adjusted so that crystal *I* is of same density in both. 60 kv·$\alpha_{ob} \simeq 3\times10^{-3}$.

regular habit, such as MgO smoke, equally spaced intensity maxima and minima[5,6] are observed in the images as seen in Fig. 3a, Fig. 3b, and Fig. 3c. These striations are not observed unless the crystals are precisely oriented with respect to the electron beam. They are regularly spaced when the crystal is in the form of a wedge whose sides are planar. If the crystal thickness does not change linearly, such striations would be expected to exhibit a variable spacing[15] as will be seen.

The reason these intensity maxima and minima occur in the image is to be found in the fact that all the pictures presented thus far have been taken with an objective limiting diaphragm in the objective lens intercepting a half-angle of $\alpha_{ob} \simeq 10^{-3}$ radian at the specimen plane. Any beams leaving the crystal at angles greater than α_{ob} are removed from the optical system and hence are not recorded in the image. Figure 4 illustrates the situation with the beam incident upon a thin crystal at the Bragg angle giving rise to a transmitted and reflected beam.

If the beam I_0 is incident upon the crystal at the Bragg angle θ_0 with a set of net planes, then the reflected beam leaves the crystal at an angle $2\theta_0$ with the optic axis where θ_0 is given by $n\lambda = 2d \sin\theta_0$. The case of an illuminating aperture other than zero will be considered later.

If Fig. 4 correctly describes the process giving rise to the observations, then two cases present themselves. In one case, $2\theta_0 > \alpha_{ob}$ and in the other, $2\theta_0 < \alpha_{ob}$. For 60-kv electrons with $\lambda = 0.05$A and considering only first-order and single reflections, it is evident that reflected beams will be excluded from the image for interplanar spacings such that

$$\frac{0.05}{d} > \alpha_{ob}, \quad d < \frac{0.05}{\alpha_{ob}}, \tag{1}$$

or for spacings $d < 34$A if $\alpha_{obj} = 3\times10^{-3}$ radian. Thus, except for reflections that might arise because of some very long spacings, reflected beams from ordinary crystals do not enter the objective aperture with so small a diaphragm present. This view can be checked by removing the objective diaphragm so that the reflected beams are recorded in the image plane. If the microscope is thrown out of focus, the reflected and transmitted images will separate depending upon the distance between the specimen plane and focal plane and upon $2\theta_0$. Even in best focus, however, the transmitted and reflected images do not coincide because of spherical aberration of the lens.

Figure 5 shows a sequence of "extra-focal"* micrographs of molybdenum oxide smoke crystals taken with the objective diaphragm removed and clearly show the reflected beams. It is now evident that in an ordinary micrograph taken with a limiting objective diaphragm the transmitted intensity in the image of a given crystal will depend, first of all, upon the orientation of crystal and beam. If the incident beam does not enter the crystal near the Bragg angle for a set of planes, then the intensity in the image is determined by the incoherent scattering. At the Bragg angle, however, the transmitted intensity may be very small (depending upon the thickness) giving the impression that the crystal is thick. This effect is analogous to the phenomenon of primary extinction in the case of x-rays. Micrographs similar to Fig. 5 have been published by Boersch[8] in which the reflected images have been termed "Nebenbilder."

Some crystals of molybdenum oxide smoke

[15] M. v. Ardenne, Zeits. f. Physik **116**, 736 (1940).

* Here "extra-focal" means that focal plane and specimen plane do not coincide.

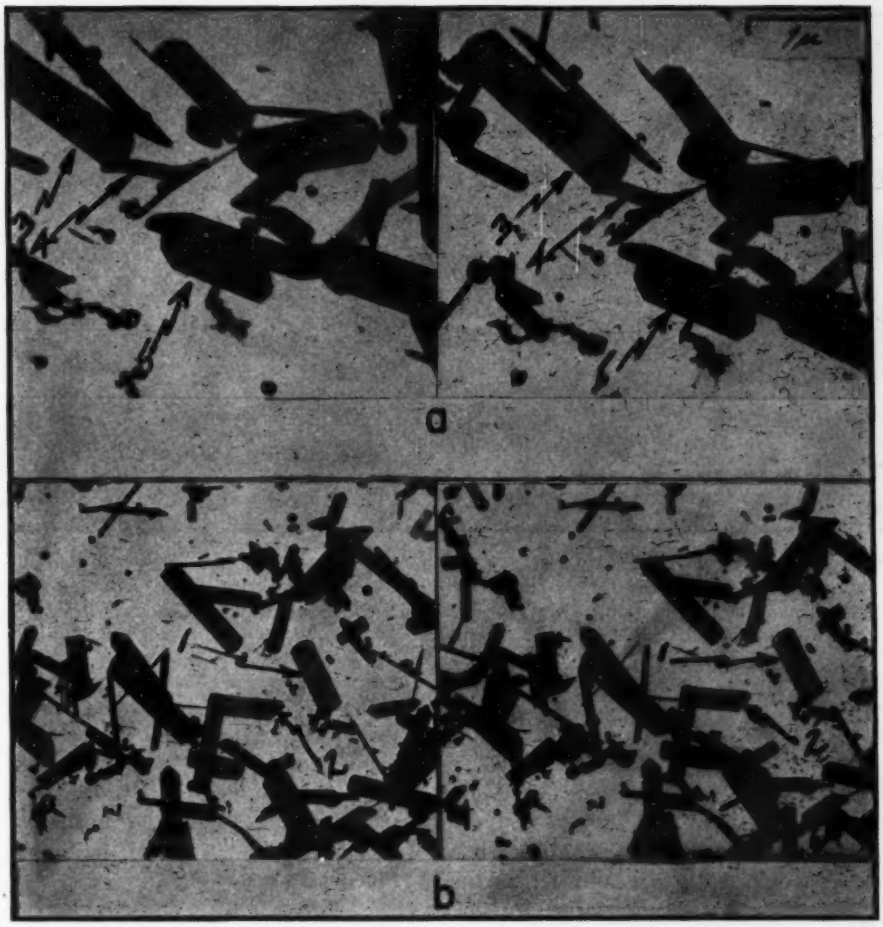

FIG. 2. Stereomicrographs of molybdenum oxide smoke crystals illustrating effect of orientation on intensity. 60 kv·$\alpha_{ob} \backsimeq 3\times10^{-3}$. (a) Stereo angle; $\sigma = \pm 10°$. (b) Stereo angle; $\sigma = \pm 4° 58'$ (5700×).

exhibit an interesting interior pattern. This pattern is illustrated in the transmitted image in Fig. 6a, and in the reflected image in Fig. 6b. A second-order reflection is also seen in Fig. 6b, as identified by the interior markings. The patterns are likely caused by orientation changes within the crystal, since changing the angle of illumination completely changes the pattern in cases where this has been tried.

Finally, in Fig. 7 is shown a micrograph of MgO crystals taken with the objective diaphragm removed and printed to illustrate both the reflected and transmitted images. Crystal *1* corresponds to the orientation of Fig. 3a, while the reflected image from crystal *2* can be faintly seen and corresponds to the orientation of Fig. 3c.

In order to check the observations against theory, it is necessary to know what planes are responsible for the reflections. From the orientation of the crystal and the direction of displacement of the reflected beam, it is not difficult to deduce the set of planes operative. A single extra-focal micrograph is not sufficient, however, in the case of a crystal such as *2* in Fig. 7. A sequence of extra-focal images, through focus, will make the direction of displacement evident. The arrows in Fig. 7 between the transmitted and reflected images indicate the directions of motion of the reflected images determined from a sequence of four extra-focal micrographs. Even in best focus, however, the reflected and transmitted images do not exactly coincide. The displacement is evident in Fig. 7, where the

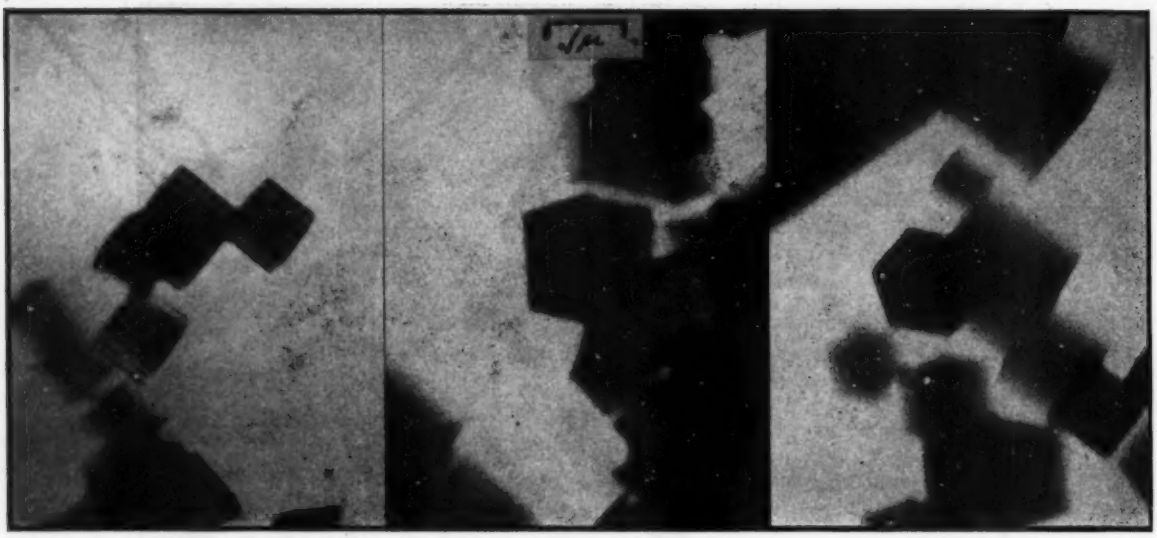

(a) (b) (c)

FIG. 3. Intensity maxima and minima in MgO crystals illustrating different orientations and reflection planes. 60 kv·$\alpha_{ob} \leqq 3\times10^{-3}$. (a) (200) reflections. (b) (220) reflections. (c) (220) reflections.

reflected image of crystal *1* obviously does not line up with the transmitted image.

The thickness increments between two successive maxima or minima, Fig. 7, for a given crystal are of chief interest here. Denote this "characteristic" thickness by D_0 and let s_0 be the spacing of the striations measured in the micrograph. Table I will then serve to summarize the information obtained from the micrographs. The spacings s_0 were all measured on in-focus images.

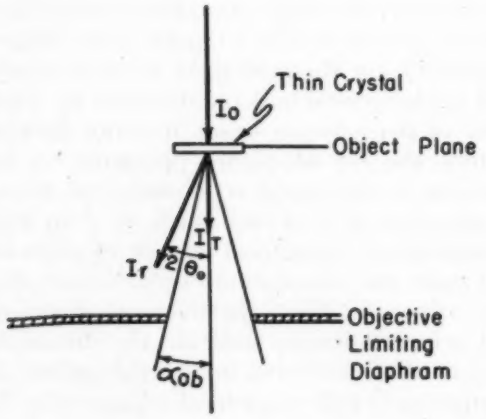

FIG. 4. Reflected and transmitted beams relative to small objective diaphragm. I_r = Reflected beam. I_T = Transmitted beam. θ_0 = Bragg angle.

It would be desirable to have data for many more crystals but a severe limitation is set by the necessity for regular habit, such as exhibited by MgO and CdO smokes, so that the relation between spacing and thickness is accurately known. MgO and CdO have different lattice constants, however, and even more important, their scattering cross sections are considerably different. Consequently, they should constitute a reasonably good check of the theory.

TABLE I. $E=60$ kv. $\lambda=0.05$A.

Crystal	(*hkl*)	s_0	D_0	
MgO	(200)	210A	$2s_0=420$A	Fig. 3a
	(220)	300	$2s_0=600$	Fig. 3b
		200	$\sqrt{6}s_0=500$	Fig. 3c
CdO	(200)	125	$2s_0=250$	

s_0 = measured spacing. Error is ±10 percent.
D_0 = characteristic thickness.

THEORY

In the first report[5] describing the equally spaced intensity maxima and minima, it was suggested that the phenomena were explicable on a geometrical basis utilizing a process of mul-

FIG. 6. Transmitted and reflected images in extra-focal micrographs of molybdenum oxide smoke showing internal markings. 60 kv. Diaphragm removed.

tiple reflections. The relation $D_0=\Delta t=j(4d^2/\lambda)$ was derived for the characteristic thickness where j was a number. A more fundamental explanation is highly desirable. The dynamical theory of electron diffraction offers a method of dealing with the results wherein numerical values of the spacing of the maxima and minima can be obtained. On the other hand, the dynami-

FIG. 5. Extra-focal sequence showing reflected images in molybdenum oxide crystals. 60 kv. Diaphragm removed.

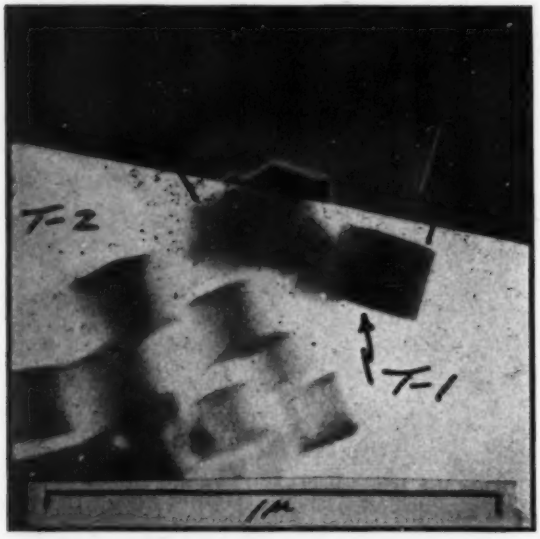

FIG. 7. Transmitted and reflected images of MgO crystals. 60 kv. Diaphragm removed.

cal theory has not been positively confirmed[16,17] by ordinary diffraction experiments and hence the data obtained from the electron micrographs may be considered as a partial test of the dynamical theory.

The problem of the dynamical theory[11,12,16,17] is the solution of the wave equation for an electron wave front incident upon a crystal. The potential of an electron in the crystal is represented as a three-dimensional Fourier series and the Schrödinger equation written as

$$\nabla^2\Psi+\left(\frac{8\pi^2me}{h^2}E+\sum_g v_g e^{2\pi i(g\cdot r)}\right)\Psi=0, \quad (2)$$

where g is a vector to a point of the reciprocal lattice and r is the position vector. The solution of (2) for an electron wave incident upon a thin crystal of infinite extent and thickness D with the application of the usual boundary conditions has been carried out by MacGillavry.[12] The final expression obtained for the intensity of the reflected beam after incorporating several approximations is given by him as

$$\frac{I_r}{I_0}=\left\{\frac{v_g}{K^2}\frac{\sin\frac{1}{2}KD\left[(\theta-\theta_0)^2\sin^2 2\theta_0+\frac{v_g^2}{K^4}\right]^{\frac{1}{2}}}{\left[(\theta-\theta_0)^2\sin^2 2\theta_0+\frac{v_g^2}{K^4}\right]^{\frac{1}{2}}}\right\}^2, \quad (3)$$

where $v_g=\frac{8\pi^2me}{h^2}V_{hkl}$ and V_{hkl} is the Fourier coefficient of potential for the (hkl) plane, $K/2\pi=1/\lambda=$wave number, $D=$thickness of crystal, $\theta=$angle between incident beam and planes (hkl), $\theta_0=$Bragg angle for planes (hkl), and $\theta-\theta_0=$deviation from Bragg angle. Values of V_{hkl} are computed from the relation

$$V_{hkl}=\frac{d_{hkl}^2e}{\pi R}\sum_j (Z_j-f_j)\exp\left[2\pi i(g_{hkl}\cdot r_j)\right], \quad (4)$$

where $R=$volume of unit cell, $\sum_j=$electronic structure factor, $d_{hkl}=$interplanar spacing, and $e=$electronic charge.

Equation (3) can be conveniently written in the form

$$\frac{I_r}{I_0}=\frac{V_{hkl}^2}{E^2\gamma^2}\sin^2\pi\frac{D}{D_0};\quad D_0=\frac{\lambda}{\gamma}, \quad (5)$$

with

$$\gamma=\left[(\theta-\theta_0)^2\frac{\lambda^2}{d^2}+\frac{V_{hkl}^2}{E^2}\right]^{\frac{1}{2}},$$

where E is the accelerating potential applied to the incident beam.

If the beam is incident upon the crystal such that $\theta=\theta_0$ then the reflected intensity is

$$\frac{I_r}{I_0}=\sin^2\pi\frac{D}{D_0}\quad\text{with}\quad D_0=\frac{\lambda E}{V_{hkl}}. \quad (6)$$

Equation (5) is restricted to an incident plane-parallel wave and only a single strong reflected wave is assumed. Inelastic scattering is neglected with the result that the periodic reflected intensity is of amplitude unity, which, of course, is not correct. Even so, Eq. (6) yields values of D_0 which check surprisingly well with observed values in Table I. Table II summarizes the calculations for incidence at the Bragg angle. Considering that D_0 is quite sensitive to deviations from the Bragg angle, the agreement between theory and experiment is quite good so far.

It appeared rather significant that in all the micrographs taken under various conditions over

[16] G. P. Thompson and W. Cochrane, *Theory and Practice of Electron Diffraction* (The Macmillan Company, 1939), Chapter 19.

[17] R. Beeching, *Electron Diffraction* (Methuen and Company, Ltd., London, 1936), p. 65.

the past two years, the spacing of the bands was always the same within experimental error when they were observed. In ordinary electron diffraction reflection experiments, observable intensities are obtained even when the incident beam deviates as much as half a degree from the Bragg angle. This has been pointed out by Beeching[17] in the case of diamond and taken as evidence against the dynamical theory since theory predicts nearly zero intensity when the deviation from the Bragg angle exceeds about two minutes. It is possible that either surface fragmentation or electrical charging up, or both, is responsible for the observations of Beeching.

The effect of deviations from the Bragg angle upon both the intensity and values of D_0 as computed from Eq. (5) is shown in Fig. 8 for (200) reflections in MgO. As stated before, these calculations neglect inelastic scattering which

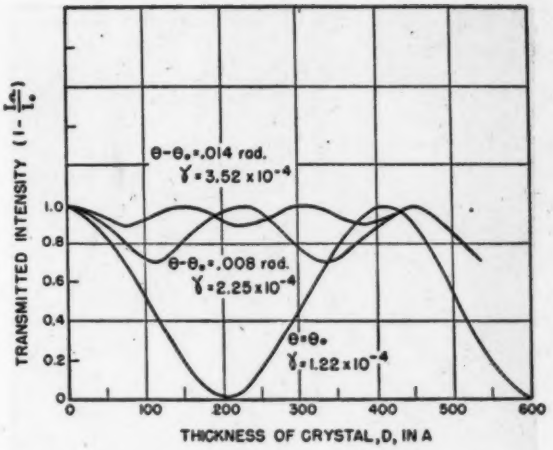

FIG. 8. Effect of deviation from the Bragg angle upon intensity and values of D_0 as computed from Eq. (5) for (200) reflection of MgO. 60-kv electrons.

TABLE II. $E=60$ kv. $\lambda=0.05$A.

Crystal	(hkl)	*V_{hkl}	D_0 (calc.)	D_0 (obs.)	
MgO	(111)	1.56 volts	1940A		
	(200)	7.42	410	420A	Fig. 3a
	(220)	5.37	560	600	Fig. 3b
				500	Fig. 3c
CdO	(200)	13.9	216	250	
	(220)	9.78	310		

* Temperature correction neglected.

would alter the transmitted intensity at the Bragg angle as illustrated in Fig. 9. Now if a change in relative intensity of about 0.1 is the smallest difference that can be observed on the photographic plate it would follow that the value $\theta-\theta_0=0.014$ radian would be sufficient to bring about extinction of the maxima and minima as far as observation is concerned. If inelastic scattering were included, this lower limit might be decreased to 0.01 radian or below for MgO, but it would still be expected that values of s_0 down to perhaps 150A could be observed. There is still another factor to be considered, though, and that is the angular aperture of the incident beam since the actual illumination is not plane-parallel. If the axis of the illuminating beam entered the crystal at the Bragg angle there would still be electrons entering with a maximum deviation from the Bragg angle of α_c, where α_c is the half-angle of the illuminating aperture. A continuous range of D_0 values from 420A down to about 300A would be obtained, thus broadening the bands and reducing the intensity. Now the average value of s_0 is 210A$\pm$25A, so the value of D_0 would have to fall to about 350A before it could be positively detected. Considering all of these factors, it is unlikely that a reduction in D_0 would be detected before the intensities fell below the minimum value that can be observed.

The results of Kinder[6] were explained by Kossel[10] on the assumption that the reflections were (220) where a value of $D_0=700$A would be expected at the Bragg angle. The observed value was 400A with the result that Kossel com-

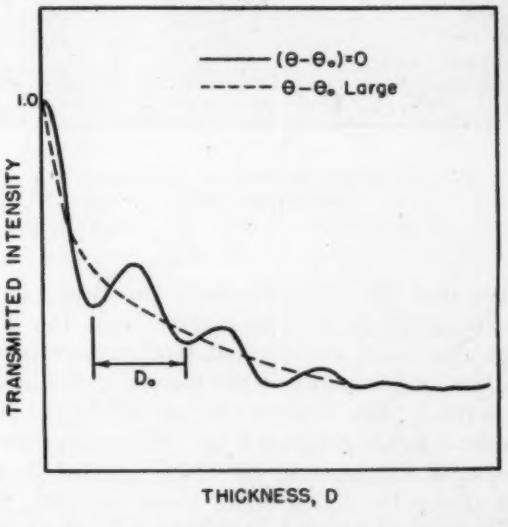

FIG. 9. Intensity distribution in transmitted image with absorption taken into account (qualitative).

FIG. 10. Localized reflections or contour lines in split mica sheet.

puted that the deviation from the Bragg angle [θ_0 for (220) is 44′] must have been 13′. This large deviation would most likely result in extinction of the bands if the foregoing discussion is correct. Since there is no evidence that Kinder's bands resulted from (220) reflections it is more likely that they are (200) as concluded in this paper for the spacing given by him. For 96-kv electrons with $\lambda = 0.038$A, the value of D_0 for (200) reflections at the Bragg angle is 460A as computed from Eq. (6) which is in reasonably good agreement with the observed value. This is additional evidence for the dynamical theory.

Boersch[8] has recently exhibited a micrograph of a MgO crystal showing the reflected image similar to Fig. 7. The value of s_0 measured from his image is 250A so that the experimental D_0 is 500A. The micrograph was taken with 103-kv electrons giving a theoretical value of $D_0 = (0.037 \times 103{,}000)/7.42 = 510$A, if incidence at the Bragg angle is assumed. Again, the agreement is as good as can be expected and the theory checks the experimental results for 60-, 96-, and 103-kv electrons.

There is, at present, no evidence from the electron micrographs that large deviations from the Bragg angle give rise to crystalline reflections. Under these circumstances, the intensity in the image should depend almost entirely on incoherent scattering following a law of the form $e^{-\beta D}$, where β is the total cross section for scattering and D the thickness. Figure 9 illustrates this point.

Examination of numerous micrographs such as shown in Fig. 6 indicate that the assumption of a single strong reflected beam in the crystal is not always correct and may lead to errors in computing the reflected intensity in a particular image.

GENERAL CONSIDERATIONS

The foregoing experimental results and theory indicate that it is possible to obtain considerable information concerning crystalline materials by means of electron microscope images. The experimental procedure would include observation with varying illuminating aperture, varying objective aperture, and different orientations of the crystal as in stereomicrographs. This is not convenient with the standard microscope but a modified instrument could make possible a detailed analysis of thin crystals.

There are two main considerations in interpreting markings and intensities in images of these crystals: (a) Orientation of the crystal with respect to beam, and (b) thickness of the crystal. By varying the illuminating aperture or orientation of the crystal to obtain images with very low reflected intensities, the question of thickness variations in a crystal rests upon detection by means of inelastic scattering. As previously mentioned, the internal markings in the molybdenum oxide crystals were concluded to be a result of

change in orientation rather than change in thickness. These crystals are hence not perfect single crystals but possess a kind of "lineage" structure. In addition, the crystals may be warped or bent such that local regions are oriented at nearly the Bragg angle as evidenced by crystal *4* in Fig. 2a. These "contour lines" in crystal *1* of Fig. 2b are again consistent with the conclusion that only a small deviation from the Bragg angle is required to extinguish a reflection. This is based on the sharpness of the contour lines, which very often do not shade out gradually as would be expected if large deviations were permissible.

A final example is shown in Fig. 10a. This is a micrograph of split mica taken with an objective aperture of about 10^{-3} radian. Boersch[7] has exhibited dark field micrographs demonstrating a similar pattern but not so pronounced. The dark contour lines in Fig. 10 appear bright in dark field and are caused by reflections from regions where incidence at the Bragg angle occurs. It was noticed that these patterns could be varied both by altering the illuminating aperture and by changing the intensity of the incident beam. It seems likely that the crystal is badly distorted because of heating by inelastic collisions or that charging up affects the angle of incidence.

That the regions of reflection can be very localized is illustrated in Fig. 10b where a curious pattern has been obtained. Contour lines less than 100A in width are present and if these are caused by orientation changes, only a small deviation from the Bragg angle is necessary to bring about extinction of the reflection.

It is hoped that results for other crystals with regular habit can be obtained in order to check further the dynamical theory and that more critical observations of images of crystals will be made as a result of this work.

Sustained Subharmonic Response in Non-Linear Series Circuits

CHARLES F. SPITZER
Department of Electrical Engineering, Yale University, New Haven, Connecticut

(Received September 27, 1944)

This paper presents an experimental analysis of oscillatory current responses peculiar to certain types of non-linear series circuits containing resistance, inductance, and capacitance. Methods of initiating the oscillations, and the effect of the boundary conditions necessary to sustain them, are summarized. This is followed by a discussion reviewing the effect of resistance and capacitance variation on sustained subharmonic response. For several values of capacitance, the effect of varying the inductor turns is presented in the form of curves. These curves are correlated in a plot of effective value of impressed voltage *versus* the product $N^2C^{1.5}$ (N is the number of turns on the inductor core, and C is the capacitance). The voltage across the inductor appears to consist of only two sinusoidal components, when the circuit undergoes subharmonic oscillations.

INTRODUCTION

BY definition, subharmonics are periodic oscillations of current whose lowest frequency component completes one cycle while the sinusoidal impressed voltage completes two or more cycles. Since the circuit contains a non-linear element, the subharmonic currents are non-sinusoidal. If several critical boundary conditions are fulfilled, the non-sinusoidal current through a circuit consisting of resistor, capacitor, and saturable inductor may, for example, have a component of half the frequency of the impressed voltage. Such a current would then be termed "subharmonic of the second order." In a similar manner there may exist subharmonics of the third, fourth, fifth, sixth, seventh order, etc.

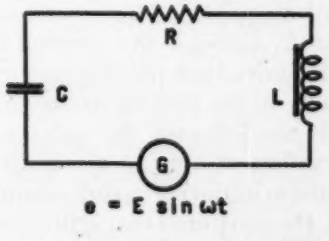

FIG. 1. Basic circuit permitting subharmonic response.

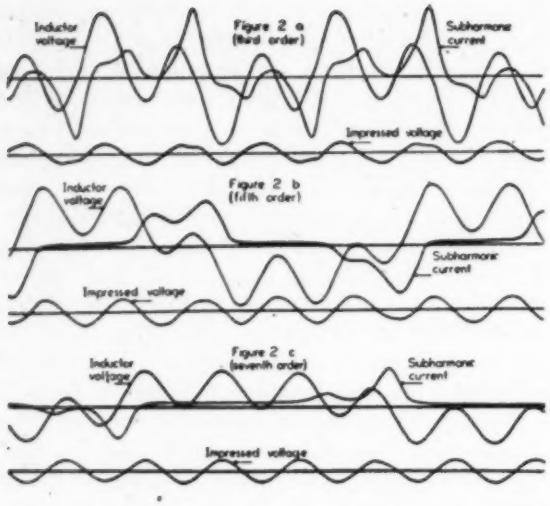

FIG. 2. Oscillograms of subharmonic currents of orders three, five, and seven, showing waves of current, inductor voltage and impressed voltage.

Oscillograms of such currents have been published elsewhere.[2, 4, 8, 10, 11, 13, 19] The oscillograms of Fig. 2 also reveal the presence of third-, fifth-, and seventh-order subharmonics, in the circuit of Fig. 1.

Mathematical expressions defining the relations between current and voltage in non-linear circuits are usually unwieldy. Thus, precise solutions applicable to one and all non-linear circuits cannot be found, although approximate solutions have been presented.[16, 17]

Fallou,[2] one of the first investigators of the phenomenon, attempted to analyze the problem on an experimental basis; this plan has been followed by subsequent investigators.[8, 10, 11, 19, 21] Approximately ten years after Fallou reported his investigations, Rouelle[19] determined the effect of frequency variation on the subharmonic response of the circuit. The test circuit employed by Rouelle is shown in Fig. 3, the results of his work in Fig. 4. In the circuit of Fig. 3, the generator G supplies a sinusoidal voltage to the circuit consisting of capacitor C, iron-cored inductor L, and resistor R, through the transformer T. To facilitate the initiation of subharmonic oscillations, Rouelle made provisions to short circuit momentarily the inductor through a resistor R_1, since the random closing of the knife switch S was unreliable in initiating sustained subharmonic oscillations. He also found that still easier starting was achieved by the use of an auxiliary generator G_1, connected as shown in Fig. 3, and that the circuit can be forced to oscillate by impressing frequencies of subharmonic order on the inductor by means of this auxiliary generator. Oscillations created in this manner were found to persist even after the removal of the voltage supply produced by the generator G_1. This procedure of adjusting the frequency of the generator G_1 to a submultiple of the frequency of the generator G was termed "harmonic synchronization" by Rouelle.

INITIATION OF SUBHARMONIC OSCILLATIONS

In a non-linear circuit the initial, or boundary, conditions determine the possibility of producing sustained subharmonic oscillations.[16] This has been recognized both in theory and in practice. These initial conditions are: (a) initial flux linkages of the inductor; (b) initial capacitor charge; (c) applied voltage at the instant of energizing the subharmonic circuit (voltage switching angle).

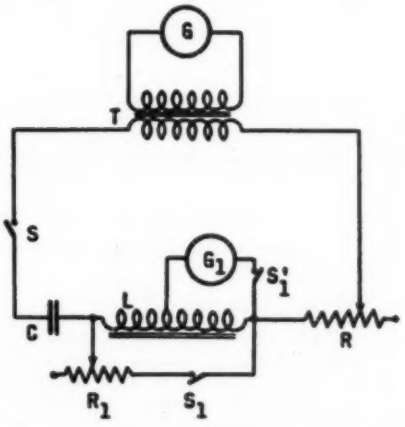

FIG. 3. Test circuit used by Rouelle: G = main generator; L = iron-cored inductor; C = capacitor; G_1 = auxiliary generator; T = transformer; S, S_1, S_1' = switches; R, R_1 = resistors.

Of these three boundary conditions, the influence of the initial flux linkages of the inductor is probably the most difficult to determine. Experiments have shown that demagnetization of the inductor core, prior to an attempt to initiate the subharmonic oscillations by means of placing a large initial charge on the condenser, had no observable effect on the ease with which the oscillations were initiated and maintained.

Under condition of subharmonic oscillation the voltage across the inductor appears to be made

up of only two sinusoidal components. This is illustrated in Fig. 2, and is also evident in the oscillograms published by previous investigators.[2,4,8,19,21] Corresponding to these voltages there must exist two sinusoidal components of flux in the inductor core. Energy in the magnetic field of the inductor is proportional to the square of the flux at any instant. Thus, if power is supplied to the non-linear circuit at twice subharmonic frequency, the initiation of sustained oscillations is facilitated. The circuit shown in Fig. 3 was devised by Rouelle to provide power at this particular frequency, through the auxiliary generator. This generator produces voltage at subharmonic frequency, and the power delivered is therefore of twice subharmonic frequency.

Another method that could be used to start sustained subharmonic response would be that of placing a certain minimum charge on the capacitor, prior to energizing the circuit. Figure 5 is a plot of the minimum capacitor charges that permitted sustained subharmonic oscillations.

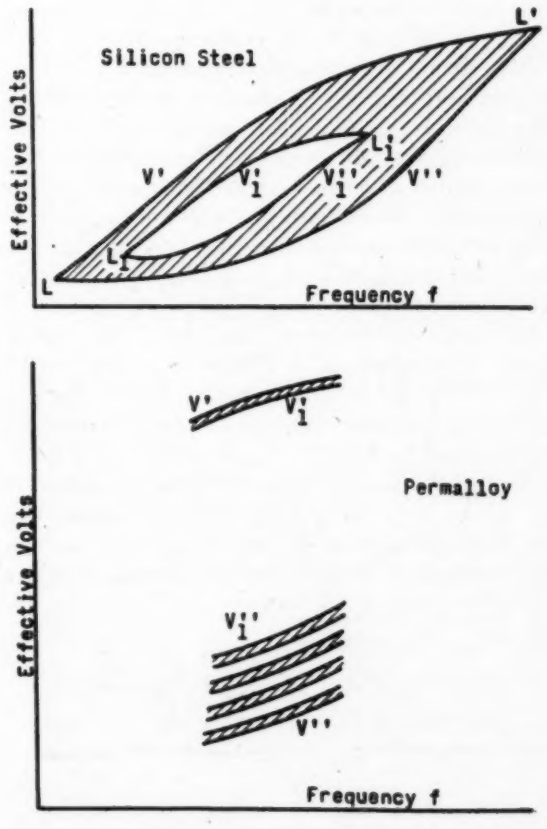

FIG. 4. Plot of voltage *versus* frequency for third-order subharmonic oscillations (after Rouelle).

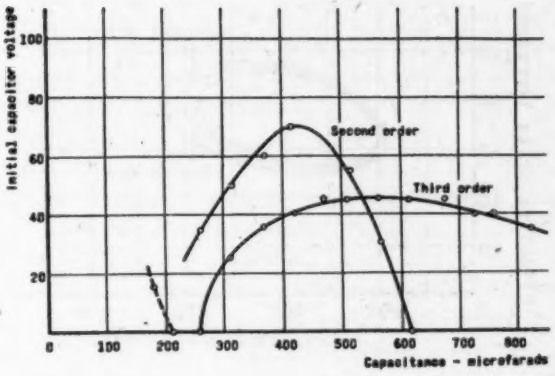

FIG. 5. Curves of minimum initial capacitor voltages permitting the initiation of subharmonic oscillations of orders three and two.

Smaller initial capacitor charges produced only transient oscillations which died out after a fraction of a second. The effective values of applied voltages for the various capacitances of Fig. 5 corresponded to the upper border of the lower range of voltages permitting sustained subharmonic oscillations, in Fig. 6. An effect similar to that of charging the capacitor initially is produced in the non-linear circuit by an instantaneous short circuit of the inductor. The high transient currents resulting from such an operation are likely to place high charges on the capacitor, facilitating the self-excitation of subharmonic oscillations. This process is called "shock excitation."

The method of starting the oscillations by means of initial capacitor charge is dependent on the voltage existing at the instant the circuit is energized (voltage switching angle). Indeed, it is found that no initial charge on the capacitor is required, if the non-linear circuit is energized at an instant at which the applied voltage is zero, or very small.[20,21]

If the non-linear circuit is dissipative, subharmonic oscillations can be sustained only if the amplitude of the impressed voltage lies between two definite limits. This can be seen from Figs. 4 and 6, and is also demonstrated by the oscillogram of Fig. 7, in which the capacitor was charged to a certain d.c. voltage, and discharged through a resistance-inductance series circuit. The voltage across the inductor-capacitor combination is equal to the resistor voltage, which is in turn proportional to the current recorded in Fig. 7. It can be seen from the oscillogram that the frequency of the current wave depends upon

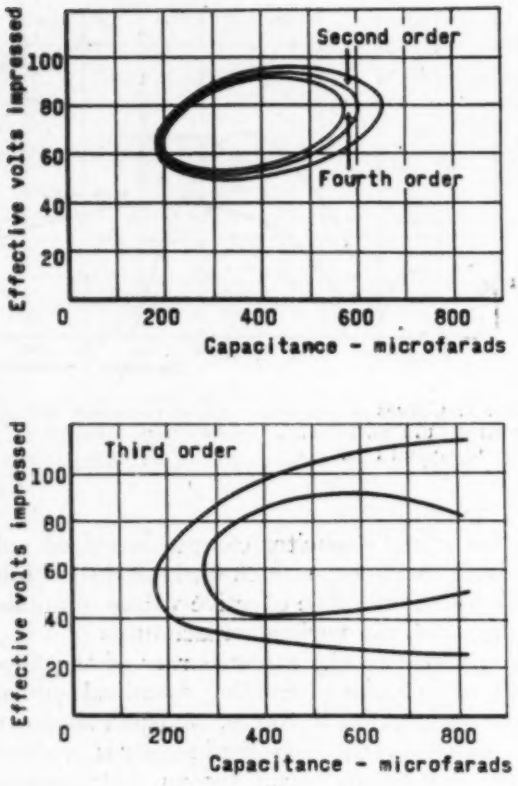

FIG. 6. Region of subharmonic responses of orders three, and two and four.

the voltage applied to the series circuit consisting of inductance and capacitance.

VARIATION OF CIRCUIT PARAMETERS

The simplest electrical circuit known to produce subharmonic oscillations consists of a resistor, a capacitor, and an iron-cored inductor connected in series. The effect of varying these parameters has been studied and reported by various authorities. Results of an investigation on the effect of resistance variation were presented by McCrumm,[19] who plotted curves of effective values of impressed voltages for which subharmonic oscillations could exist, as functions of the effective values of subharmonic currents, for various values of capacitances. These curves defined the region of sustained subharmonic response. Figure 6 shows a plot similar to those published by McCrumm, except that the effective values of voltages permitting sustained subharmonic response have here been plotted as functions of the circuit capacitance. The area between the two curves indicates the region of subharmonic currents. From McCrumm's results it can be concluded that the area between the two curves in Fig. 6 becomes narrower, if the resistance of the circuit is decreased. It might therefore be further concluded that the area would collapse to a line in the case of extremely small resistances. The oscillations would then be unstable, and the slightest fluctuation of applied voltage cause them to disappear. A moderate value of resistance helps to accentuate the non-linearity of the circuit, by distorting the voltage applied to the inductor-capacitor combination, while an excessive amount of resistance would load the circuit too much to permit sustained oscillations.

Since the flux in the inductor core is not a linear function of the magnetomotive force producing it, the concept of inductance is in this case subject to interpretation and cannot be clearly defined. However, inductance is related to the number of turns on the inductor core, and a variation of inductance could be obtained through a variation of the number of turns on the core. The curves of Fig. 8 show the voltage range of sustained subharmonic response as a function of the inductor turns and the circuit capacitance. It is evident from the variables illustrated in Fig. 8 that an increase of the number of turns on the inductor core extends the voltage ranges that permit subharmonic responses. Similarly, for any given number of turns on the core, an increase in capacitance also extends the voltage range.

An attempt to correlate the data of Fig. 8 is illustrated in Fig. 9. Various values were assumed for the exponents of the product N^aC^b (where N is the number of turns on the core, C the capacitance). The values of N^aC^b for the experimental points of Fig. 8 were then plotted *versus* effective values of impressed voltage. The best correlation was obtained by finally selecting $a=2$ and $b=1.5$; the loci of the points thus obtained are shown in Fig. 9. A curve indicating their proximity has been added, which becomes a straight line for the higher values of $N^2C^{1.5}$. Points corresponding to

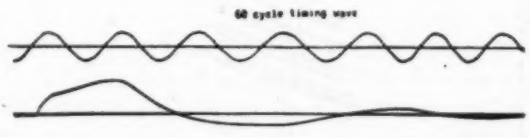

FIG. 7. Transient response, resulting from discharge of the initially charged capacitor through the subharmonic circuit. Note the change in period as the amplitude of the oscillatory current decreases.

circuits containing large capacitances lie outside the general pattern, which fact may be attributable to the excessive distortion of the originally sinusoidal wave form of applied voltage, owing to the large currents in such circuits. It is entirely possible that for oscillations of orders other than three and five, the exponents a and b might differ from the values of 2 and 1.5, respectively.

No regard was given to the change in resistance resulting from a change in number of turns on the inductor core, or to the residual flux linkages, which may also be important factors.

HYSTERESIS LOOP AND INDUCTOR VOLTAGE

Mathematical analysis based on sinusoidal impressed voltage has shown that in the absence of hysteresis effects in the inductor core, a retracing of the magnetization curve must take place several times in each cycle of impressed voltage, if subharmonic oscillations are to occur.[4,16,17] If hysteresis is present, the retraces will then be replaced by minor loops attached to the major hysteresis loop. This is shown by the illustrations of Fig. 10. Such loops can be produced artificially if two sinusoidal voltages of proper frequency ratio are impressed on the inductor simultaneously. This effect is shown by Fig. 11, which has qualitative value only, since fluxes were added directly, as were their respective magnetomotive forces. Impressing two sinusoidal voltages of the

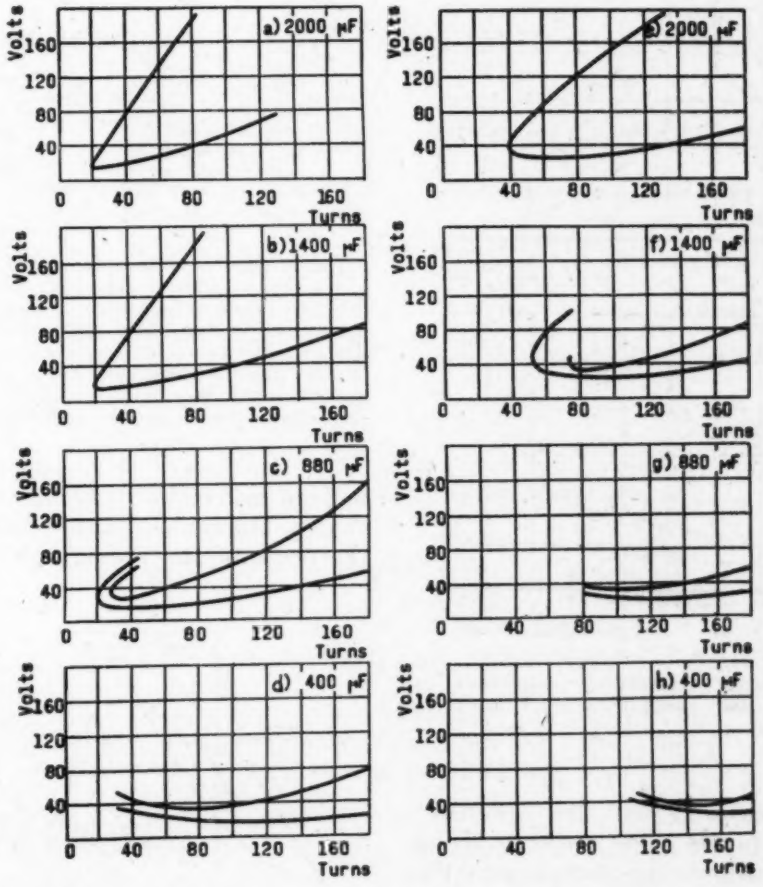

FIG. 8. Within the voltage regions of Figs. (a) to (d) subharmonic oscillations of the third order can be initiated and sustained. The circuit capacitances range from 2000 microfarads in Fig. (a) to 400 microfarads in Fig. (d). The graphs show the curves of critical voltages as functions of the number of turns on the inductor core. Figures (e) to (h) show curves of critical voltages as functions of the number of turns on the inductor core for sustained subharmonic oscillations of the fifth order.

proper frequency ratio upon the inductor to simulate subharmonic response approximates very closely the conditions obtained in the non-linear circuit, as can be seen from the inductor voltage waves of Fig. 2, and from similar curves shown in other articles on this subject.

SUMMARY

1. The extent of the ranges of effective values of impressed voltage for which subharmonic oscillations of a particular order can exist has been shown to depend upon the resistance, in any given non-linear circuit.[19] For extremely small resistances the two ranges corresponding to any

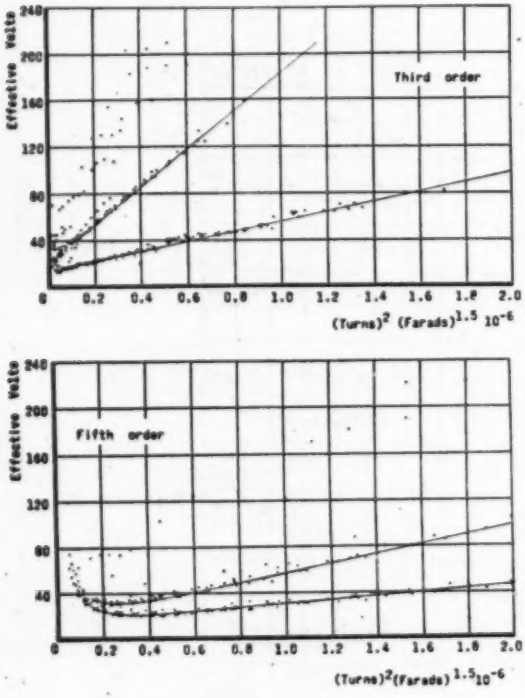

FIG. 9. Voltage ranges, correlating capacitance and number of turns on the inductor core, for third- and fifth-order oscillations.

one value of capacitance may be expected to collapse to two points. The series of points corresponding to various capacitances would then define the locus of voltages permitting sustained subharmonic response, but the oscillations would be unstable and disappear at the slightest voltage fluctuation.

2. For portions of these voltage ranges, the oscillations cannot be initiated and sustained

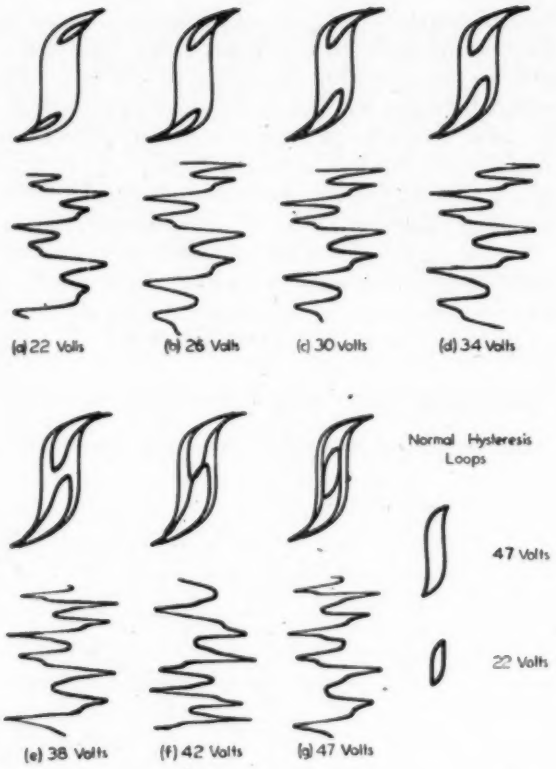

FIG. 10. Hysteresis loops during subharmonic oscillations of the third order. Figures (*a*) to (*g*) show increasing effective values of impressed voltage. With each loop are shown two cycles of the subharmonic exciting current. The current waves start at the bottom, with time increasing in the upward direction. There are 580 microfarads capacitance in the circuit, and 38 turns on the inductor core. The frequency of the applied voltage is 60 c.p.s.

without a certain minimum initial capacitor charge. The amount of this charge depends upon the order of the subharmonic, as well as the

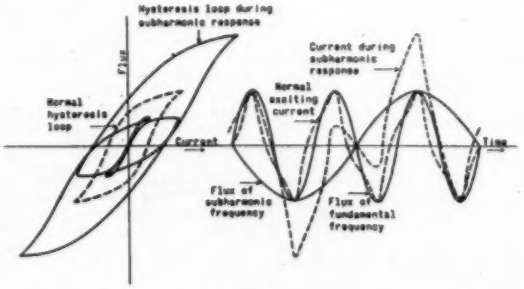

FIG. 11. Production of a major hysteresis loop with two minor loops through superposition of a flux of fundamental frequency and a flux of subharmonic frequency and their respective magnetomotive forces. This method has only qualitative value, since the principle of superposition is inapplicable to non-linear circuits.

instantaneous value of applied voltage at the moment of energizing the circuit.

3. Capacitance and number of turns on a given core can be correlated in a single plot for any value of both parameters. The resultant curves define the region within which subharmonic oscillations can be initiated and sustained, for all combinations of capacitance and number of turns on a given core.

4. The hysteresis loop during subharmonic response consists of a major loop, to which minor loops are attached. Also, the inductor voltage appears to consist of only two sinusoidal components, one of subharmonic frequency and one of the frequency of the applied voltage. Thus subharmonic response could be simulated by superposition on the inductor of two sinusoidal voltages of proper frequency ratio and amplitudes.

BIBLIOGRAPHY

(1) Lord Rayleigh, *Theory of Sound* (MacMillan and Company, 1894), second edition, Vol. 1, pp. 91–95.
(2) Jean Fallou, "Sur un demultiplicateur de frequency statique," Rev. Gen. de l'Elec. **19**, 987–991 (1926).
(3) Thomas Spooner, *Properties and Testing of Magnetic Materials* (McGraw-Hill Book Company, Inc., New York, 1927).
(4) E. A. Guillemin and P. P. Rumsey, "Frequency multiplication by shock excitation," Proc. I. R. E. **17**, 629–651 (1929).
(5) C. G. Suits, "Studies in non-linear circuits," Trans. A. I. E. E. **30**, 724–736 (1931).
(6) C. L. Dudley and E. H. Snyder, "Why not series capacitors for distribution feeders?" Elec. World **103**, 924–945 (1933).
(7) W. S. Hill, "Series capacitor improves 4150 volt line operation," Gen. Elec. Rev. **36**, 461–463 (1933).
(8) E. Aretz, "Mehrere stabile Gleichgewichtszustaende bei Reihenschaltung von Eisendrossel und Kondensator," Elektrotech. Zeits. **57**, 305–310 (1936).
(9) J. J. Lewis, "Series capacitor wipes out feeder flicker," Elec. World **106**, 3488–3490 (1936).
(10) Edmond Rouelle, "Quelques nouvelles experiences de demultiplication de frequence dans un circuit oscillant dont la bobine est a noyau de fer," Rev. Gen. de l'Elec. **40**, 811–819 (1936).
(11) E. Aretz, "Ueber das Wesen der stabilen Gleichgewichtszustaende bei Reihenschaltung von Eisendrossel und Kondensator," Elektrotech. Zeits. **58**, 1160–1162 (1937).
(12) R. C. Buell, "Improved voltage regulation with series capacitors," Gen. Elec. Rev. **40**, 174–179 (1937).
(13) J. W. Butler and C. Concordia, "Analysis of series capacitor application problems," Trans. A. I. E. E. **56**, 976–988 (1937).
(14) P. H. Odyssey and E. Weber, "Critical conditions in ferroresonance," Trans. A. I. E. E. **57**, 444–452 (1937).
(15) E. G. Keller, "Resonance theory of series non-linear control circuits," J. Frank. Inst. **225**, 561–577 (1938).
(16) Irven Travis and C. N. Weygandt, "Subharmonics in circuits containing iron-cored reactors," Trans. A. I. E. E. **57**, 423–431 (1938).
(17) Irven Travis, "Subharmonics in circuits containing iron-cored inductors, II," Trans. A. I. E. E. **58**, 735–746 (1939).
(18) Claude M. Summers, "An unstable non-linear circuit," Trans. A. I. E. E. **59**, 273–276 (1940).
(19) John D. McCrumm, "An experimental investigation of subharmonic currents," Trans. A. I. E. E. **60**, 533–540 (1941).
(20) Stephen J. Angello, "The effect of initial conditions on subharmonic currents in non-linear circuits," Trans. A. I. E. E. **61**, 625–627 (1942).
(21) Charles F. Spitzer and Thomas P. Evans, "Subharmonic oscillations and the effect of initial conditions on their initiation," Swarthmore College thesis (1942).
(22) E. C. Starr and R. D. Evans, "Series capacitors for transmission lines," Trans. A. I. E. E. **61**, 963–973 (1942).
(23) R. B. Bodine, C. Concordia and G. Kron, "Self-excited oscillations of capacitor compensated long distance transmission systems," Trans. A. I. E. E. **62**, 58–65 (1943).

An X-Ray Diffraction Study of the Fatigue in Metals at High Stresses

ARTHUR G. BARKOW
Physical Laboratories, Marquette University, Milwaukee, Wisconsin

(Received September 30, 1944)

INTRODUCTION

THE study and analysis of fatigue in rapidly rotating machine parts are of the utmost importance. To be able to indicate fatigue or to predict failure would be of tremendous help to the designing engineers and metallurgist. A large percentage of numerous experimental studies of fatiguing of metals consists of subjecting the samples to repeated cycles of stress and recording the number of cycles required to cause failure. The application of x-ray diffraction to this problem requires a diffraction picture to be taken after a definite number of cycles; and the effects on the crystals, i.e., rotation of grains, fragmentation, strain, etc. are analyzed. The study of fatigue by means of x-ray diffraction have met

with varied results. The present investigation was performed on an aluminum alloy, 14 ST.

Commercial metals are composed of aggregations of small crystals with random orientations. The crystals themselves are usually non-isotropic. Experiments indicate that some crystals in a stressed piece of metal reach their limit of elastic action sooner than others, owing, no doubt, to their unfavorable orientation, which permits slip to occur. Also, the distribution of stress from crystal to crystal within a piece of stressed metal is probably uniform; and when a piece is subjected to cyclic stress variation, the constituent particles tend to move slightly with respect to one another. This movement finally weakens some minute element to such an extent that it ruptures. In the zone of failure a stress concentration develops, and with successive repetitions of stress the fracture spreads from this nucleus across the entire section. Fatigue failures occur suddenly without any appreciable deformation, and the fracture is coarsely crystalline as in the case of a static failure of cast iron or brittle steel. The appearance of the fracture and the characteristic suddenness with which failure occurs gave rise to a theory of cold crystallization of metal. There are still those who refer to metal that has failed by fatigue as having become "crystallized." Many experiments have shown that this idea is incorrect, although it is fostered by the fact that sudden failures display the crystalline structure of a metal, which, in the case of gradual failure as in a static test, is disguised by the distortion of the piece owing to its ductility.

Fatiguing of a specimen might be expected to cause any one, or all, of the following reactions: (1) Radial streaks on a Laue pattern because of distorted or bent single crystal or large-grained aggregates. (2) Permanent rearrangement of Laue spots by rotation or reorientation of grains upon the application of large stresses. (3) Fragmentation of large crystals. (4) Broadening of line width. (5) Aligning of grains in a preferred orientation or fiber structure.

In the case where the specimen possesses large crystals, all of the above reactions, with the exception of (4) and (5), will produce a detectable change in the x-ray diffraction picture.

In the present investigation special emphasis was placed on (1), (2), and (3), since the aluminum alloy used possessed large-grained aggregates and hence, the strain, fragmentation, and rotation of spots could be easily observed.

X-ray diffraction studies of the fatigue in metals under repeated stresses have been subject to various tests by numerous investigators. Gough and Wood[1,2] have conducted a series of fatigue experiments on normalized and cold-rolled mild steel (0.1 percent C). Their fatigue tests were of three distinct types involving cycles of reversed torsional stresses, cycles of reversed direct stresses, and cycles of alternating direct stresses. It was found that the diffraction pattern of the specimen subjected to cycles of a safe range of stress was practically identical with that of the unstressed material. In the unsafe range, however, the formation of the pattern differed distinctly. The pattern showed changes in the number of reflection spots, blurring and elongation of individual spots and the production of continuous lines; these changes were progressively more marked when greater values of applied stress were used. A further examination at different depths after the surface had been etched away showed no appreciable change from the state of the specimen at the surface. They concluded that the unsafe range is distinguished from the safe range by changes in the structure of the grains which affect the diffraction pattern. These changes start with the dislocation of the grains and end in their complete breakdown, depending, to a degree, on the applied range of stress.

The work of Wever and Möller[3] was performed on specimens subjected to cyclic stresses. A small spot on the surface was etched and the specimen locked in the x-ray camera so that this etched spot was always irradiated. They concluded that they can differentiate between safe and unsafe stresses. Wever, Hemple, and Möller[4] working with specimens of cold-worked steel conclude that they can differentiate between safe and unsafe stresses.

A rather extensive investigation of fatigue in metals by x-ray diffraction has been carried out by Barrett[5–7] using both steel and aluminum alloys and copper specimens. Barrett found that for specimens fatigued at stresses above the

[1] H. J. Gough and W. A. Wood, Proc. Roy. Soc. **A154**, 510–539 (1936).
[2] H. J. Gough and W. A. Wood, Proc. Roy. Soc. **A165**, 358–371 (1938).
[3] F. Wever and H. Möller, Naturwiss. **25**, 449 (1937).
[4] Wever, Hemple, and Möller, Arch. Eisenhütt. **11**, 313–318 (1937–38).
[5] C. S. Barrett, Metals and Alloys **8**, 13 (1937).
[6] C. S. Barrett, Metals Prog. **32**, 677 (1937).
[7] C. S. Barrett, Trans. A. S. M. **25**, 1115 (1937).

endurance limit there was only a slight blurring of spots as the number of cycles increased. There was severe distortion of the grains at the surface of a fatigue break and at the ends of a fatigue crack. In areas slightly removed from these places the grains were less distorted. The distortion is equal at all places of equal stress and decreases with decreasing stress down to stresses below the yield point and endurance limit, provided the specimen had received a large number of cycles.

A further examination, made at two different areas that had been subjected to the same stress, showed no significant difference in the diffraction pattern of the pair. Barrett also found that with aluminum alloys, diffraction patterns fell into two classes: those with sharp or nearly sharp spots and those in which plastic deformation had multiplied and blurred the spots until they formed practically continuous rings. The former class invariably corresponds to stresses below the yield point, the latter to stresses above the yield point. He suggests, therefore, that in these materials it is the relation of a stress to the yield point, and not to the endurance limit, that is the determining factor for the severity of the deformation and the type of x-ray pattern. He also states that the changes in the diffraction pattern reveal cold work caused by fatigue, not necessarily fatigue damage, and that cold work may take place at stresses both above and below the endurance limit.

MATERIALS USED AND PREPARATION OF THE SPECIMEN

14 ST aluminum alloy, specially prepared bars of which were kindly furnished by Mr. Ray Entringer of the Aluminum Company of America, were used in all of the tests described below. The 14 ST ingot was hot-rolled to $\frac{3}{4}$ of an inch diameter, straightened, and heat-treated at 940°F followed by a quench in water at 16°F. Aging took place at 340°F. The heat-treat cycle amounts to a minimum of 4 hours, the aging was for 10 hours. The samples were handled in such a manner that no internal strains could have been introduced into them prior to the time that they were put into the fatigue machine. Mr. Entringer states that 14 ST aluminum alloy has a tensile strength of 71,000 p.s.i., a yield strength of 64,000 p.s.i., a Brinell hardness number 131, and an endurance limit at 500,000,000 cycles of 17,000 p.s.i.

The chemical analysis of the bars is as follows:

Cu	Fe	Si	Mn	Mg
4.41	0.28	0.62	0.75	0.37.

Each specimen was machined to one-half inch diameter. A constriction of circular contour was then machined near one end. The smallest diameter of this constriction was $\frac{3}{8}$ of an inch. The last half-dozen cuts of the lathe tool when machining the constriction were about 0.0005 of an inch in depth. The specimen was then polished with fine aloxite cloth. Finally, the specimen was etched to remove any crystallites which might have been strained during the process of machining and polishing and to remove any finely powdered aluminum and abrasive dust which might have been imbedded in the surface. Specimens with etched surfaces, of course, have a lower endurance limit than polished surfaces. However, crystallites which have been broken up or strained by machining and polishing must be removed from the surface or the results will be confusing. A study of surfaces prepared in this manner will reveal what changes occur because of fatiguing not confused by strains or fragmentation of crystallites which have been produced by other processes before fatiguing has started.

THE CAMERA

A back reflection camera similar to the one designed by G. Pish[8] pictured in Fig. 1 was used

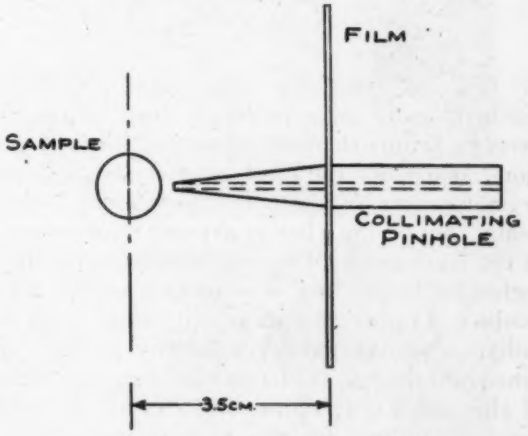

FIG. 1.

[8] Clark, Pish, and Seabury, J. App. Phys. 14, 284–290 (1943).

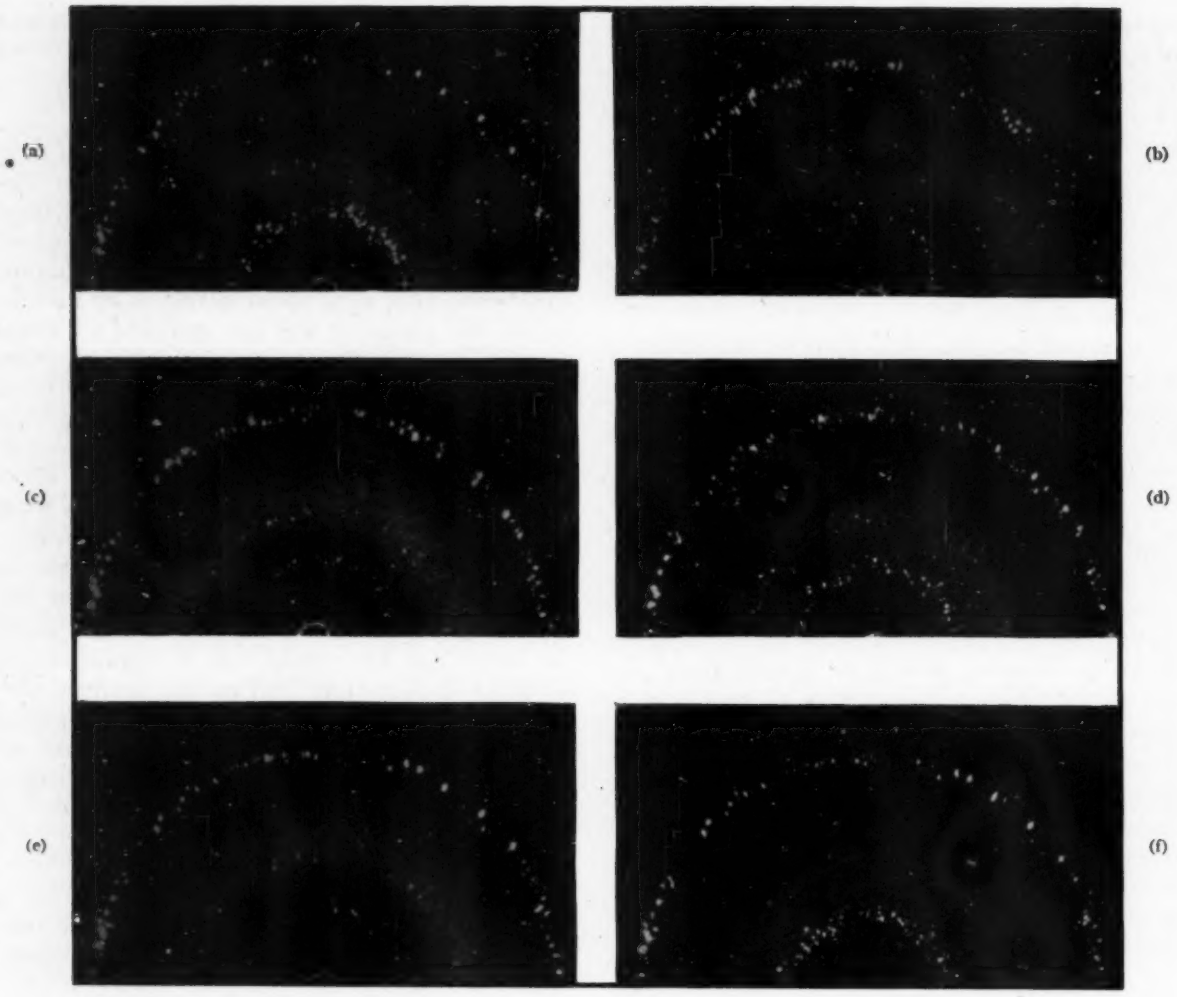

FIG. 2. X-ray diffraction pattern from Specimen No. 3. Stress 25,000 p.s.i. (a) Before fatigue. (b) After 5000 cycles. (c) 400,000 cycles. (d) 1,100,000 cycles. (e) 1,550,000 cycles. (f) 2,392,000 cycles.

in this investigation. This rapid "focusing" method, using large pinholes, gives a more divergent beam, thereby decreasing the exposure time. Also, when the specimen is made up of large crystals, more of them can be included in the beam, thus giving a better average representation of the test sample. The only disadvantage in the technique is the loss of resolution of the $K\alpha_1\alpha_2$ doublet. Copper radiation was used. This soft radiation penetrated a comparatively short distance into the specimen and gave large deviations of the diffracted beams. Both of these factors have advantages for this type of work. All exposures were for 10 minutes at 35 kv and 15 milliamp. The large ring in all diffraction pictures was analyzed for changes. This ring is caused by second-order reflection from the (111) plane. The 14 ST aluminum specimens were fatigued in an ordinary rotating beam machine in the laboratories of the A. O. Smith Corporation of Milwaukee. The aluminum rods were removed from the machine at intervals as fatiguing progressed so that diffraction patterns could be made. The back reflection camera was designed with a saddle jig, so that the rods could be removed for fatiguing and locked exactly in position for the diffraction picture. In this manner, the same area was irradiated each time an exposure was made. After a specimen failed it was placed in the camera in exactly the same position as before, regardless of the position of the fatigue crack. If the fracture itself was to be studied, the position of the rod was changed so that the area directly over or adjacent to the crack was irradiated. In

testing most of the specimens the machine was stopped before the excessive vibration actually broke the rod. The presence of a small surface crack on the specimen rotating at 1750 r.p.m. set up sufficient vibration to trip the automatic shut-off. Five of the specimens actually broke into two pieces upon failure, because of the large applied stress. These conditions are discussed in the section entitled Results. All specimens were fatigued at stresses above the endurance limit.

RESULTS

Fourteen specimens of aluminum alloy 14 ST were studied at various cycles and stresses. The result of six of these will be discussed in detail. The area under test in all cases was a circle 0.063 inch in diameter—the diameter of the x-ray beam striking the test bar. In all cases the larger ring, caused by x-ray reflection from the second order of the (111) plane, was analyzed and studied for changes that would suggest fatigue damage to the test specimen.

Specimen No. 3 was fatigued at a stress of 25,000 lb./sq. in. (a) is the diffraction pattern taken before fatiguing started, (b) after 5000 cycles, (c) after 400,000 cycles, (d) after 1,100,000 cycles, (e) after 1,550,000 cycles, and (f) after 2,392,000 cycles—at which point the specimen failed. The vibration caused by the cracked specimen was sufficient to trip the automatic shut-off, which stopped the machine before the specimen broke. The fatigue crack did not occur in the area under observation, but took place on the opposite side of the circumference of maximum stress. The spots in this series of pictures are clear and sharp and give no indication of fragmentation, distortion, or strain.

Specimen No. 4 was fatigued at a stress of 26,000 lb./sq. in. (a) is the diffraction pattern taken before fatiguing started, (b) after 5000 cycles, (c) after 1,400,000, (d) after 1,700,000, and (e) after 1,727,500 cycles—at which point the specimen failed. The fatigue crack occurred in the area under test. It will be noted that between (d) and (e) only 27,500 cycles were necessary to produce failure. It is interesting to note that between (c) and (d) there is an appreciable change in the diffraction patterns of the specimen, which

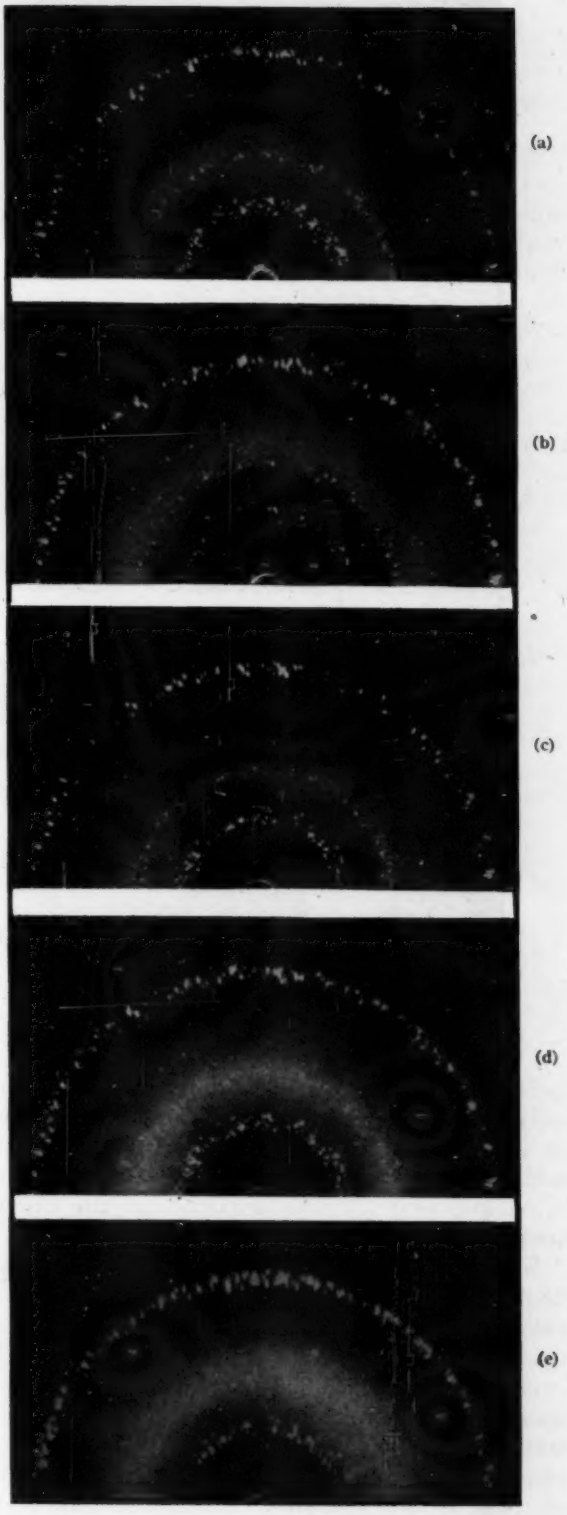

FIG. 3. X-ray diffraction pattern from Specimen No. 4. Stress 26,000 p.s.i. (a) Before fatigue. (b) After 5000 cycles. (c) 1,400,000 cycles. (d) 1,700,000 cycles. (e) 1,727,500 cycles.

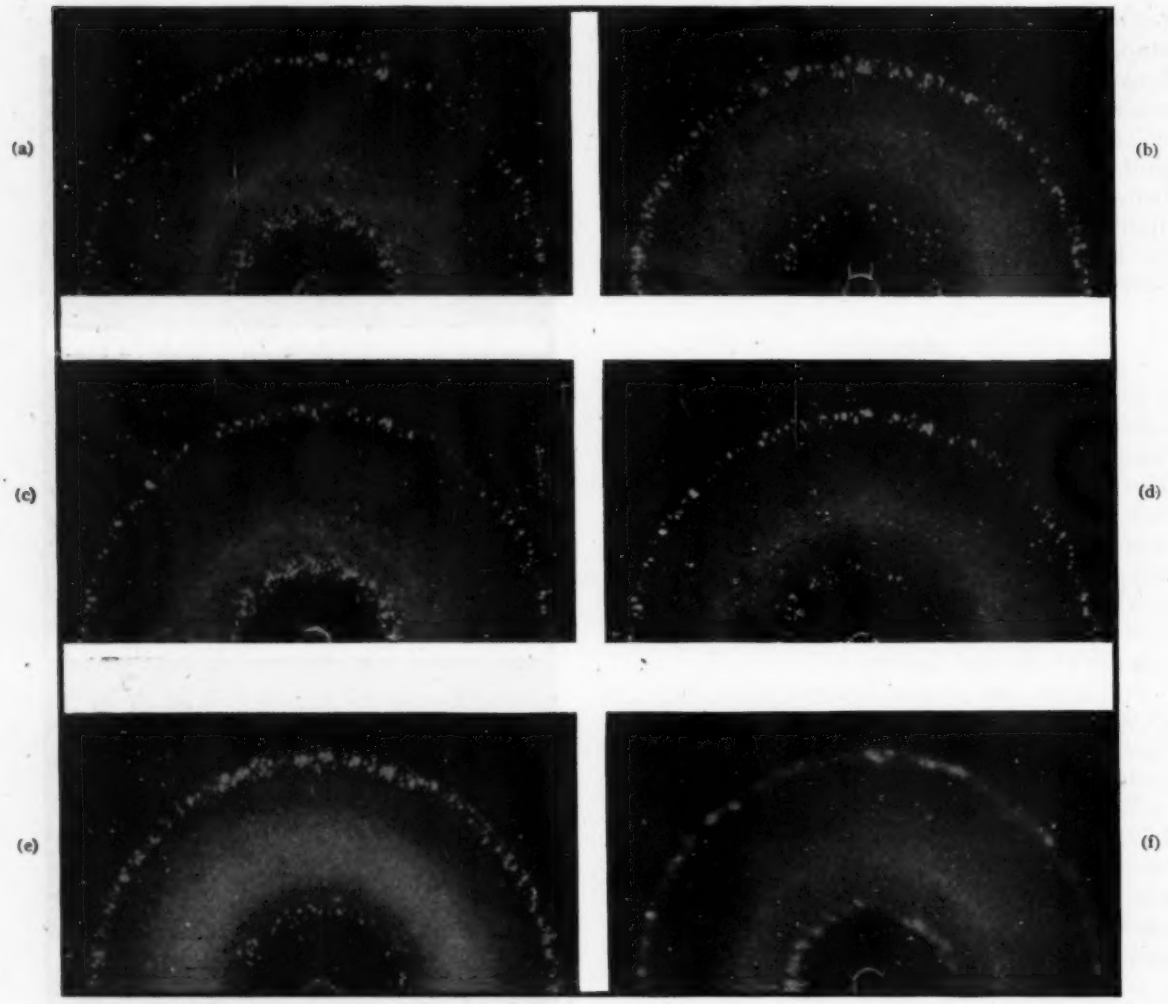

FIG. 4. X-ray diffraction pattern from Specimen No. 6. Stress 28,000 p.s.i. (a) Before fatigue. (b) After 5000 cycles. (c) 500,000 cycles. (d) 1,035,000 cycles. (e) 1,535,000 cycles. (f) 1,859,900 cycles.

becomes increasingly more prominent in (e) after only 27,500 cycles have been added. The increase in the number of spots indicates fragmentation while elongation of the spots suggests strain. It is obvious that the greater portion of the strain took place in the last 27,500 cycles.

Specimen No. 6 was fatigued at a stress of 28,000 lb./sq. in. (a) is the diffraction pattern taken before fatiguing started; (b) after 5000 cycles, (c) after 500,000 cycles, (d) after 1,035,000 cycles, (e) after 1,535,000 cycles, and (f) after the specimen had broken, through the area under test, at 1,859,900 cycles. There is no appreciable change in the diffraction pattern of the first four pictures. (e) indicates a definite fragmentation and (f) shows the great amount of strain produced on the crystals at the breaking point. Without a doubt, the greatest portion of this strain and deformation took place during the process of breaking.

Specimen No. 8 was fatigued at a stress of 30,000 lb./sq. in. (a) is the diffraction pattern taken before fatiguing started, (b) after 5000 cycles, (c) after 500,000 cycles, and (d) after the specimen had fractured after 572,500 cycles. The fracture occurred in the area under test. The change in the diffraction pattern as shown in print (d) must have taken place in the last 72,500 cycles or at the instant of fracture.

Specimen No. 12 was fatigued at a stress of 34,000 lb./sq. in. (a) is the diffraction pattern taken before fatiguing started, (b) after 5000

cycles, (c) after 275,000 cycles, and (d) after the specimen had fractured at 282,300 cycles. The fracture did not take place through the area under test, but appeared on the opposite side of the circumference of maximum stress. There is no appreciable change in the nature of the diffraction pattern.

Specimen No. 14 was fatigued at a stress of 40,000 lb./sq. in. (a) is the diffraction pattern taken before fatiguing started, (b) after 5000 cycles, (c) after 35,000 cycles, (d) after 90,000 cycles, and (e) after the specimen had broken at 105,700 cycles. The break did not take place in the area under test, but just outside of the area. (f) is the diffraction picture taken after the specimen was moved so that the edge of the break was tangent to the area of the x-ray beam irradiating the specimen. Careful measurements on the location of the three clusters of spots that appear at the left end of the horizontal diameter of print (e) indicate a slight clockwise rotation, while the position of the two large spots that appear at the right end of the horizontal diameter remained unchanged. Print (e) of Fig. 7 was the only pattern in which a rotation of the grain was observed at the time of fracture. In (f) there exists a definite change in the diffraction pattern. The pattern indicates that the crystals are highly strained. This strained condition exists only in the region adjacent to the break, and disappears entirely a short distance away.

DISCUSSION AND CONCLUSION

Fourteen test specimens were examined and the results obtained vary. Of the fourteen specimens two broke through the area under test and three broke outside the area. The two that broke through the area irradiated showed marked changes, while the three that failed outside the area produced no effect on the diffraction pattern. The only change noted was when the area directly adjacent to the break was analyzed. Figure 7 illustrates this point.

Of the nine remaining specimens in which fatigue cracks resulted, six cracked outside the area and three within the area under test. In all six cases no detectable damage, previous to failure, manifested itself on the diffraction pattern. Figures 2 and 6 illustrate this point. When the specimen was moved so that the region adjacent to the fatigue crack was irradiated, definite damage was noted by the diffraction pattern. In the remaining three the fatigue crack took place directly in the area under consideration, and all three showed marked detectable damage

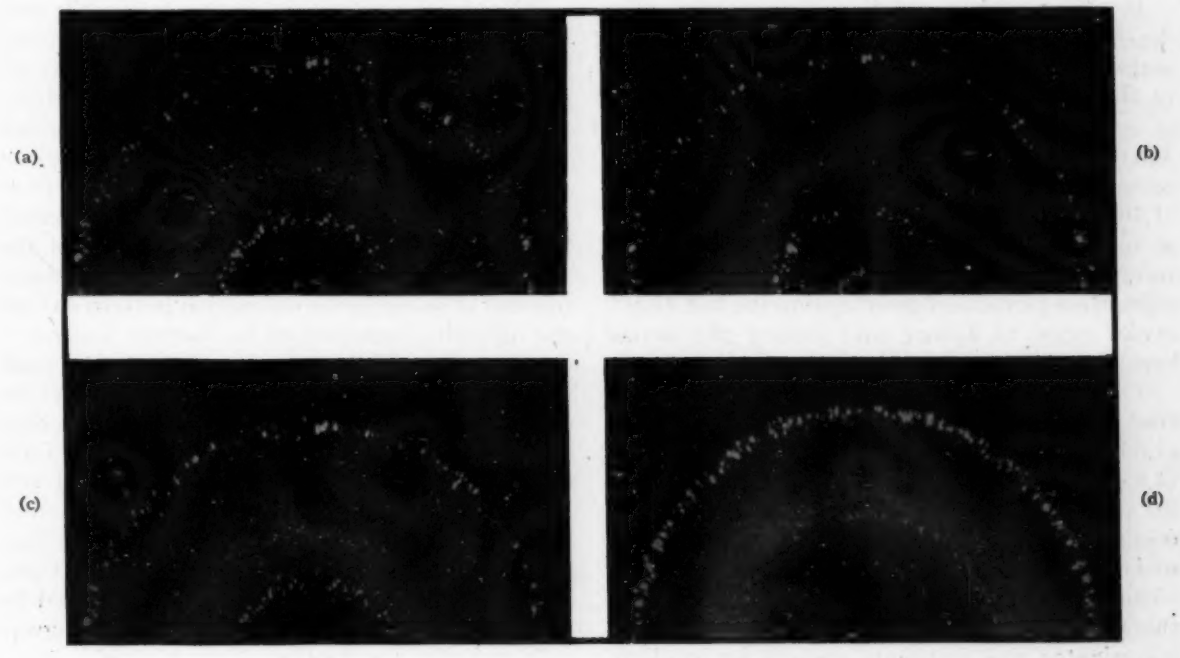

FIG. 5. X-ray diffraction pattern from Specimen No. 8. Stress 30,000 p.s.i. (a) Before fatigue. (b) After 5000 cycles. (c) 500,000 cycles. (d) 572,500 cycles.

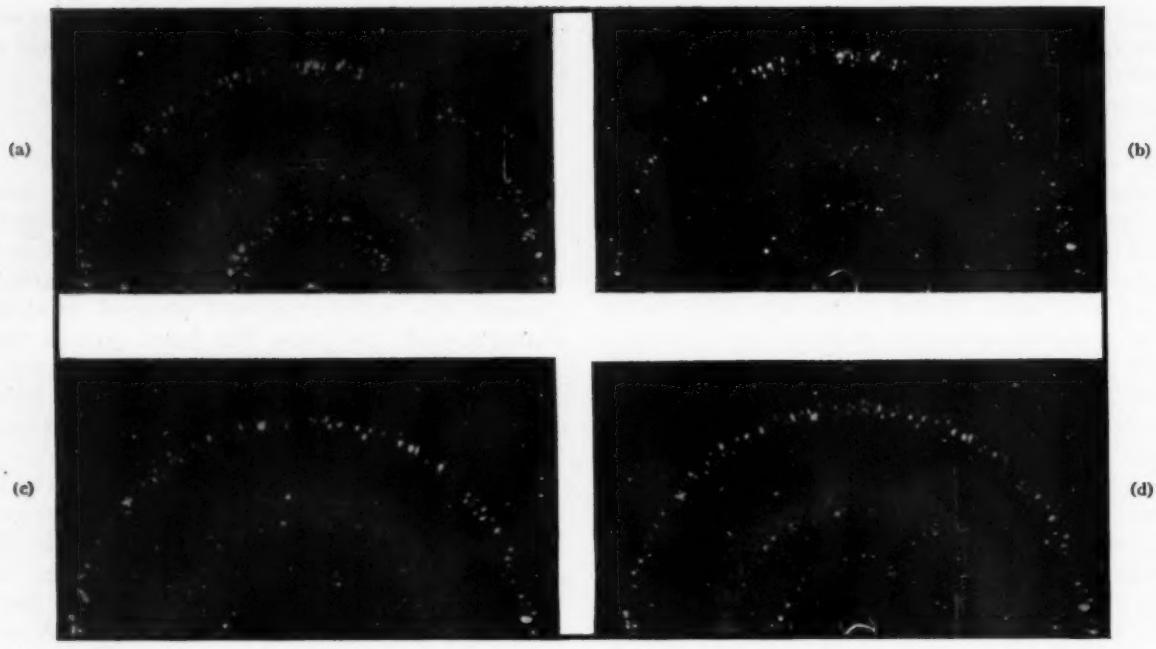

FIG. 6. X-ray diffraction pattern from Specimen No. 12. Stress 34,000 p.s.i. (a) Before fatigue. (b) After 5000 cycles. (c) 275,000 cycles. (d) 282,300 cycles.

previous to failure. Figures 3–5 illustrate this point.

In all cases failure followed very soon after detectable damage occurred. This is illustrated rather clearly in Fig. 3 where between picture (c) (1,400,000 cycles) and (d) (1,700,000 cycles) there is a distinct change that occurred within the 300,000 cycles; and this detectable damage occurred before failure. Between pictures (d) (1,700,000 cycles) and (e) (1,727,500 cycles) there is an appreciable change in the diffraction pattern. The detectable damage represented by the diffraction picture occurred during the last 27,500 cycles prior to failure and during the actual breaking of the test specimen.

This is again illustrated in Fig. 4. In Fig. 4, there is a definite change between picture (d) (1,035,000 cycles), (e) (1,535,000 cycles), and (f) (1,859,900 cycles). The change shown in picture (e) is definitely the effect of fatigue damage that occurred previous to failure and cannot be associated with changes caused by the tensile nature of the actual failure of the test bar. From this we can conclude that in the case where the investigator was fortunate enough to irradiate the area in which the fatigue crack was to take place, an x-ray diffraction picture could predict failure. This prediction is limited to the last 20,000–300,000 cycles.

The above results agree rather favorably with other investigations performed with aluminum alloys. In the initial study on 25 ST, Barrett[7] found the grain size too large for suitable analysis. Only 3 or 4 spots were present on the diffraction pattern. Kies and Quick[9] continued the work of Barrett on 25 ST. The specimens were cut from an airplane propeller, which was re-heat-treated to the 25 SW condition. The grain size of the material was small enough to produce a large number of spots on the diffraction pattern so that the difficulty encountered by Barrett was not a consideration. The specimen was locked in such a position that the same spot could be used for each successive diffraction pattern. The x-rays were directed at the specimen at grazing incidence. The diffraction patterns obtained are therefore representative of the same specimen in the course of a series of fatigue-stress applications. They found no progressive changes in the x-ray diffraction patterns that could be considered as significant for foretelling failure in a fatigued

[9] J. A. Kies and G. W. Quick, N.A.C.A. Report 659 (1939).

specimen. Van Horn[10] in performing his experiment with 25 ST took x-ray patterns after every million cycles, each time taking pictures at eight different areas on the circumference of maximum stress. His results showed no change in the crystalline pattern until after failure. Then the change was very noticeable caused, most likely, by the tensile nature of the actual failure in parts of the fatigue bar. Spencer and Marshall[11] conducted an investigation with aluminum alloy 17 ST and concluded, among other things, that fatigue failure is always preceded by fatigue damage which is detectable by x-ray methods. All of the detectable damage occurred in the last 300,000 cycles and consisted of rotation of some of the grains, introduction of strains into some of the crystallites and fragmentation of some of the crystallites.

The slight variation in findings between the various aluminum alloys, i.e., 25 ST, 17 ST, and 14 ST would stimulate the question: are differences between these results always or sometimes owing to the use of different alloys or alloys in different conditions? The author feels that the results are in good agreement with one another inasmuch as the various techniques are concerned. To conclude from a series of diffraction patterns that no change took place in the

[10] K. R. Van Horn, communicated results.
[11] R. G. Spencer and J. W. Marshall, J. App. Phys. **12**, 191 (1941).

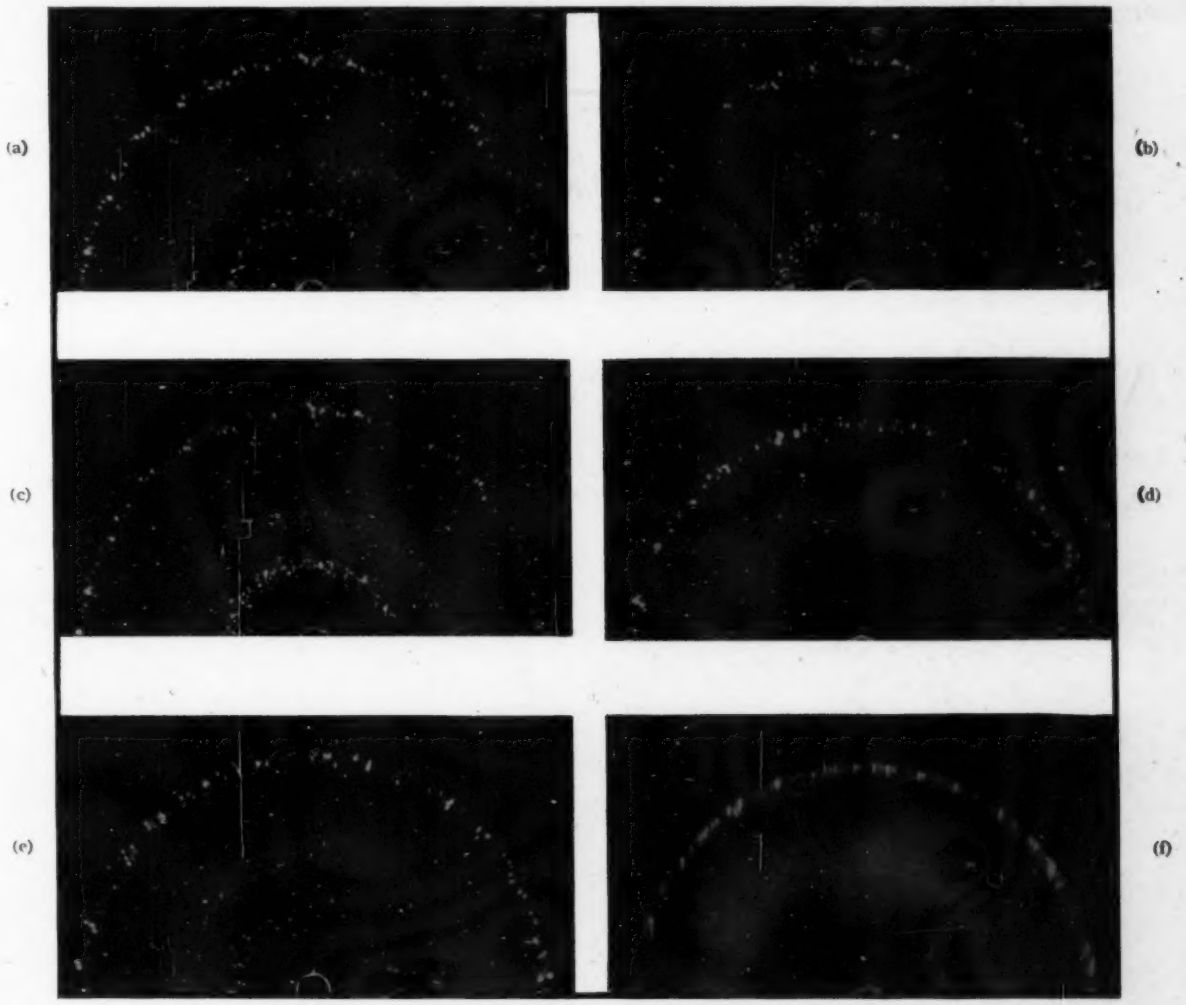

FIG. 7. X-ray diffraction pattern from Specimen No. 14. Stress 4000 p.s.i. (a) Before fatigue. (b) After 5000 cycles. (c) 35,000 cycles. (d) 90,000 cycles. (e and f) 105,700 cycles.

crystalline pattern until after failure, or that detectable changes do take place in the last 300,000 cycles depends on the good fortune of the investigator to have taken a diffraction pattern of the specimen just 300,000 cycles or less before failure, and to have the fatigue crack take place in the area under test. It will be noted that in the case of Figs. 3–5, no appreciable changes occurred in the diffraction patterns until the very last stages of fatigue, and that in all these cases the fatigue crack occurred in the area under test.

Barrett[7] has also indicated in his investigation that the changes in the diffraction pattern reveal cold work owing to fatigue. Since the changes take place in the last 300,000 cycles or less, and since these changes are only detected when the fatigue crack lies in the area irradiated, it seems necessary to conclude that the changes manifested are not caused by cold work owing to fatigue. These changes could hardly be caused by cold work effected by fatigue unless we contend that the cold-work fatigue took place in the last 300,000 cycles and was localized to the area in which the actual fatigue crack took place. This does not conform with cold-work phenomena. Hence, it is safe to conclude that the changes in the diffraction pattern are the effects of the repeated cyclic stresses which gradually weakened the intercrystalline bonds which caused the metal to fail.

ACKNOWLEDGMENTS

Acknowledgments are due the Production Laboratories of the A. O. Smith Corporation of Milwaukee, especially Messrs. L. Heise, J. Bach, and M. Zimmerman for their kind cooperation in the study.

Erratum: Fatigue of Fabrics

[J. App. Phys. 13, 715 (1942)]

W. F. Busse, E. T. Lessig, D. L. Loughborough, and L. Larrick

A NUMERICAL error was made in the calculation of activation energy given in Table V of the paper "Fatigue of fabrics." Table V in the correct form is given herewith.

Table V.

Material	Activation energy
Nylon	45,700 cal./°
Cotton	28,800 cal./°
Rayon	19,000 cal./°